Green City, Clean Waters

Tributary Water Quality Model for Dissolved Oxygen

Consent Order & Agreement

Deliverable VII

City of Philadelphia Combined Sewer Overflow Long Term Control Plan Update

Submitted to

The Commonwealth of Pennsylvania

Department of Environmental Protection

By The Philadelphia Water Department

June 1, 2014

Table of Contents

1.0 Introduction

1.1 TTF Creek Dissolved Oxygen Model Extent 1-6
1.2 Cobbs Creek Dissolved Oxygen Model Extent 1-7
1.3 Model Objectives 1-10
1.4 Modeling Approach 1-10

2.0 Tributary H&H Models

2.1 H&H Model Refinements 2-3

3.0 Dissolved Oxygen Model

3.1 Dissolved Oxygen Model 3-1
3.1.1 Algae 3-1
3.1.2 BOD 3-3
3.1.3 SOD 3-3
3.1.4 Reaeration 3-6
3.1.5 Modeling DO in Urban Streams 3-6
3.2 Summary of Available Data 3-8
3.2.1 TTF and Cobbs Creeks Comprehensive Characterization Reports 3-8
3.2.2 Periphyton 3-10
3.2.3 SOD 3-16
3.2.4 Reaeration 3-17
3.2.5 Continuous Data 3-22
3.3 Model Validation Periods 3-23
3.4 Algae 3-24
3.5 Linkage from H&H Model to DO Model 3-26
3.6 Water Quality Model Input Data 3-29
3.6.1 Boundary Conditions 3-29
3.6.1.1 Stormwater 3-30
3.6.1.2 Sanitary Base Wastewater 3-31
3.6.1.3 Baseflow 3-32
3.6.1.4 Water Temperature and PAR 3-35
3.6.2 Model Parameterization 3-35
3.6.2.1 Canopy Cover 3-37
3.6.2.2 Sediment Oxygen Demand 3-38
3.6.2.3 Algae Habitat 3-38
3.6.2.4 Dam Reaeration 3-39
3.7 Water Quality Model Sensitivity Analysis 3-43
3.8 Model Validation 3-49
3.8.1 TTF Creek 3-49

3.8.2 Cobbs Creek 3-61
3.9 Dissolved Oxygen Model Limitations 3-73
3.10 Potential Areas for Improvement 3-74
3.11 Conclusions........ 3-75

References

List of Tables

2.0 Tributary Hydrologic and Hydraulic Models

Table 2-1 Baseflow Ranges for DO Model Validation Periods 2-3

3.0 Water Quality Model

Table 3-1 Measured and Calculated Reaeration Rates from USGS Study 3-19
Table 3-2 TTF Creek Reach Properties from USGS Reaeration Study 3-19
Table 3-3 Calculated Reaeration Coefficients from Published Reaeration Equations 3-20
Table 3-4 TTF DO Model Validation Periods 3-23
Table 3-5 Cobbs DO Model Validation Periods 3-23
Table 3-6 TTF DO Model Segmentation 3-26
Table 3-7 Cobbs DO Model Segmentation 3-27
Table 3-8 National EMCs Derived from Published Sources 3-31
Table 3-9 Water Quality Constituents Derived from EMCs as Required by WASP 3-31
Table 3-10 Dry Weather Regulator Sampling Data of Base Wastewater 3-32
Table 3-11 Water Quality Constituents Derived from Base Wastewater as Required by WASP 3-32
Table 3-12 Summary of Dry Weather Water Quality Data for TTF Creek Inside City, March-September of 2000-2013 3-33
Table 3-13 Summary of Dry Weather Water Quality Data for Cobbs and East/West Indian Creeks Inside City, March-September of 1999-2013 3-33
Table 3-14 Summary of Dry Weather Water Quality Data for Cobbs Creek Watershed Outside City, January-December of 1999-2013 3-34
Table 3-15 Water Quality Baseflow Concentrations Applied to TTF and Cobbs DO Models 3-34
Table 3-16 Headwater Concentrations Applied to TTF and Cobbs DO Models 3-35
Table 3-17 Global Constant Values Applied in Validation 3-36
Table 3-18 Spatially Variable Parameters in Cobbs DO Model 3-39
Table 3-19 Spatially Variable Parameters in TTF DO Model 3-42
Table 3-20 TTF DO Model Evaluation Statistics for Validation Periods T-1 through T-5 3-60
Table 3-21 Cobbs DO Model Evaluation Statistics for Validation Periods C-1 through C-4 3-73

List of Figures

1.0 Introduction

Figure 1-1 Nontidal TTF Creek Watershed 1-2
Figure 1-2 Nontidal Cobbs Creek Watershed 1-3
Figure 1-3 Land Use in Nontidal TTF Creek Watershed 1-4
Figure 1-4 Land Use in Nontidal Cobbs Creek Watershed 1-5
Figure 1-5 CSO Outfalls in the Nontidal TTF Creek Watershed 1-7
Figure 1-6 CSO Outfalls in the Nontidal Cobbs Creek Watershed 1-9
Figure 1-7 Modeling Approach for DO in Tributaries 1-12

3.0 Water Quality Model

Figure 3-1 SOD Sampling Apparatus for Profile Method 3-5
Figure 3-2 Water Chemistry Monitoring Sites in the Nontidal TTF Creek Watershed 3-9
Figure 3-3 Water Chemistry Monitoring Sites in the Nontidal Cobbs Creek Watershed 3-10
Figure 3-4 Benthic Algal Density and Streamflow in the TTF Creek, June-July 2011 3-11
Figure 3-5 Benthic Algal Density and Streamflow in the TTF Creek, August-September 2011 3-12
Figure 3-6 Benthic Algal Density and Streamflow in Cobbs Creek, April/July/September 2012 3-13
Figure 3-7 Periphyton and SOD Monitoring Sites in the Nontidal TTF Creek Watershed 3-14
Figure 3-8 Periphyton and SOD Monitoring Sites in the Nontidal Cobbs Creek Watershed 3-15
Figure 3-9 SOD Monitoring Results, 2011-2012 (n=20) 3-16
Figure 3-10 Dye Injection and Propane Gas Diffusion on September 3, 2009 in TTF Creek near US Route 1 (from Senior and Gyves, 2010) 3-17
Figure 3-11 USGS Reaeration Study Sites in TTF Creek 3-18
Figure 3-12 Calculated vs. Observed Reaeration Coefficient 3-22
Figure 3-13 WASP7.5 Advanced Eutro Modeling Schematic (from Ambrose *et al*., 2006) 3-25
Figure 3-14 Sensitivity of Benthic Algal Density to Maximum Growth Rate 3-44
Figure 3-15 Sensitivity of DO to Maximum Growth Rate 3-45
Figure 3-16 Sensitivity of Nitrogen Uptake Rate to Maximum Growth Rate 3-45
Figure 3-17 Sensitivity of Phosphorus Uptake Rate to Maximum Growth Rate 3-46
Figure 3-18 Sensitivity of Photosynthesis Rate to Maximum Growth Rate 3-46
Figure 3-19 Sensitivity of SOD to SOD Temperature Coefficient 3-47

Figure 3-20 Sensitivity of Benthic Algal Density to CNP Ratio 3-47
Figure 3-21 Sensitivity of DO to CNP Ratio 3-48
Figure 3-22 Sensitivity of DO to Dam Reaeration 3-48
Figure 3-23 Sensitivity of DO to SOD.. 3-49
Figure 3-24 Observed and Simulated Benthic Algal Density at Site TF316, Validation Period T-3 3-50
Figure 3-25 Observed and Simulated Benthic Algal Density at Site TF316, Validation period T-4 3-51
Figure 3-26 Observed and Simulated Benthic Algal Density at Site TF316, Validation Period T-5 3-51
Figure 3-27 Observed and Simulated DO Concentration at Site TF280, Validation Period T-3 3-53
Figure 3-28 Observed and Simulated DO Percent Saturation at Site TF280, Validation Period T-3 3-53
Figure 3-29 Observed and Simulated CDF of DO Concentration at Site TF280, Validation Period T-3 3-54
Figure 3-30 Observed and Simulated DO Concentration at Site TF280, Validation Period T-4 3-54
Figure 3-31 Observed and Simulated DO Percent Saturation at Site TF280, Validation Period T-4 3-55
Figure 3-32 Observed and Simulated CDF of DO Concentration at Site TF280, Validation Period T-4 3-55
Figure 3-33 Observed and Simulated DO Concentration at Site TF280, Validation Period T-5 3-56
Figure 3-34 Observed and Simulated DO Percent Saturation at Site TF280, Validation Period T-5 3-56
Figure 3-35 Observed and Simulated CDF of DO Concentration at Site TF280, Validation Period T-5 3-57
Figure 3-36 Observed and Simulated DO Concentration at Site TF280, Validation Period T-1 3-57
Figure 3-37 Observed and Simulated DO Percent Saturation at Site TF280, Validation Period T-1 3-58
Figure 3-38 Observed and Simulated CDF of DO Concentration at Site TF280, Validation Period T-1 3-58
Figure 3-39 Observed and Simulated DO Concentration at Site TF280, Validation Period T-2 3-59
Figure 3-40 Observed and Simulated DO Percent Saturation at Site TF280, Validation Period T-2 3-59
Figure 3-41 Observed and Simulated CDF of DO Concentration at Site TF280, Validation Period T-2 3-60
Figure 3-42 Observed and Simulated Benthic Algal Density at Site DCC770, Validation Period C-2 3-61

Figure 3-43 Observed and Simulated Benthic Algal Density at Site DCC251, Validation Period C-2 3-62
Figure 3-44 Observed and Simulated Benthic Algal Density at Site DCC770, Validation Period C-3 3-63
Figure 3-45 Observed and Simulated Benthic Algal Density at Site DCC251, Validation Period C-3 3-63
Figure 3-46 Observed and Simulated Benthic Algal Density at Site DCC770, Validation Period C-4 3-64
Figure 3-47 Observed and Simulated Benthic Algal Density at Site DCC251, Validation Period C-4 3-64
Figure 3-48 Observed and Simulated DO Concentration at Site DCC251, Validation Period C-1 3-66
Figure 3-49 Observed and Simulated DO Percent Saturation at Site DCC251, Validation Period C-1 3-66
Figure 3-50 Observed and Simulated CDF of Do Concentration at Site DCC251, Validation Period C-1 3-67
Figure 3-51 Observed and Simulated DO Concentration at Site DCC251, Validation Period C-2 3-68
Figure 3-52 Observed and Simulated DO Percent Saturation at Site DCC251, Validation Period C-2 3-68
Figure 3-53 Observed and Simulated CDF of DO Concentration at Site DCC251, Validation Period C-2 3-69
Figure 3-54 Observed and Simulated DO Concentration at Site DCC251, Validation Period C-3 3-70
Figure 3-55 Observed and Simulated DO Percent Saturation at Site DCC251, Validation Period C-3 3-70
Figure 3-56 Observed and Simulated CDF of DO Concentration at Site DCC251, Validation Period C-3 3-71
Figure 3-57 Observed and Simulated DO Concentration at Site DCC251, Validation Period C-4 3-71
Figure 3-58 Observed and Simulated DO Percent Saturation at Site DCC251, Validation Period C-4 3-72
Figure 3-59 Observed and Simulated CDF of DO Concentration at Site DCC251, Validation Period C-4 3-72

Appendices

Appendix A1: Sediment Oxygen Demand Measurements Collected in the Tacony Creek, Philadelphia, Pennsylvania

Appendix A2: Sediment Oxygen Demand Measurements Collected in Tacony and Cobbs Creeks, Philadelphia, Pennsylvania

Appendix B: USGS Gage Data Processing & Analysis Procedures

Glossary of Acronyms

ADV	Acoustic Doppler Velocity Profiler
BOD	Biochemical Oxygen Demand
CBOD	Carbonaceous Biochemical Oxygen Demand
CCR	Comprehensive Characterization Report
CDF	Cumulative Distribution Function
COA	Consent Order and Agreement
CSO	Combined Sewer Overflow
CSS	Combined Sewer System
DCIA	Directly Connected Impervious Area
DO	Dissolved Oxygen
EMC	Event Mean Concentration
FAS	Fraction of Bottom Area in Each Segment Providing Suitable Substrate for Growth
FLI	Fraction of Light Intercepted by Tree Canopy
GIS	Geographic Information Systems
H&H	Hydrologic and Hydraulic
LTCPU	Long Term Control Plan Update
MAE	Mean Absolute Error
NBOD	Nitrogenous Biochemical Oxygen Demand
NREL	National Renewable Energy Laboratory
NSQD	National Stormwater Quality Database
PADEP	Pennsylvania Department of Environmental Protection
PAR	Photosynthetically Active Radiation
PCSWMM	Support Software of the Storm Water Management Model
RMSE	Root Mean Square Error
SOD	Sediment Oxygen Demand
SWMM	Storm Water Management Model
SWMM4	Storm Water Management Model version 4
SWMM4.4	Storm Water Management Model version 4.4
SWMM5	Storm Water Management Model version 5
TMDL	Total Maximum Daily Load
TTF	Tookany-Tacony/Frankford
US EPA	United States Environmental Protection Agency
USGS	United States Geological Survey
UTC	Urban Tree Canopy
WASP	Water Quality Analysis Simulation Program
XP-SWMM	Expert System of the Storm Water Management Model

1.0 Introduction

This report focuses on Deliverable Item 7 of the 2011 Consent Order and Agreement (COA) between the Pennsylvania Department of Environmental Protection (PADEP) and the Philadelphia Water Department (Water Department), the Tributary Water Quality Model for Dissolved Oxygen. The COA requires the development of Dissolved Oxygen (DO) models for the nontidal extents of two tributaries that receive combined sewer overflow (CSO) discharges within the City of Philadelphia (City), Tookany/Tacony-Frankford (TTF) Creek and Cobbs Creek (Figures 1-1 and 1-2). The Cobbs Creek Watershed and Tookany/Tacony-Frankford Creek Watershed have been extensively described in their 2004 and 2005 Comprehensive Characterization Reports (CCRs), respectively (Philadelphia Water Department, 2004 and 2005). These documents can be referenced for more detailed information on watershed characteristics and for summaries of physical, chemical, and biological water quality monitoring results. The highly developed degree of land use in each watershed is depicted in Figures 1-3 and 1-4.

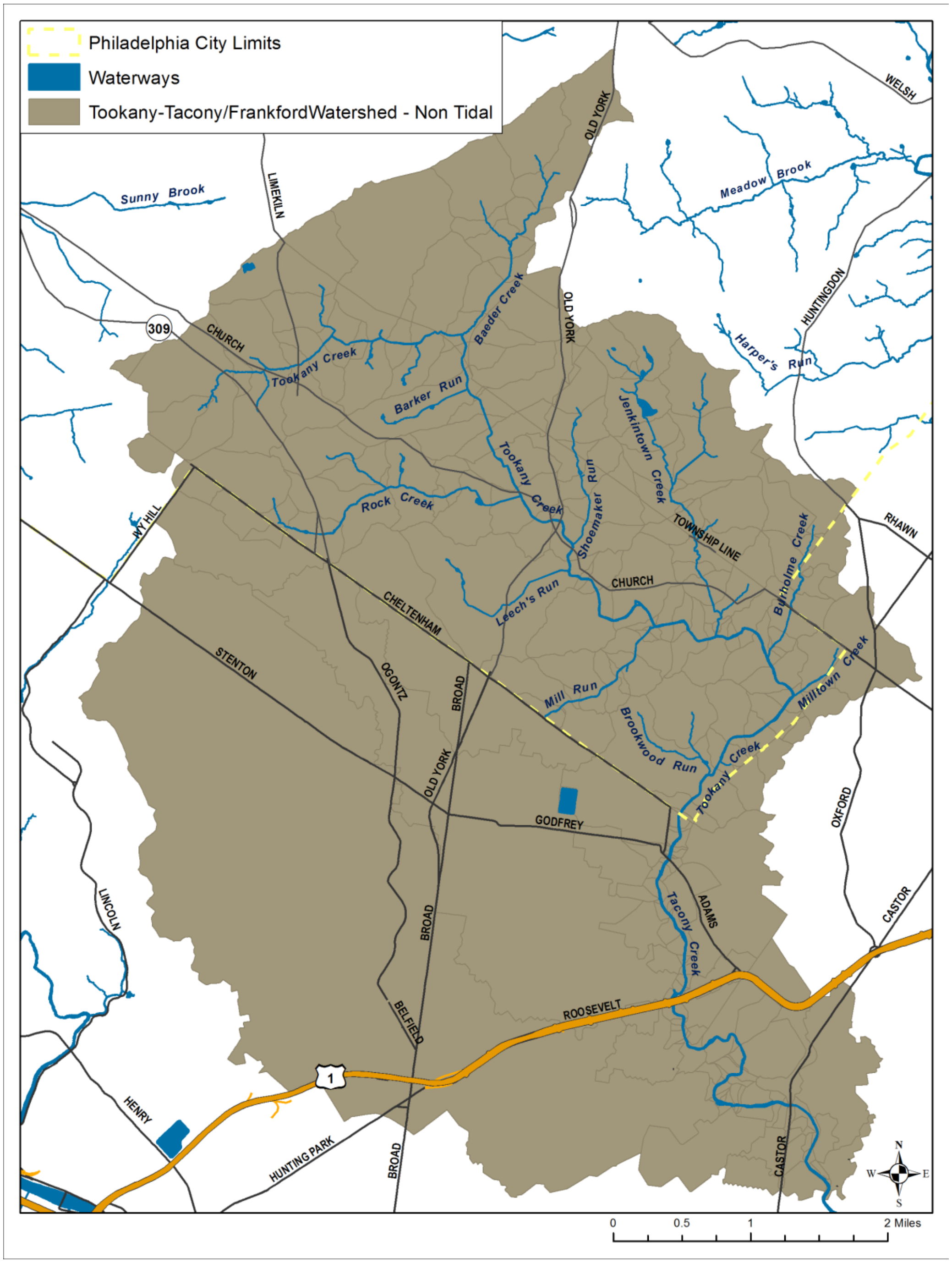

Figure 1-1: Nontidal TTF Creek Watershed

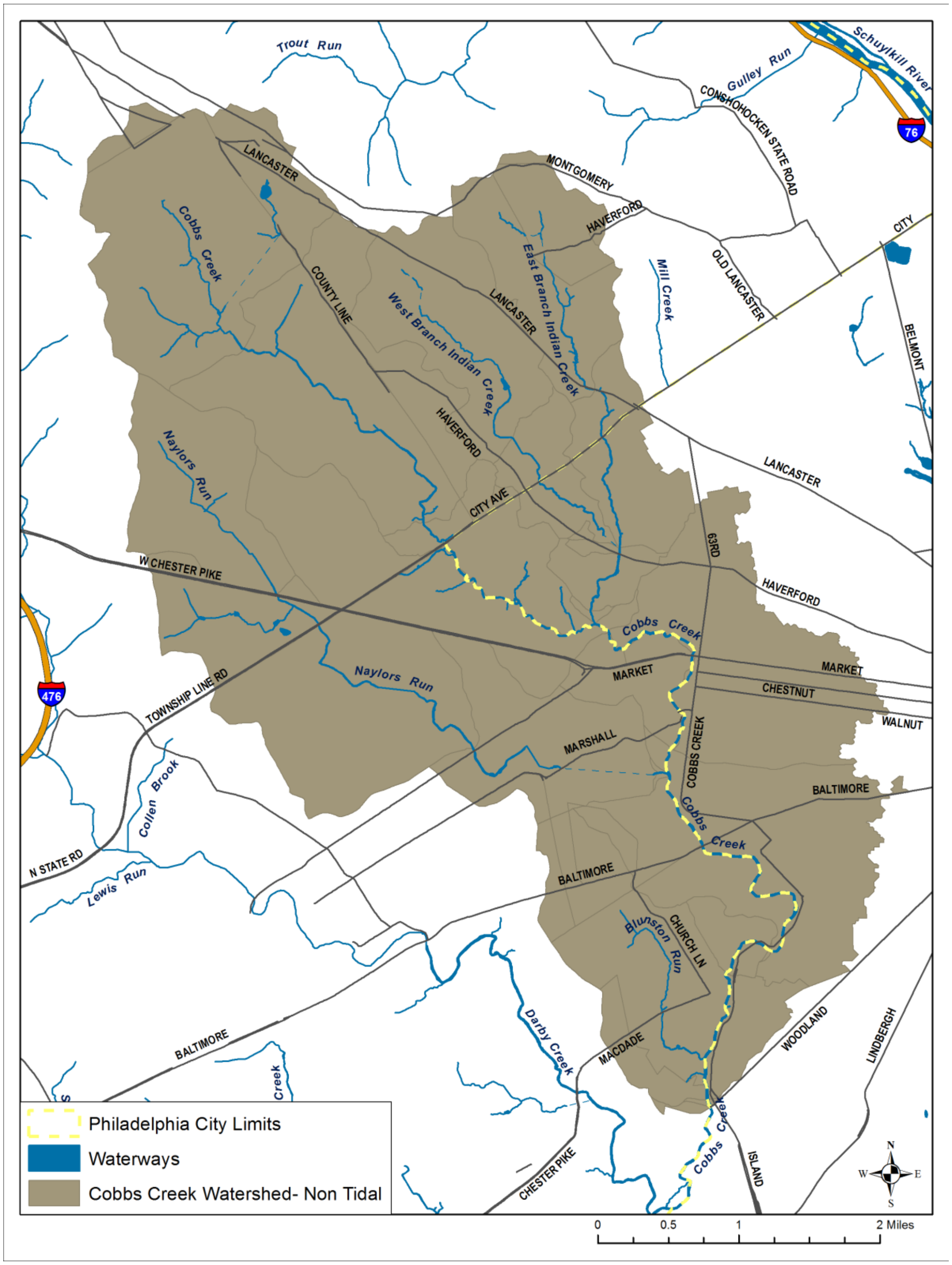

Figure 1-2: Nontidal Cobbs Creek Watershed

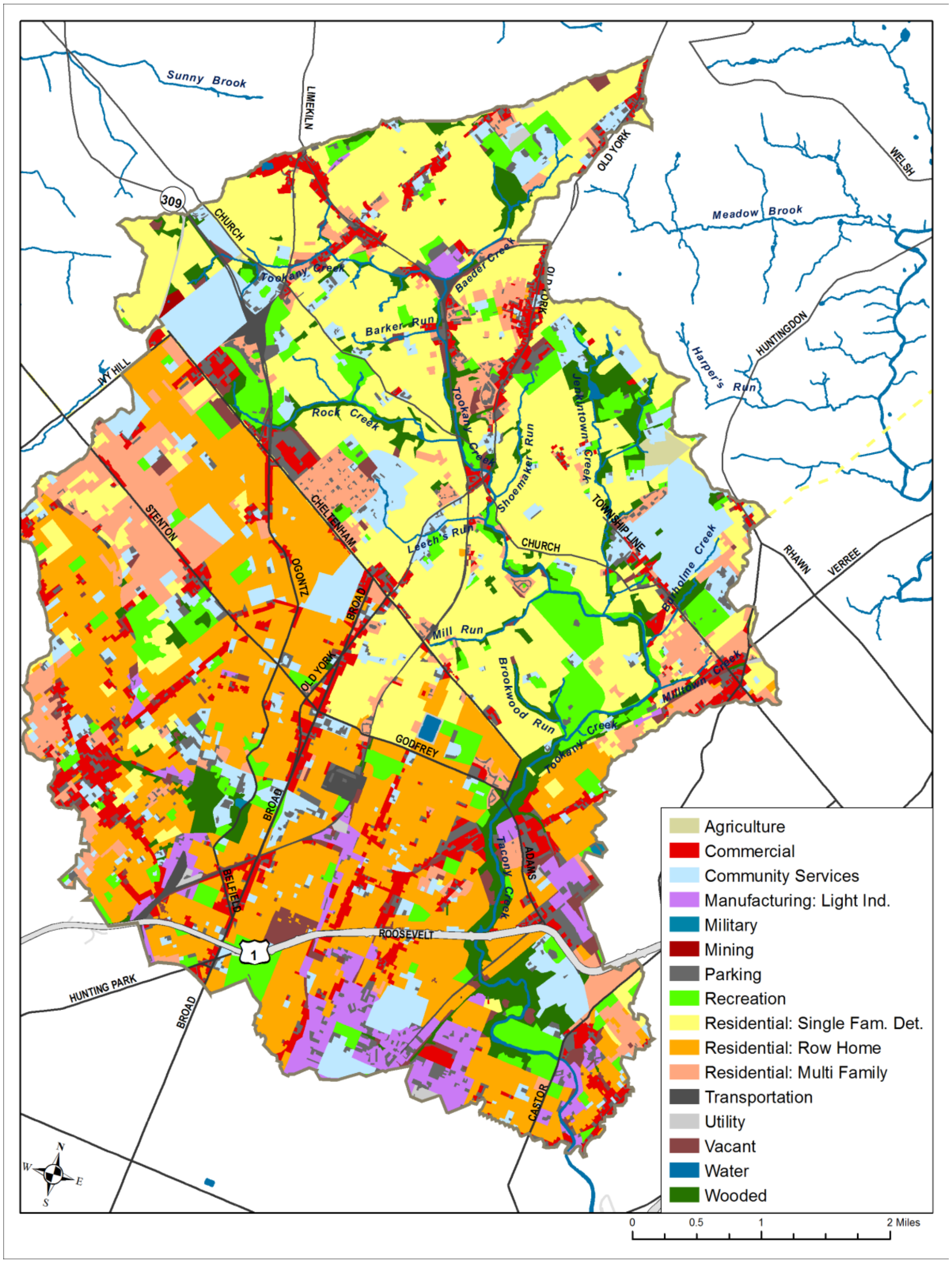

Figure 1-3: Land Use in Nontidal TTF Creek Watershed

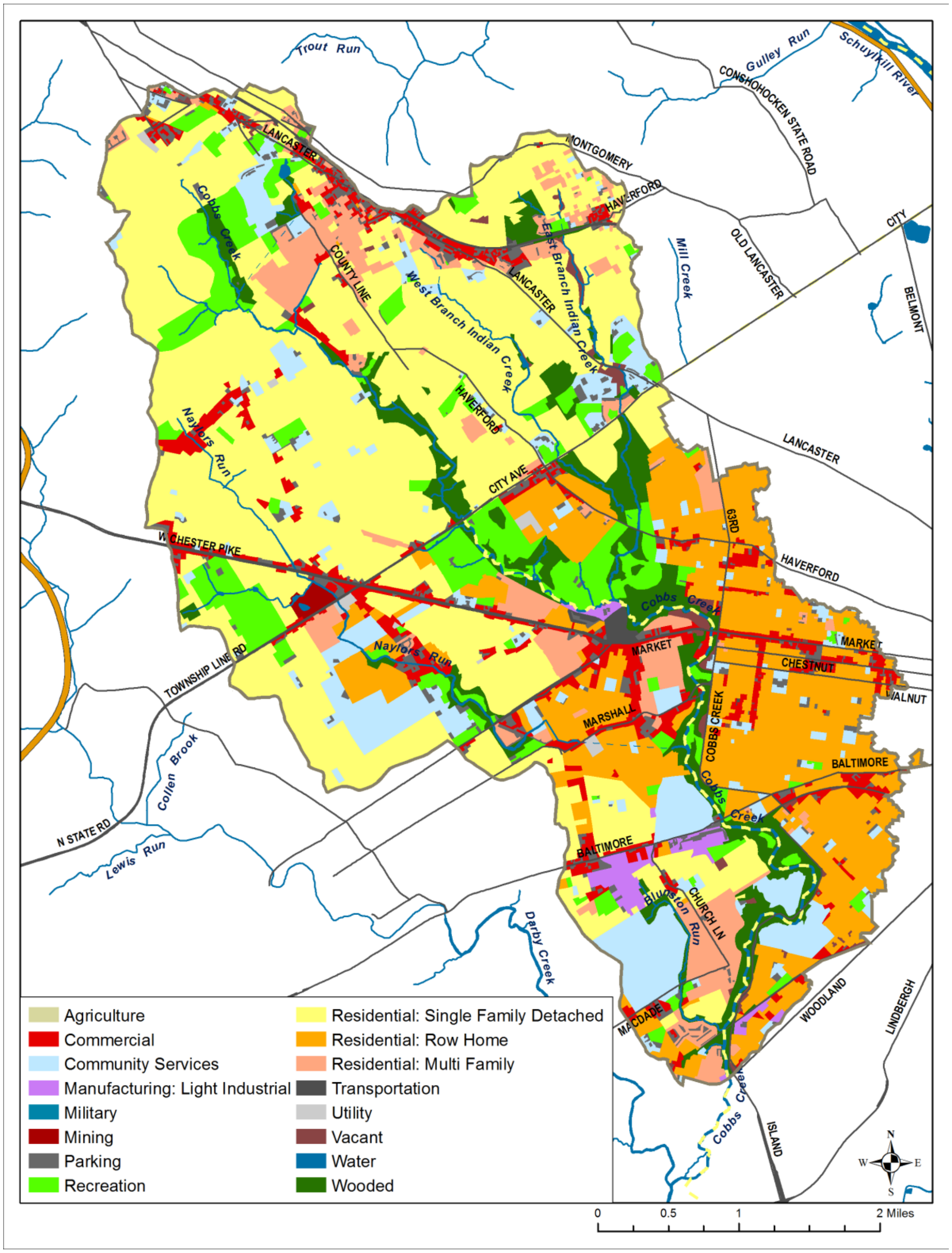

Figure 1-4: Land Use in Nontidal Cobbs Creek Watershed

1.1 TTF Creek Dissolved Oxygen Model Extent

The TTF Creek dissolved oxygen model (or TTF DO Model) explicitly simulates in-stream DO conditions in nontidal reaches within City limits. In the TTF DO Model extent, there are 20 outfalls that release combined stormwater and sanitary wastewater during storms that exceed the Northeast Water Pollution Control Plant treatment capacity (Figure 1-5). Based on model simulations for the typical year precipitation, as described in the Long Term Control Plan Update (LTCPU) Supplemental Documentation Volume 4 (Philadelphia Water Department, 2011), the outfalls in the TTF DO Model extent discharge, at present, a total annual volume of almost 4 billion gallons of combined stormwater and sanitary wastewater.

The upstream boundary of the TTF DO Model extent is at River Mile 6.32 (*i.e.*, 6.32 miles upstream of the end of TTF Creek), site of United States Geological Survey (USGS) Gage 01467086 above Adams Avenue near the City boundary. The downstream boundary of the TTF DO Model is at River Mile 1.77, the Torresdale Avenue weir dam, which is regarded to be the head of tidal influence. The modeling of DO dynamics for the tidal reach of Frankford Creek will be included in the June 1, 2015 deliverable for water quality models of tidal receiving waters.

It should be noted that outfall T-01 is the only outfall in the nontidal watershed that discharges to receiving waters outside the City, and thus outside the TTF DO Model extent. The nontidal reach outside the City was excluded from the TTF DO Model extent because there is insufficient continuous DO data available in these stream segments to perform model validation; and because the effects of the T-01 discharge are implicitly captured at the upper boundary of the model. (USGS Gage 01467086 above Adams Avenue). Note model simulations for the typical year precipitation suggest that the discharge from T-01 is 1.2% of the total discharge of all 21 outfalls in the nontidal TTF Creek.

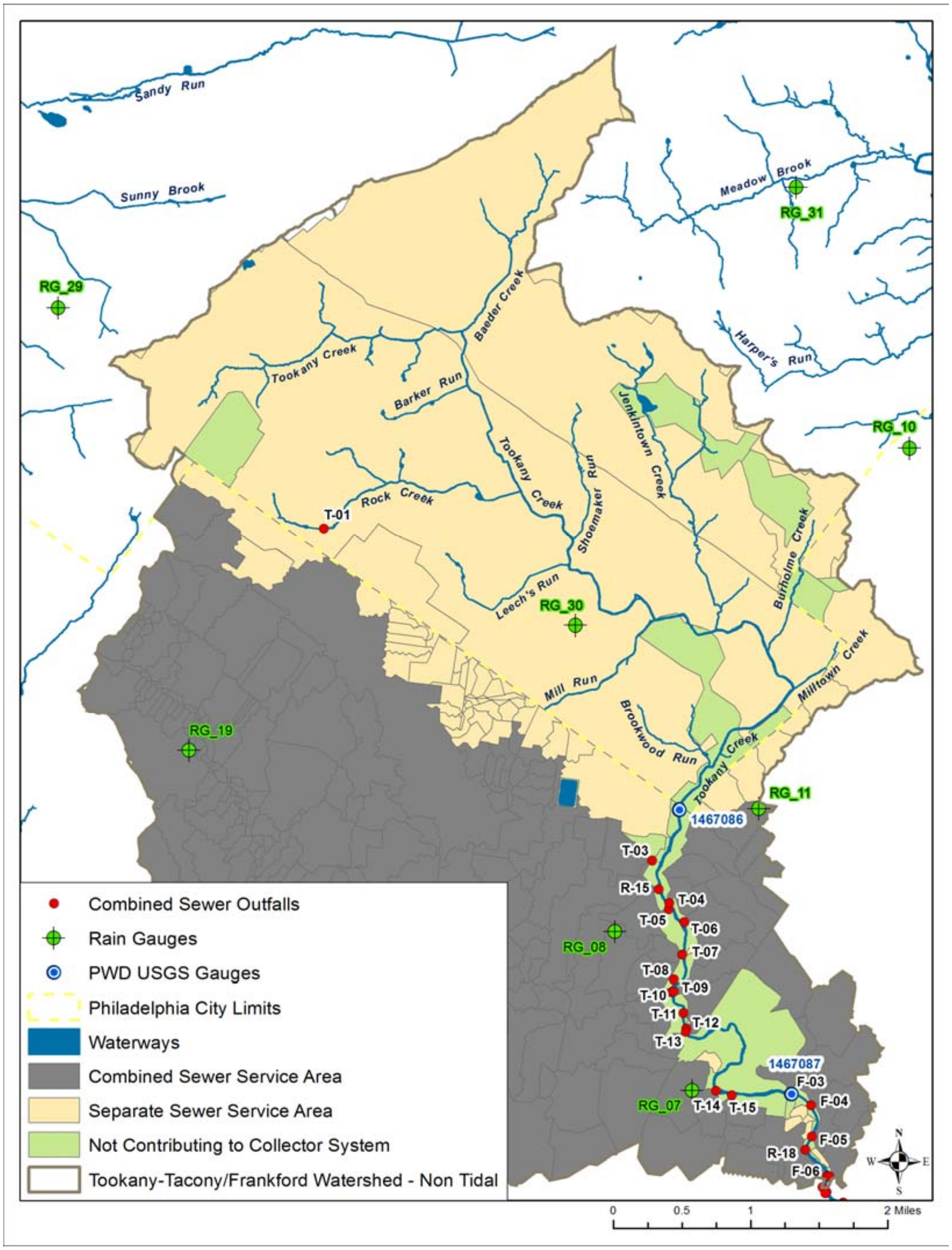

Figure 1-5: CSO Outfalls in the Nontidal TTF Creek Watershed

1.2 Cobbs Creek Dissolved Oxygen Model Extent

The Cobbs Creek dissolved oxygen model (or Cobbs DO Model) explicitly simulates in-stream DO conditions in the nontidal reaches of the Cobbs, East Indian, and West Indian Creeks , that receive City CSO discharges. In the Cobbs DO Model extent, there are 30 outfalls that release combined stormwater and sanitary wastewater during storms that exceed the capacity of the interceptors in the Southwest Water Pollution Control drainage district (Figure 1-6). During a typical year of precipitation, as described in the LTCPU Supplemental Documentation Volume 4 (Philadelphia Water Department, 2011), the outfalls in the Cobbs DO Model extent discharge a total annual volume in excess of 700 million gallons of combined stormwater and sanitary wastewater.

The Cobbs DO Model extends upstream on the mainstem Cobbs Creek from the head of tidal influence near Woodland Avenue crossing, to the USGS Gage 01475530 located near the boundaries of Philadelphia and Delaware Counties at the Route 1 crossing, River Mile 7.70. The entire spans of the East and West Indian Creeks and Naylors Run were explicitly simulated to better capture their effects on DO in Cobbs Creek. The downstream boundary of the Cobbs DO Model is at River Mile 1.10, the Woodland Avenue dam, is taken here to be the head of tide. The Cobbs DO Model extent covers the entire nontidal zone of City discharge influence on the Cobbs, East Indian, and West Indian Creeks. The modeling of DO dynamics for the tidal reach of Cobbs Creek will be included in the June 1, 2015 deliverable for water quality models of tidal receiving waters.

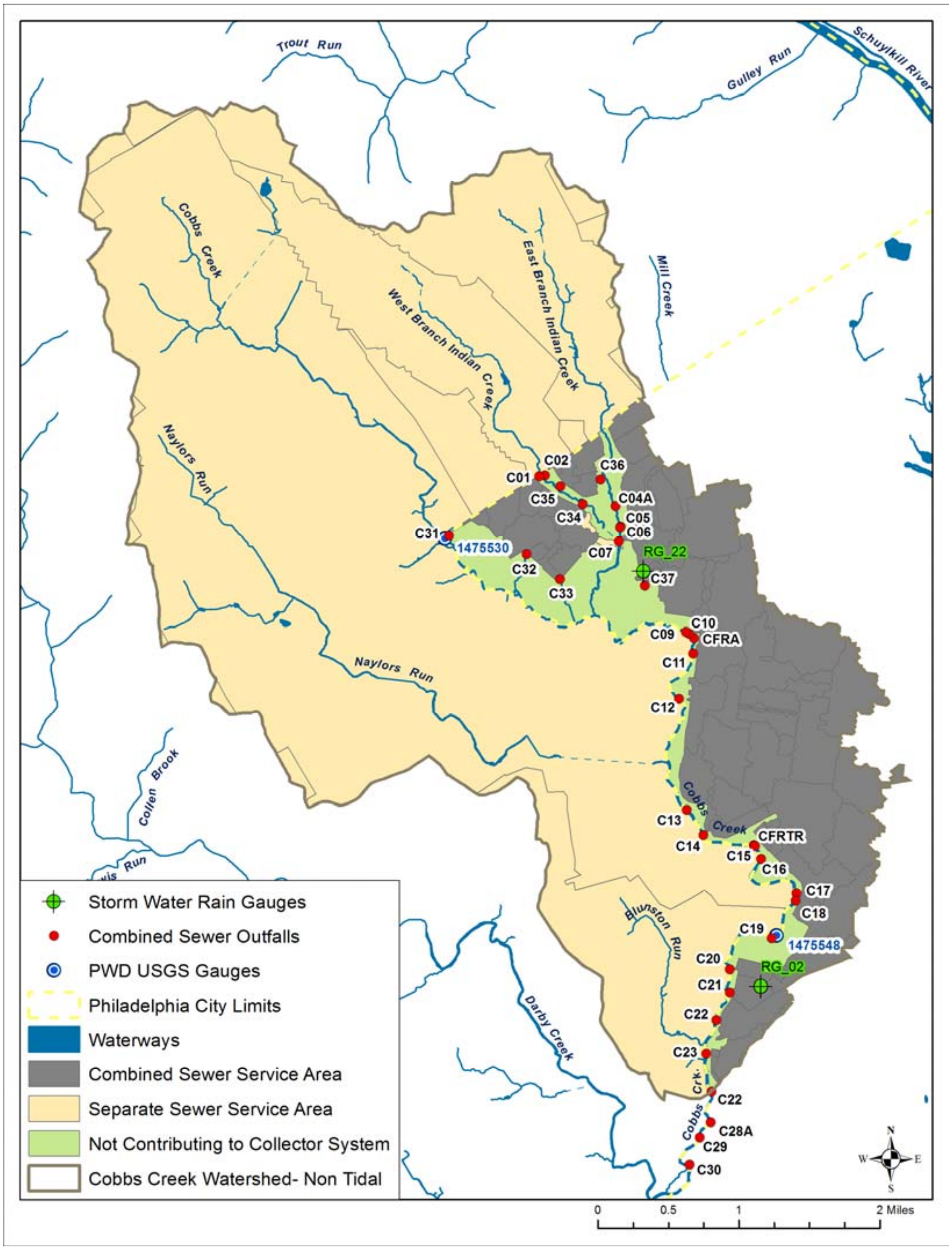

Figure 1-6: CSO Outfalls in the Nontidal Cobbs Creek Watershed

1.3 Model Objectives

The objectives of the model development were to represent existing DO conditions and underlying stream processes in the receiving waters through comparison of predicted and observed DO concentrations and benthic algal densities during past events. In particular, spring and summer benthic algal bloom conditions, and DO during wet weather were simulated. Chemical and algal sampling data were used to validate the model results for DO and benthic algal density to measurements including continuous DO monitoring, dry weather chemical data grab samples,wet weather chemical data collected via grab and automated samples, and benthic algal density, taxonomy and intracellular nutrient concentrations.

1.4 Modeling Approach

The COA requires the Water Department to develop a DO model appropriate for characterizing flow and dissolved oxygen quality concentrations in the receiving waters of the TTF and Cobbs Creeks.

Flow and pollutants can enter the receiving waters through:

- Overflows from sewer systems
- Runoff (direct and through stormwater collection systems)
- Secondary tributaries
- Baseflow (groundwater)

The Water Department Tributary Hydrologic and Hydraulic (H&H) Models were developed and validated to provide reasonable estimates of combined sewer overflows resulting from precipitation events, as described in the LTCPU Supplemental Documentation Volume 4 (Philadelphia Water Department, 2011). The H&H Models simulate and couple the sewer system, contributing watershed area, and open channel (*i.e.,* mainstem creek and tributaries). In recent years, these models were updated and re-developed from the original United States Environmental Protection Agency (US EPA) Storm Water Management Model Version 4 to the newer version 5 of that model (SWMM5). The SWMM5 application has the capability to simulate surface runoff pollutant loadings, in this case through assignment of pollutant concentrations directly to sanitary wastewater and to stormwater contributions. Stormwater and sanitary wastewater pollutants are carried through the collection system and discharge through the outfalls to the receiving waters during an overflow event. The Water Department Tributary H&H Models were used to generate pollutant loading time series from the collection systems, secondary tributaries, and baseflow to the receiving waters.

A one dimensional water quality model was considered appropriate for the receiving waters. A one-dimensional model does not take into account cross sectional differences in flow or concentration, but instead provides a uniform cross sectional average. The US EPA Water Quality Analysis Simulation Program (WASP) version 7.5 was selected to model eutrophication kinetics, with a linkage to the SWMM5 model. More detail on WASP is provided in Section 3.4.

Figure 1-7 presents a flow chart of the Water Department Water Quality Modeling approach, the major elements of which are described below.

The Tributary H&H Models included the following model domains:

- **Combined Sewer System (CSS) Models**. This model domain included:
    - The combined service area within the City borders, which drains to the Water Department Water Pollution Control Plants.
    - The sanitary portion of the separate sewered area, within and outside the City, which drains to the Water Department Water Pollution Control Plants. A simplified version of the sanitary collection system is modeled inside the City, and indirectly modeled outside the City.
    - The combined sewer overflow (CSO) and interceptor relief outfall pipes within the City, which discharge into receiving waters.
- **Watershed Models.** This model domain included:
    - Open channel representations of the receiving waters and major tributaries within the watershed.
    - The stormwater and direct runoff areas within and outside of the City borders. Stormwater collection system conduits are not explicitly modeled.

Models developed previously for these streams under the State of Pennsylvania the Act 167 Stormwater Management Plan process served as the starting point for the water quality model development. The Act 167 Models were created by merging the CSS Models with the Watershed Models, and hydraulically connecting the CSS Models' CSO outfall conduits to the Watershed Models' receiving waters. The resulting models after updates and modifications to incorporate better information on stream morphometry and water quality capabilities are the Tributary H&H Models.

The predicted flows, loads, and in-stream velocities and depths from the Tributary H&H Models drive the Tributary Water Quality Models for DO. Additional details about these modeling elements are provided throughout this report.

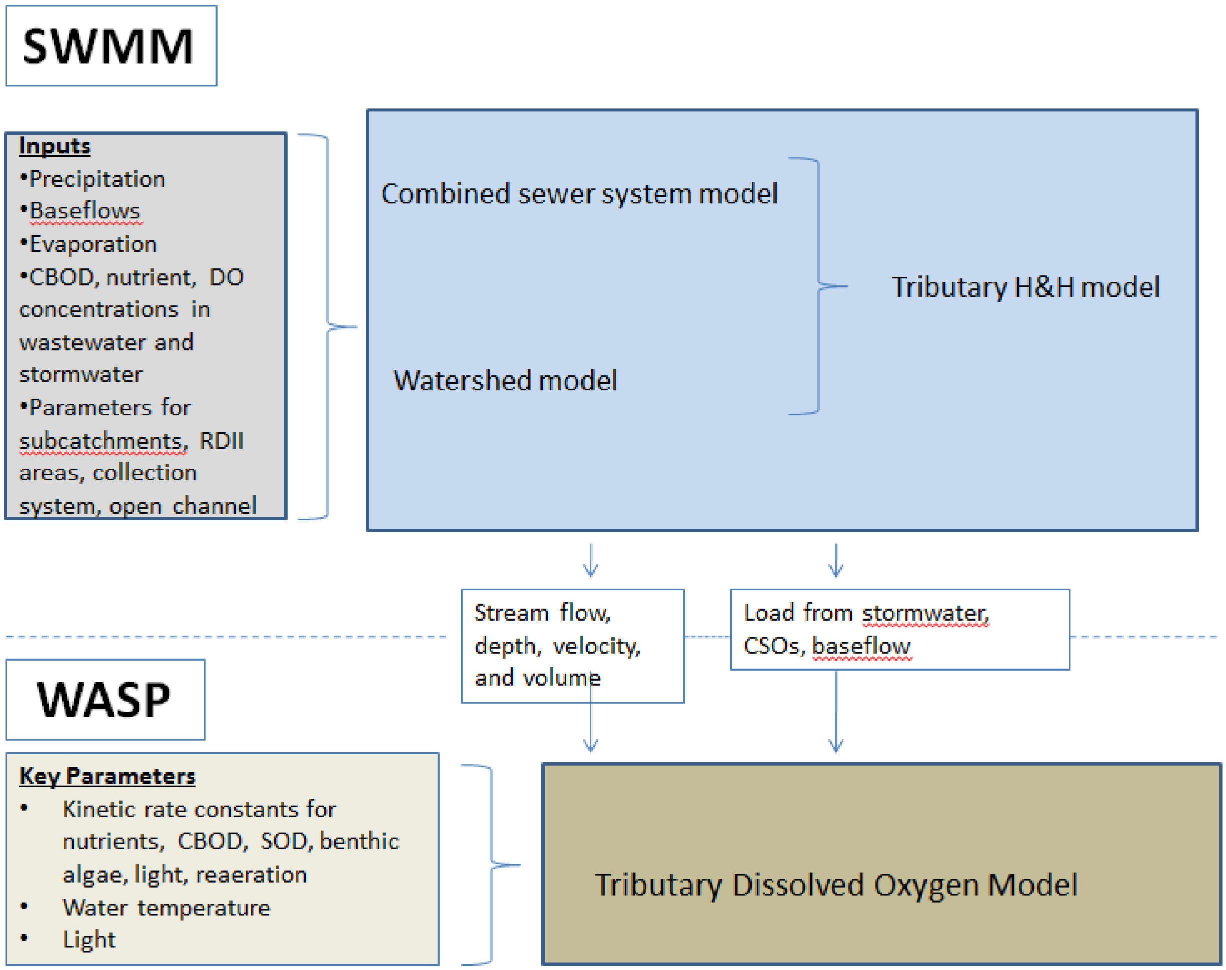

Figure 1-7: Modeling Approach for DO in Tributaries

2.0 Tributary Hydrologic & Hydraulic Models

Tributary Hydraulic & Hydrologic (H&H) Model Development

As described in Section 2.0 of this report, the Tributary H&H Models were developed by merging the combined sewer system (CSS) Models with the Watershed Models, and hydraulically connecting the CSS Models' combined sewer overflow (CSO) outfall conduits to the Watershed Models' receiving waters. The Tributary H&H Models were validated to streamflow at United States Geological Survey (USGS) gaging sites along the major tributaries.

The CSS Models were developed for each of the drainage districts contributing to the City's three Water Pollution Control Plants. The Northeast and Southwest District CSS Models were integrated into the Tookany/Tacony-Frankford (TTF) Creek and Cobbs Creek Watershed Models independently. The CSS Models were originally developed for the Long Term Control Plan (Philadelphia Water Department, 1997). Additional refinement of the CSS Models occurred as part of the Long Term Control Plan Update (LTCPU) (Philadelphia Water Department, 2009). CSS Model development and validation methodology are discussed in the LTCPU Supplemental Documentation Volume 4 (Philadelphia Water Department, 2011). Additional refinements were made to the CSS Models for Dissolved Oxygen (DO) modeling considerations. The models were refined to reflect the most recent system information and model development, and to perform water quality routing within hydrologic and hydraulic flow routing through the combined and sanitary sewer area collection systems.

The Watershed Models were also developed in Storm Water Management Model Version 5 (SWMM5) and underwent additional refinements for DO modeling applications. These models included the open channel representations of the receiving waters and major tributaries within the watersheds, and the stormwater and direct runoff areas within and outside of the City borders. These runoff areas were primarily comprised of the neighboring communities north and west of the City of Philadelphia (City). These areas contributed runoff flows and associated pollutant loads to the receiving waters either through storm water collection systems, direct runoff, or through minor tributary waterways.

These Tributary H&H Model refinements are explained in further detail in Section 2.1 of this report.

Radar Rainfall

For wet weather simulations, the refined CSS Models, Watershed Models and resultant Tributary H&H Models were driven by radar-corrected precipitation from a spatially variable rainfall record obtained under contract with Vieux & Associates, Inc. The radar grid was calibrated to the existing Water Department rain gage network, consisting of 24 gages within the City limits. Precipitation for each model subcatchment was calculated by area weighting 1 km^2 radar grids intersecting the individual subcatchment boundaries.

In-Stream Baseflow Separation

Stream baseflow was loaded into the Tributary H&H Models as a flow time series derived from USGS stream discharge data. Since TTF and Cobbs Creeks exhibit rapid runoff response to rainfall and snowmelt, and depleted baseflow conditions during dry weather conditions, an accurate representation of baseflow during low flow periods was necessary to simulate DO during the validation periods, and to reflect seasonable variability.

A sensitivity analysis of the influence of baseflow on dissolved oxygen in the stream channel was performed to determine the necessary level of detail to reliably represent in-stream DO conditions during the critical summer months. Results of the sensitivity analysis suggested a need to represent baseflow in the Watershed Models with a greater spatial and temporal resolution than that provided by a monthly average. Therefore, baseflow separation was performed on flow data available for the streams at an hourly time step. Streamflow data obtained at four USGS gages was used for the baseflow separation analysis. Two gages located on each tributary were used for the analysis. The upstream gage above Adams Ave (01467086) and the downstream gage at Castor Ave (01467087) were used for TTF Creek (Figure 1-5), and the upstream gage at Route 1 (01475530) and the downstream gage at Mt. Moriah Cemetery (01475548) were used for Cobbs Creek (Figure 1-6). The 15-minute streamflow record at each gage was smoothed and reduced to an hourly data time series. The Lyne and Hollick equation (Lyne and Hollick, 1979; Lim *et al.*, 2005) was then used to filter the hourly streamflow data and return a low frequency time series. Since the high frequency represents wet weather response, the resulting filtered low frequency time series represents streamflow at baseflow conditions (Eckhardt, 2005).

Once the hourly baseflows were estimated for each gage, the time series were loaded into the Watershed Model as area-weighted hourly inflow time series at nodes along the stream channel. The watershed areas between the USGS gages were assigned area-weighted baseflow time series that were the difference between the baseflow at the upstream and downstream gages, offset by an estimate of the low flow time of travel between the gages. Watershed areas below the most downstream gages were assigned area-weighted baseflow time series derived from streamflow at the downstream gage. Since the streamflow boundary condition at the most upstream node of the Watershed Model is the streamflow at the upstream USGS gage, it was not necessary to load the baseflow of the upstream gage independently.

Time-varying baseflow was used in the Watershed Models with the intent of improving the simulated estimate of flow, velocity and depth at baseflow conditions, and thus better simulating the impacts of processes including reaeration rates and sediment oxygen demand. This method would allow for a more accurate representation of dissolved oxygen during periods of low flow between storms and seasonally lower baseflow during dry months.

The range of baseflow at the downstream USGS gage simulated on each tributary is listed in Table 2-1 for each validation period.

Table 2-1: Baseflow Ranges for DO Model Validation Periods

Tributary	Validation Period	Dates	Base flow Range (CFS)
TTF	T-1	8/18 – 8/20/2009	13.6 – 14.1
TTF	T-2	9/1 – 9/5/2009	12.0 – 14.0
TTF	T-3	6/20 – 6/30/2011	9.2 – 11.0
TTF	T-4	7/16 – 7/25/2011	7.2 – 8.0
TTF	T-5	3/10 – 3/30/2012	11.8 – 18.4
Cobbs	C-1	7/27 – 8/7/2010	7.8 – 10.3
Cobbs	C-2	4/20 – 4/30/2012	9.9 – 12.0
Cobbs	C-3	7/23 – 7/29/2012	6.0 – 10.7
Cobbs	C-4	9/9 – 9/17/2012	6.0 – 8.1

2.1 H&H Model Refinements

Refinements of previous versions of the CSS Models and Watershed Models were implemented in developing the Tributary H&H Models. These refinements were implemented for DO modeling considerations, primarily impacting runoff characteristics, pollutant loadings, and representations of in-stream reaeration processes.

Combined Sewer System Model Domain

Numerous refinements were made to the CSS Models used for this DO modeling effort. Global refinements were made to all CSO sewersheds based on updated system information, and included refinements to the following hydrologic parameters:

- Shed area
- Gross percentage imperviousness
- Average overland slope

Another global refinement to the hydrology included switching runoff methodology. The PERVIOUS routing method was selected, so that a percentage of the impervious runoff was directed to the conveyance system, while the remainder was directed onto the catchment's pervious area. The PERVIOUS routing method allowed for complex hydrographs to be reproduced since directly connected impervious area (DCIA) results in immediate system response to precipitation, while the pervious area runoff may have a slower response.

Individual sewersheds were further refined based on validations to extensive trunk flow monitoring data coupled with the adoption of radar rainfall data used to drive the models. The trunk monitoring data used in this validation were primarily collected between years 2009 to 2011. The primary hydrologic parameters refined in this model validation included:

- Percent impervious area routed to pervious area
- Impervious depression storage
- Saturated hydraulic conductivity

Within this report, sewersheds that were monitored and validated to the trunk flow monitoring data will be referred to as Monitored CSO Sheds, whereas the other sewersheds will be referred to as Unmonitored CSO Sheds. Through the validation effort individual validation parameter values were determined for each Monitored CSO Shed. The average validation parameter values, weighted by a site grade, from the Monitored CSO Sheds were applied to the Unmonitored CSO Sheds.

Watershed Model Domain

As described in Section 3.1 of this report, within WASP 7.5 reaeration rates were calculated from simulated in-stream velocity and depth for each segment and time step. In order to better account for reaeration, particularly in dry weather flow periods, refinements were made to the in-stream hydraulic model representation. Refinements were made to the geometry of dams and a subset of bridges that act as hydraulic restrictions. Also, refinements were made to the slope, geometry, and roughness of natural and manmade stream channel sections.

Similar to the CSS Models, global hydrologic refinements were made to the Watershed Models based on updated system information.

Tributary H&H Model Validation

Tributary H&H Models were validated to streamflow at USGS gaging sites along the major tributaries primarily by refining hydrologic parameters for subcatchments within the Watershed domain, or by refining hydrologic parameters for the subset of Unmonitored CSO Sheds within the CSS modeling domain.

The same subset of hydrologic parameters refined in the CSS Model Validation was refined in the Tributary H&H Model Validation:

- Percent impervious area routed to pervious area
- Impervious depression storage
- Saturated hydraulic conductivity

The predicted flows, loads, and in-stream velocities and depths from the validated Tributary H&H Models drive the Tributary Water Quality Models for Dissolved Oxygen as described in Section 3 of this report.

3.0 Dissolved Oxygen Model

3.1 Dissolved Oxygen in Urban Streams: Summary of Key Processes

Pollutants enter the Tookany/Tacony-Frankford (TTF) and Cobbs Creeks primarily via stormwater runoff, combined sewer overflow discharges, and tributaries. Neither waterbody receives discharge from any wastewater treatment plants. The key processes which affect dissolved oxygen (DO) in the TTF and Cobbs Creeks are described below.

3.1.1 Algae

Stream metabolism is a measure of the basic ecosystem processes of primary productivity and community respiration. Primary productivity measures the total energy fixed by plants in a community by photosynthesis, and community respiration quantifies the use of reduced chemical energy by autotrophs as well as heterotrophs (Odum, 1956). Benthic algae are important primary producers in aquatic systems and are often the greatest source of energy in shallow mid-order streams with less than complete tree canopy.

Benthic algae comprise submerged plants that grow attached to rock and cobble on the stream bed. They require stable attachment points within the photic zone and hence do not occur where the bed is mobile sand or in deep, turbid water where light levels are < ~1% of incident. In shallow cobble bed rivers they can occupy the entire channel width (Rutherford and Cuddy, 2005).

Algae attached to the stream bed strongly influence water quality, notably by causing diel variations in DO concentration and pH. When actively growing they remove soluble nutrients from the water column (notably nitrogen, phosphorus and dissolved organic carbon). However, when senescent they release soluble nutrients, and when disturbed and detached by high stream flows, they contribute to particulate nutrient concentrations in the water column.

Continuous water quality data collected at some of the sites in sites in TTF and Cobbs Creeks indicate that the range of diel fluctuations in DO and pH can be reduced in magnitude in the aftermath of larger storms (*e.g.*, Figure 3-51). While some of this effect is due to reduced insolation, scouring and flushing effects of high flows are assumed to have reduced periphyton algal biomass, thereby decreasing production of oxygen via photosynthesis. Daily maximum DO concentrations and range of diel fluctuations subsequently returned to pre-flow conditions rather quickly, often within about three days. This phenomenon is assumed to be a result due to accrual of algal biomass following scouring events. As TTF and Cobbs Creek Watersheds have not been found to have large dry weather concentrations of chlorophyll in the water column that would be indicative of suspended phytoplankton, it was hypothesized that these pronounced fluctuations were due largely to periphytic algae (Philadelphia Water Department, 2004 and 2005).

Benthic algal biomass is affected by flow (*e.g.*, shear, scour, abrasion and mass transfer), light, nutrients (*e.g.*, mass transfer, uptake and release) and grazers.

With respect to flow, the disturbance regime has been found by some researchers (Uehlinger *et al.*, 1996; Biggs, 2000) to be more significant than nutrients and light in predicting biomass. In urban streams like TTF and Cobbs Creeks, discharge during storms can rapidly increase by 10-100 times above baseflow. The number of days of accrual, *i.e.*, the duration since the previous disturbance, is a major factor in determining the potential for algal blooms.

In a study of the Jackson River in Virginia, Flinders and Hart (2009) found the relationship between velocity and chl-a is nonlinear. Bott and Newbold (2000) suggested that a formula for scour is not universal and is dependent on velocity, algal type, and local conditions. A velocity-periphyton relationship developed by the Philadelphia Academy of Natural Sciences (ANS) in artificial streamside channels was used to relate the effect of stream velocity changes on periphyton scouring for the Jackson River TMDL (Louis Berger Group, 2010). Other studies have related scour to bottom shear stress (*e.g.*, Cronin *et al.*, 2007).

In terms of light, Davis (2002) studied photosynthetic rates of periphyton in shallow streams in southeastern Pennsylvania, and found that available light and nutrient flux are key factors. Available light was calculated by adjusting the incident solar irradiation for riparian shading factors such as vegetation height on streambanks, shading, stream width, elevation angle of the sun, and stream orientation relative to the North-South direction.

The relationship between nutrients and algal biomass is complicated by numerous factors, and findings are not consistent across ecoregions and water body types. Typically, nutrient enrichment stimulates periphyton growth in lotic systems and many studies have shown strong relationships between nutrient concentrations and algal biomass (*e.g.*, Jones *et al.*, 1984; Welch *et al.*, 1988; Kjeldsen, 1994; Chetelat *et al.*, 1999; Francouer, 2001). However, other studies have shown no relationship between biomass and nutrient concentration (Biggs and Close, 1989; Lohman *et al.*, 1992).

Light and temperature can affect nutrient uptake rates (*e.g.*, Faulkner *et al.*, 1980; Wynne and Rhee, 1988), and more nutrients are often needed when light and temperature conditions are less than ideal (Goldman, 1979; Rhee and Gotham, 1981a,b; Wynne and Rhee, 1986; van Donk and Kilham, 1990). Additionally, nutrient uptake rates can vary depending on nutrient conditions. In steady-state growth conditions, the rate of nutrient uptake is equivalent to the rate at which nutrients are used in growth. However, cells may take up fewer or greater amounts of nutrients (for example, during nutrient pulses) and alter the nutrient ratios within the cell (Borchardt, 1996).

Water Department studies (2004 and 2005) of the TTF and Cobbs Creek Watersheds have concluded that in both systems, phosphorus is the limiting nutrient. Overall, the most important factors shaping algal communities in TTF Creek and Cobbs Creek Watersheds are nutrient availability, substrate particle size, current velocity, and the frequency of flow disturbances that cause scour.

3.1.2 BOD

The decomposition of carbonaceous matter exerts an oxygen demand in the stream, and is referred to as carbonaceous biochemical oxygen demand (CBOD). The oxygen demand due to nitrification is termed nitrogenous biochemical oxygen demand (NBOD) (Chapra, 1997).

Sources of CBOD and NBOD in TTF and Cobbs Creeks include stormwater runoff, sanitary wastewater associated with combined sewer overflow (CSO) events, baseflow, and decomposition of detrital matter in the stream. CBOD decay and nitrification are typically modeled as first-order kinetic processes. However, a second-order CBOD decay rate was found necessary to explain rapid transient decreases in DO during CSO events in the Indianapolis Long Term Control Plan model (CDM, 2004).

Large, transient decreases in DO have also been observed in TTF and Cobbs Creeks during certain CSO events, particularly low volume CSO events in which the dilution of wastewater by stormwater is thought to be less than in a high volume event (*e.g.*, Figure 3-34). CBOD appears to be a major sink for DO in these cases.

3.1.3 SOD

Sediment oxygen demand (SOD) is the sum of two separate oxygen consuming processes: 1) biochemical oxidation of settled organic matter, and 2) the chemical oxidation of reduced chemical species (*e.g.*, HS^-, Fe^{2+}, Mn^{2+}) (Giga, 1985). In freshwater sediments, where nitrogen and carbon redox species generally dominate sulfates and other redox species, the chemical oxidation of reduced chemical species is a minor contributor to SOD (Hantush, 2007). Thus, the deposition of organic matter is most often the primary source of SOD in freshwater sediments. These organic deposits derive from several sources. Dead algal and plant biomass, wastewater particulates, leaf litter and eroded organic-rich soils can result in sediments with high organic content. Oxidation of settled organic matter, regardless of the source, results in SOD (Chapra, 1997).

Typical SOD values range from 0.2 $g/m^2/d$ for sandy bottoms to 10 $g/m^2/d$ for organic-rich sediments (Thomann and Mueller, 1987). Sediments associated with severely polluted surface waters can have even higher SOD values. Despite the long standing awareness of the importance of SOD in DO dynamics, there remains no standard method of measuring SOD (Ziadat and Berdanier, 2004).

SOD is affected by physical, chemical, and biological factors, such as temperature, overlying water velocity, sediment roughness, sediment surface area, sediment particle distribution, sediment porosity and tortuosity, sediment organic content, and biological activity (Giga, 1985; Nakamura and Stefan, 1994; Hantush, 2007).

To measure SOD, *in situ* experiments use a benthic chamber (also referred to as chamber respirometer or bell jar) while lab experiments use sediment cores sampled from the site. Both methods are limited by the potential for sediment disturbance and resuspension, and neglecting the effect of streamflow on SOD. *In situ* experiments are limited by the difficulty in many stream bottoms of completely sealing off the chamber from the surrounding water column. Each approach inevitably alters the natural environment of the sediment.

Miskewitz *et al.* (2010) attempted to improve upon benthic chamber and lab methods for measuring SOD. Their "profile method" for measuring SOD is based upon a characterization of the flow in the near sediment boundary layer and the transport of dissolved oxygen down a concentration gradient. The main advantage this method has over lab and chamber methods is the ability to measure the SOD flux as a function of the flow in its natural environment. Compared to the chamber method, the measurement time is reduced from 2 hours to between 10 and 30 minutes. The method calculates the SOD flux as the product of a turbulent diffusion coefficient, *i.e.*, the eddy viscosity, and the vertical gradient of DO (Miskewitz *et al.* 2010). Eddy viscosity is derived from Elder (1959) where friction velocity is determined by taking the square root of the covariance of the turbulent fluctuations in the vertical and horizontal velocities measured by a Sontek acoustic doppler velocity profiler (ADV) operating at 10Hz. The vertical gradient of DO is measured through DO sensors placed at varying depths above the sediment. The ADV and DO sensors are mounted on a rack structure that allows for minimal disturbance to the sediment and the flow during measurement (Figure 3-1). As described further in Section 3.2, Dr. Miskewitz was contracted to apply the profile method to measure SOD in various locations in TTF and Cobbs Creeks.

Figure 3-1: SOD Sampling Apparatus for Profile Method. Three DO probes are positioned vertically on the right. The ADV sensor is on the left.

The classic SOD model assumes that SOD follows an empirical zero-order reaction rate parameter, *i.e.*, SOD is not limited by the concentration of organic matter or overlying dissolved oxygen (Hantush, 2007). However, more sophisticated alternatives to SOD modeling have been published that develop SOD relationships to organic matter deposition (*e.g.*, Di Toro *et al.*, 1990; Higashino *et al.*, 2004; Hantush, 2007).

A sediment diagenesis modeling approach was not considered for this project because in a small, flashy urban streams like TTF and Cobbs Creeks, scouring events occur on such a frequent basis, *e.g.*, weekly to monthly, that the benthic layer 'memory' described in Wool *et al.* (2003) does not have time to accumulate. An exception might be deep scour pools, but these are a small percent of the total water surface area in the model domain. Therefore the more conventional zero-order approach was chosen, based on site-specific data reported by Miskewitz (2011, 2012).

In TTF and Cobbs Creeks, water quality data collected during dry weather suggest that neither CBOD nor NBOD is problematic, even when low DO concentrations are present. These findings suggest that in dry weather, oxidation processes in the sediment are the primary cause of low DO concentrations. Furthermore, SOD is expected to increase with temperature according to an Arrhenius relationship; this is consistent with the low DO sometimes observed in warm months (*e.g.*, Figure 3-31).

3.1.4 Reaeration

Oxygen deficient, *i.e.*, below saturation, waters are replenished via atmospheric reaeration. The reaeration rate coefficient is a function of the average water velocity, depth, and temperature; wind effects can also be included (Wool *et al.*, 2003). Some methods also use channel slope to calculate the reaeration coefficient (Bowie *et al.*, 1985).

The Covar method (Covar, 1976), which estimates reaeration as a function of velocity and depth by one of three empirical formulas, is perhaps the most-often used approach in recent developments of water quality models. The three formulations are taken from the works of Owens *et al.* (1964), Churchill *et al.* (1962), or O'Connor and Dobbins (1958). The Covar method was selected for this application of the United States Environmental Protection Agency's (US EPA) Water Quality Analysis Simulation Program (WASP) 7.5. As described in Section 3.2, empirical formulas were found to underestimate measured reaeration rates by up to an order of magnitude in downstream reaches subjected to more channel alteration.

The presence of dams can significantly affect oxygen transfer in streams (Chapra, 1997). The empirical formula developed by Butts and Evans (1983) characterizes reaeration below dams and is available in the WASP eutrophication module. As listed in Tables 3-17 and 3-18, a total of five model segments in TTF and Cobbs Creeks were simulated with dam reaeration.

3.1.5 Modeling DO in Urban Streams

In the modeling context, DO is conceptualized as having the following sinks – algal respiration; microbial respiration of organic matter in the water column (CBOD) and sediment (SOD); and nitrification. DO sources include reaeration and algal photosynthesis. The following are examples of DO modeling approaches from the literature that pertain to urban rivers.

Chicago, IL

DO in the Chicago River was simulated on a long term scale using EUTROF2, a water quality model similar to WASP (Alp and Melching, 2006). The model ran at a 15 minute time step, using 36 segments to represent 76 stream miles. Nearly 200 CSOs were consolidated into 28 loading points. In lieu of a time series, a total CSO event load was estimated via an event mean concentration (EMC) approach derived from measurements at 3 pumping stations. Tributary loading was based on the long term average dry weather concentration and wet weather EMCs. The reaeration rate was calculated according to O'Connor and Dobbins (1958). The model utilized spatially variable rates for CBOD decay, nitrification, dispersion, and diffusive exchange. The SOD algorithm used an active sediment layer and diffusive area rate term; separate processes were simulated for the water column and pore water. Sediment depth and composition were surveyed to calibrate the SOD model.

The water quality model was calibrated for a 4 month period using monthly grab sample data at 18 locations and hourly DO concentration and temperature data at 25 locations. Historical sampling data were used to supplement the monthly grab sample data in calibrating biological oxygen demand (BOD), nutrients and phytoplankton.

Detroit, MI

DO in the Rouge River was modeled to investigate the potential benefit of CSO controls to CBOD-driven DO impairments in wet weather, and SOD-driven DO impairments in dry weather (Kluitenberg *et al.*, 1999). Hydrology and hydraulics were modeled with Storm Water Management Model (SWMM4), and linked to a one dimensional WASP model to simulate water quality on primarily an event scale. The WASP model spans 126 stream miles. Notably, SWMM4 river hydraulics were performed using the TRANSPORT block, using kinematic rather than dynamic wave routing. SOD was modeled as a zero-order rate process. For the evaluation of potential future control scenarios, the simulated SOD in the CSO area was reduced to approach that of *in situ* SOD measurements made in river reaches that were not CSO impacted.

Columbus, OH

DO was modeled as part of the Columbus, Ohio Long Term Control Plan (Smith and Hothem, 2006). The RUNOFF block of XP-SWMM was used to simulate watershed hydrology. The combined sewer system (CSS) area was simulated by the City's PCSWMM model. The TRANSPORT block of SWMM4.4 was used to model river hydrodynamics with kinematic wave routing, and linked to WASP to simulate water quality on event and long term scales. The WASP model was chosen in part because it can represent low-head dams, a key feature required for modeling the system. Phytoplankton, rather than benthic algae, was the primary algal assemblage affecting DO. The principal model validation parameters were source concentrations for CBOD, organic phosphorus, and orthophosphate; CBOD decay rate; dam reaeration variables; and algae growth rate. The SOD was not mentioned in the article cited. Continuous in-situ DO concentrations at 34 locations were used in the calibration, which spanned 6 wet weather events.

The authors critique WASP for having a global CBOD decay rate, and point out that "in one-dimensional applications, WASP averages the water quality parameters in the dam pools over the large stored volume; this dampened diel variations in the pools, but the diel swings returned once the flow left the pool." A similar phenomenon was observed in outfall scour pool segments in the TTF and Cobbs Creeks DO Models. However, the dampening of the diel swings in Water Department-modeled pools likely is due to greater light extinction and less algal biomass on an areal basis than in shallower neighboring segments without pools.

Indianapolis, IN

DO in the White River and its tributaries were modeled as part of the Indianapolis Long Term Control Plan (CDM, 2004). A total of 94 outfalls were included in the modeled CSO area of 37.4 square miles. Hydrology and hydraulics were modeled using the SWMM4 RUNOFF and EXTRAN blocks, and linked to a one dimensional WASP model to simulate water quality on an event scale. Water quality segments averaged 2 miles in length. A time varying BOD rate from CSOs was applied to mimic the first flush effect. The WASP code was modified to utilize a second order BOD decay rate during wet weather, in order to simulate the rapid transient decreases in DO during CSO events. Higher SOD rates were assigned just upstream of dams. Dam reaeration formulas were used. Stormwater runoff was represented by EMC values based on land use. DO concentrations in runoff were assumed to be 75% of saturation. Validation periods were split according to dry or wet weather. Predicted DO concentrations were compared to continuous in-situ DO measurements at 6 locations.

3.2 Summary of Available Data

3.2.1 TTF and Cobbs Creeks Comprehensive Characterization Reports

Extensive sampling and monitoring programs were conducted from 2000-2004 to inform development of the TTF Creek Watershed Comprehensive Characterization Report (CCR), and from 1999-2003 for the Cobbs Creek Watershed CCR. The programs included hydrologic, water quality, biological, habitat, and fluvial geomorphological aspects.

Water quality samples (*i.e.*, BOD, N and P series constituents) were collected in dry weather and wet weather conditions via grab samples and automated samplers (Isco, Inc.). During wet weather sampling, several discrete samples were collected just before and during the course of a wet weather event. Automated samplers were configured to collect samples throughout the wet weather event, at intervals ranging from 20 to 90 minutes. The data allowed characterization of water quality responses to stormwater runoff and CSOs.

The CCR data offered the main set of observations used to characterize dry and wet weather in-stream concentrations in TTF and Cobbs Creeks. Water quality data has also been collected quarterly since 2009 at each USGS gage site in TTF Creek (01467086 and 01467087) and Cobbs Creek (01475530 and 01475548). Along with quarterly data from the USGS gages, other water quality data collected in the TTF Creek and Cobbs Creek watersheds through separate monitoring programs were added to the CCR data set to enable a more complete analysis of water quality concentration statistics by season, weather condition and site.

Monitoring sites that were used in the TTF and Cobbs DO Models are mapped in Figures 3-2 and 3-3.

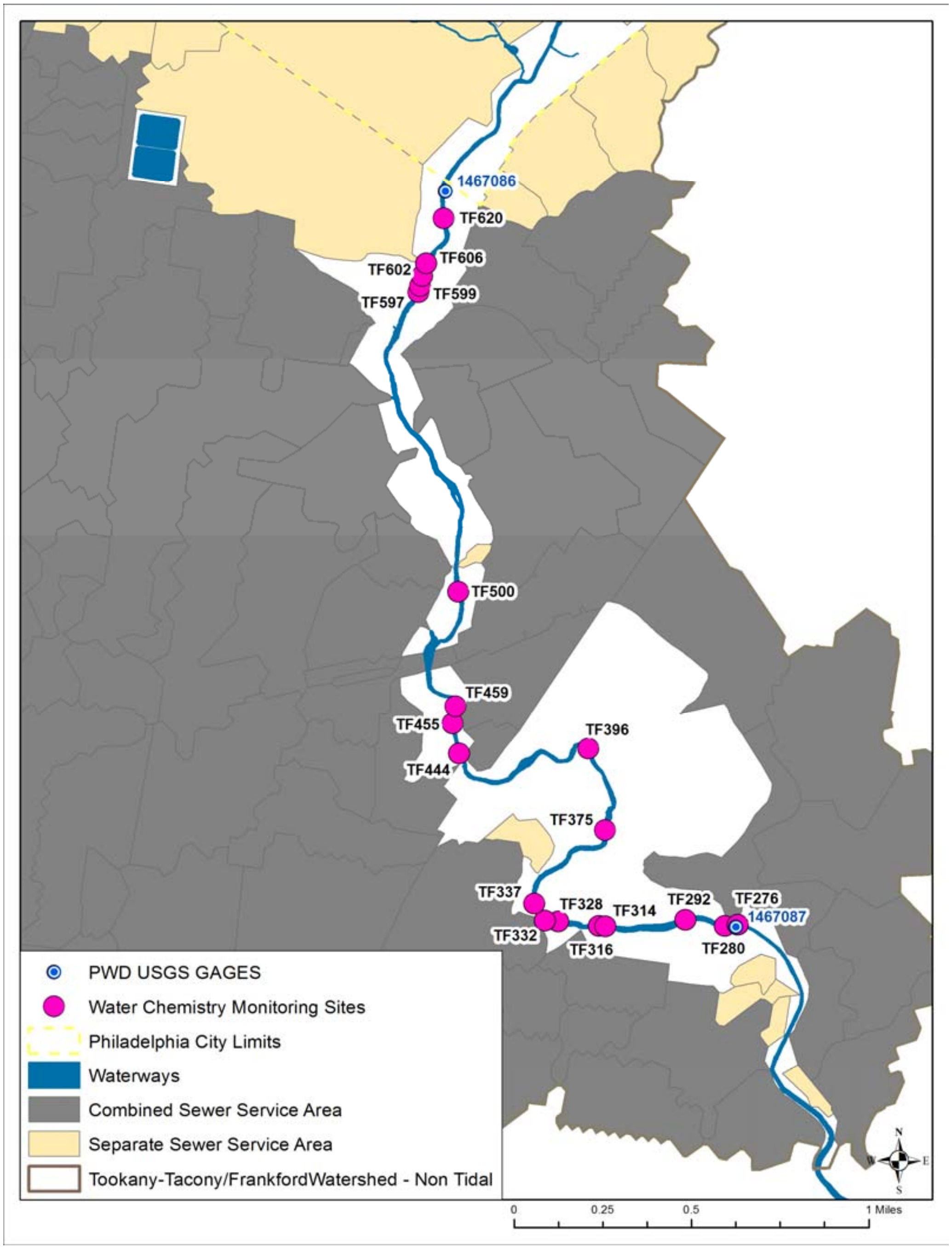

Figure 3-2: Water Chemistry Monitoring Sites in the Nontidal TTF Creek Watershed

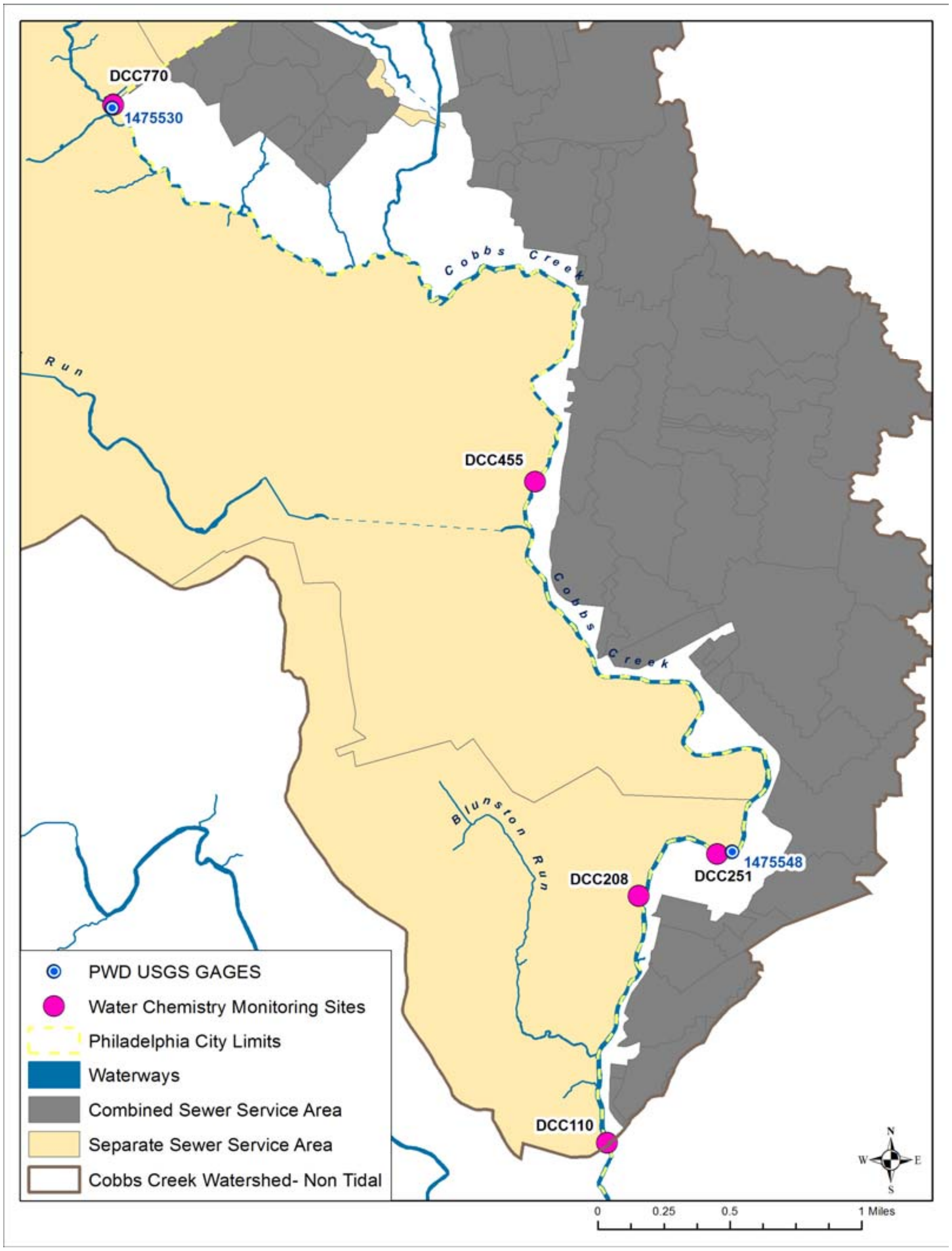

Figure 3-3: Water Chemistry Monitoring Sites in the Nontidal Cobbs Creek Watershed

3.2.2 Periphyton

Sampling of periphyton density, taxonomy and intracellular carbon, nitrogen, phosphorus, (CNP) ratios in TTF and Cobbs Creeks was conducted in 2011-2012 at two sites on each stream (Figures 3-7 and 3-8). (The upstream site on TTF Creek proved to be outside the DO Model extent). The intent was to capture the effect of scour and regrowth on the benthic algal community. The sampling program was designed to characterize benthic algal densities a day prior to and in the immediate days after a storm of sufficient discharge to cause scouring.

In June 2011, one storm in TTF Creek was studied that yielded the expected pattern of scour and regrowth; a study of another storm in July 2011 captured scour but did not extend long enough to observe regrowth (Figure 3-4). August to early September 2011 proved to be an extremely wet period. This disrupted the sampling design since the stream underwent a high frequency of disturbance; accrual was only observed in the last 2 samples of the dataset (Figure 3-5). It should be noted that Hurricane Irene and Tropical Storm Lee occurred in the latter part of this period.

The expected pattern of scour and regrowth was observed in three of the four 2012 study periods in Cobbs Creek (Figure 3-6).

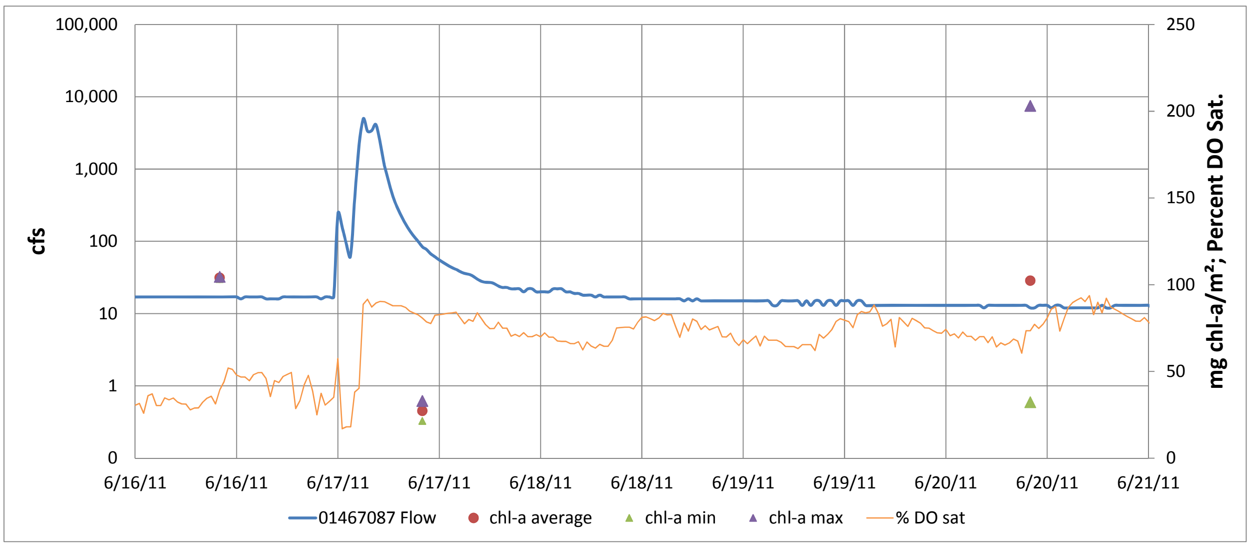

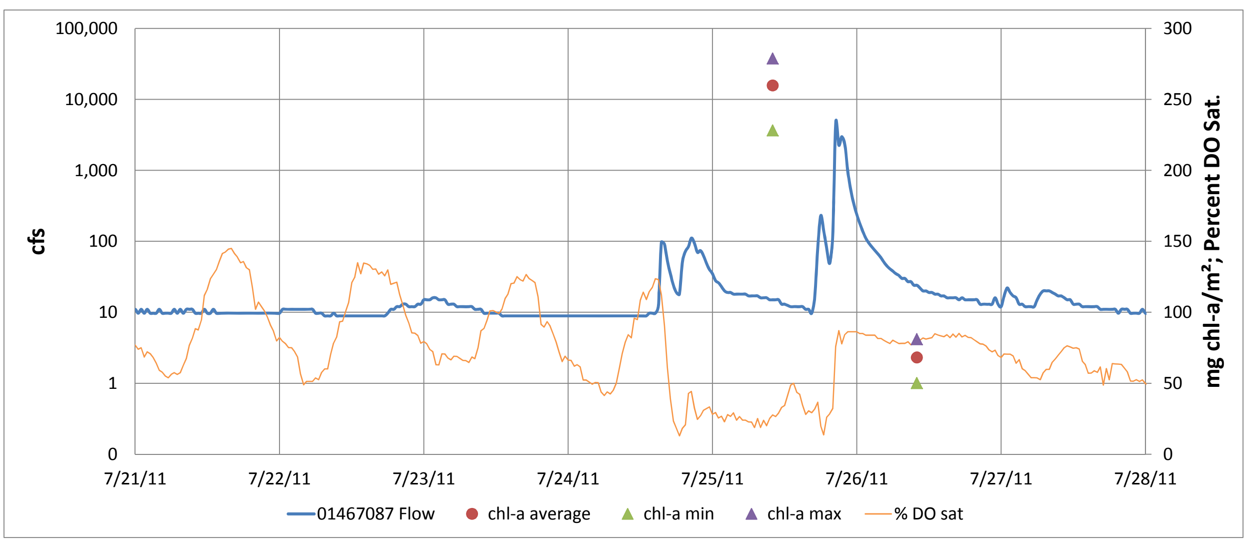

Figure 3-4: Benthic Algal Density and Streamflow in TTF Creek, June-July 2011

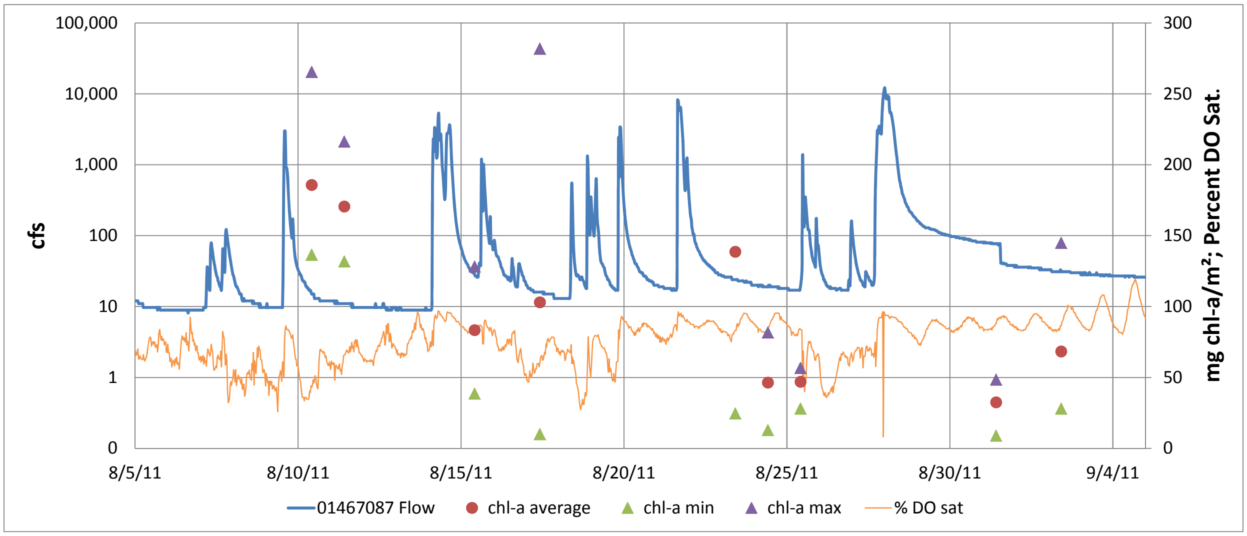

Figure 3-5: Benthic Algal Density and Streamflow in TTF Creek, August-September 2011

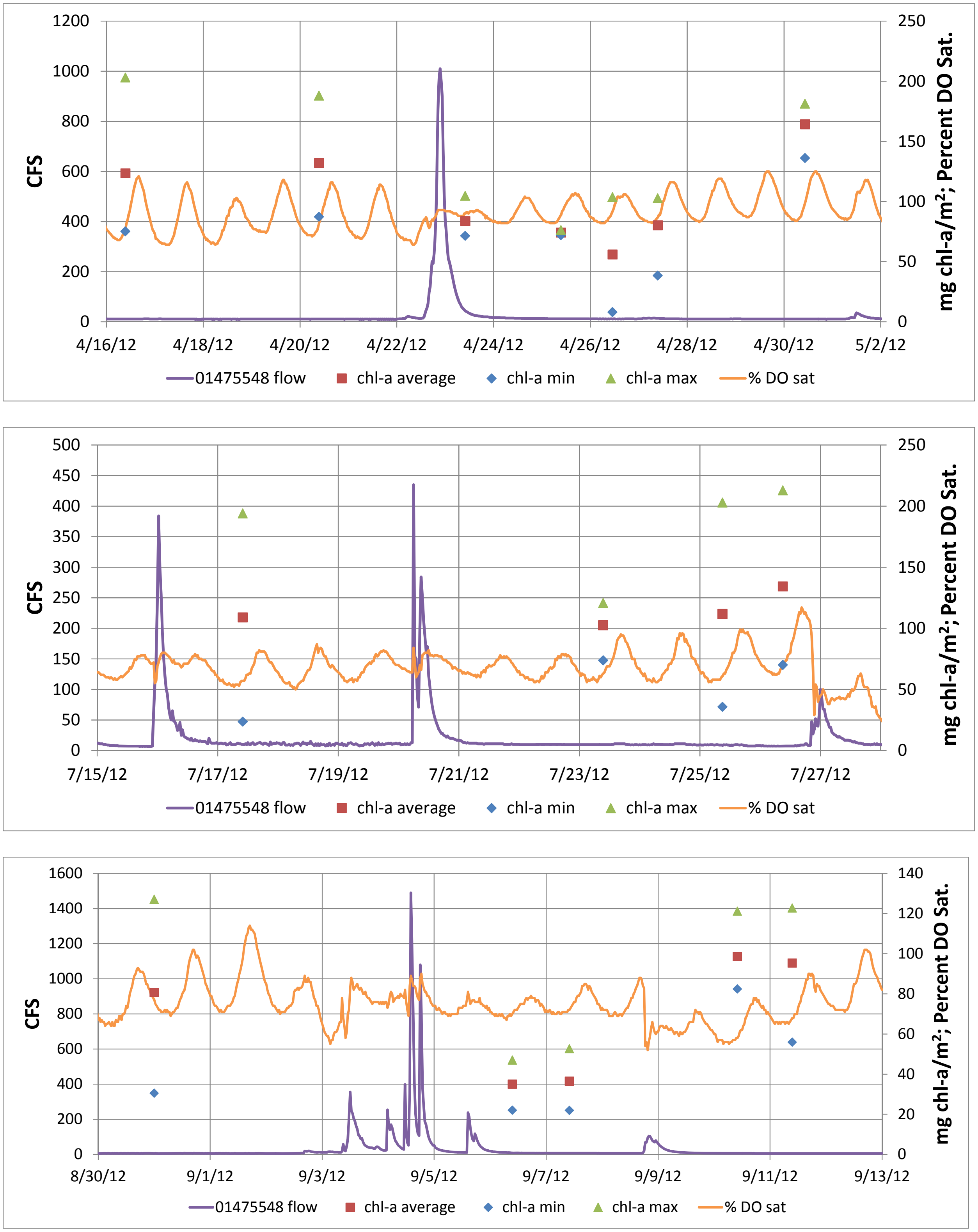

Figure 3-6: Benthic Algal Density and Streamflow in Cobbs Creek, April/July/September 2012.

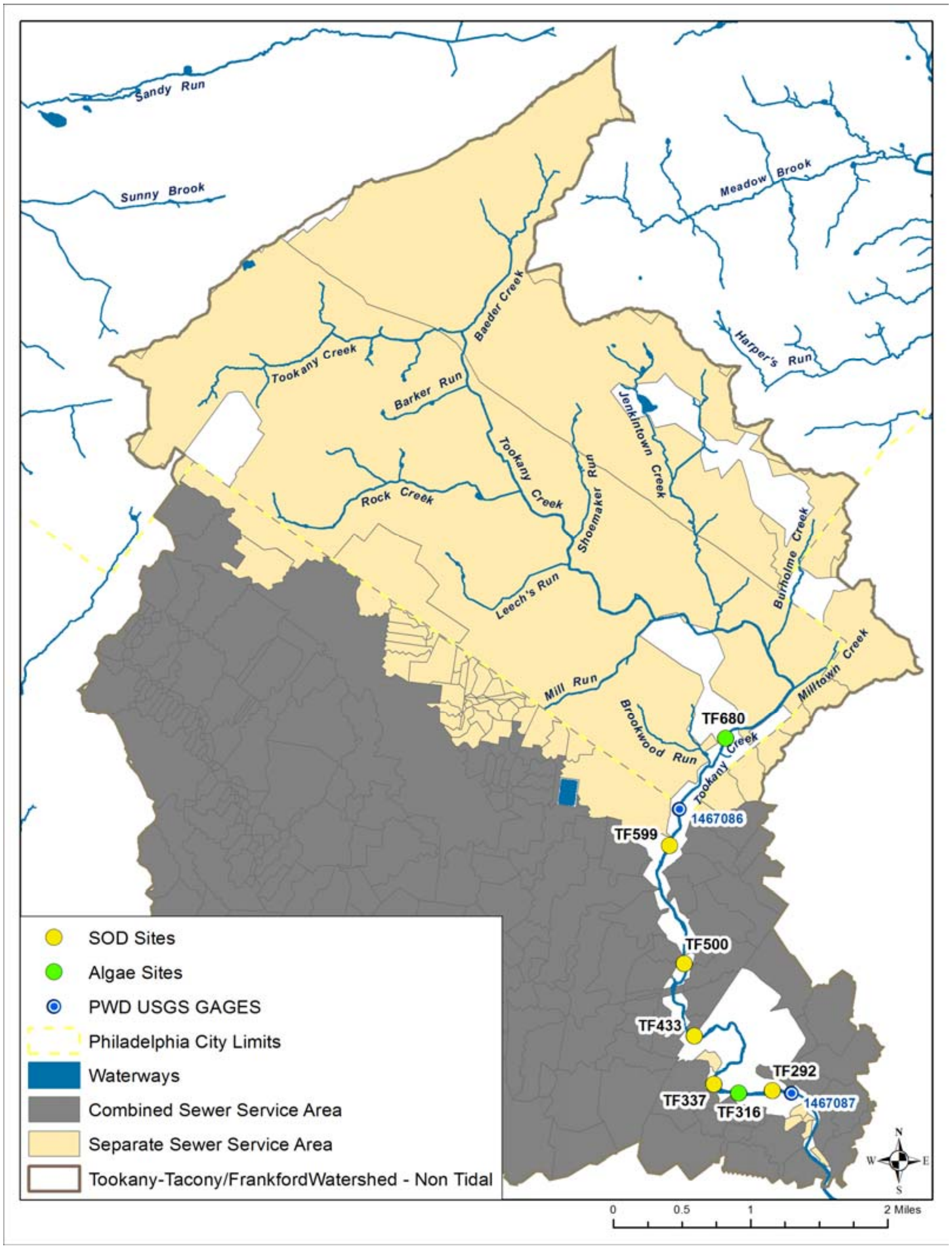

Figure 3-7: Periphyton and SOD Monitoring Sites in the Nontidal TTF Creek Watershed

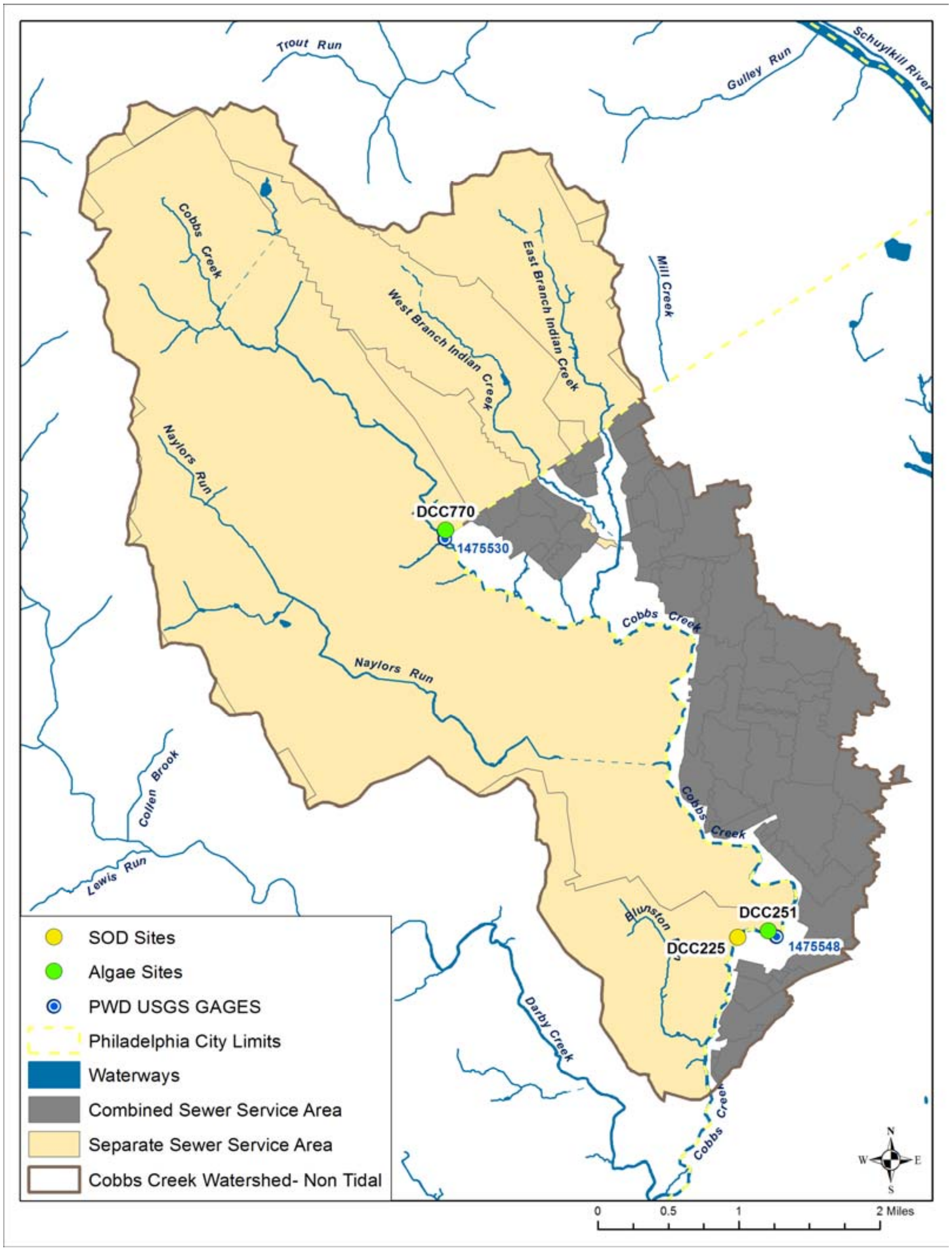

Figure 3-8: Periphyton and SOD Monitoring Sites in the Nontidal Cobbs Creek Watershed

A total of 40 periphyton samples were analyzed by the ANS for intracellular carbon, nitrogen, phosphorus, (CNP) ratios, and taxonomy. The Redfield ratio assumes 1000 mg Dry Weight: 400 mgC: 72 mgN: 10 mgP: 10 mg chl-a (Redfield *et al.*, 1963). The average stoichiometric ratio measured in TTF Creek was 1000 mg Dry Weight: 154 mgC: 20 mgN: 3 mgP: 14 mg chl-a. In Cobbs Creek, the measured ratio was 1000 mg Dry Weight: 142 mgC: 19 mgN: 4 mgP: 10 mg chl-a. Compared to the Redfield ratio, TTF and Cobbs Creeks samples had less than half as much carbon per dry weight; 30-50% greater C:N ratios; similar N:P ratio in TTF Creek, and

34% smaller N:P ratio in Cobbs Creek. Chl-a:carbon ratio was 22% smaller in Cobbs Creek than in TTF Creek samples. The taxonomy analysis found the greatest relative abundance (based on cell counts) of blue green algae and diatoms in TTF Creek, and blue green algae and chlorophytes in Cobbs Creek, respectively.

3.2.3 SOD

In collaboration with Dr. Robert Miskewitz of Rutgers University, the profile method (described in Section 3.1) was applied to gather SOD estimates in TTF and Cobbs Creeks in 2011-2012. The data reports from Dr. Miskewitz are attached in Appendix A. Data points were considered questionable if the uncertainty exceeded the mean flux, or if the velocity field as measured with the acoustic doppler velocimeter (ADV) indicated the assumption of a logarithmic boundary layer of fluid flow was not applicable. Overall, twenty measurements of SOD were considered acceptable data.

Results of SOD sampling, with SOD rates normalized to 20 degrees C, are presented in Figure 3-9. Overall, the distribution of SOD rates in TTF Creek meets expectations, in that the maximum rate of 17.3 $g/m^2/d$ was observed just upstream of the dam at TF292, and the minimum rate of 2.1 $g/m^2/d$ was observed at TF599, upstream of any CSO discharges into the mainstem. Unfortunately, in Cobbs Creek, only one of the three attempted sampling stations yielded quality data. At site DCC225 the average flux was 4.71 $g/m^2/d$.

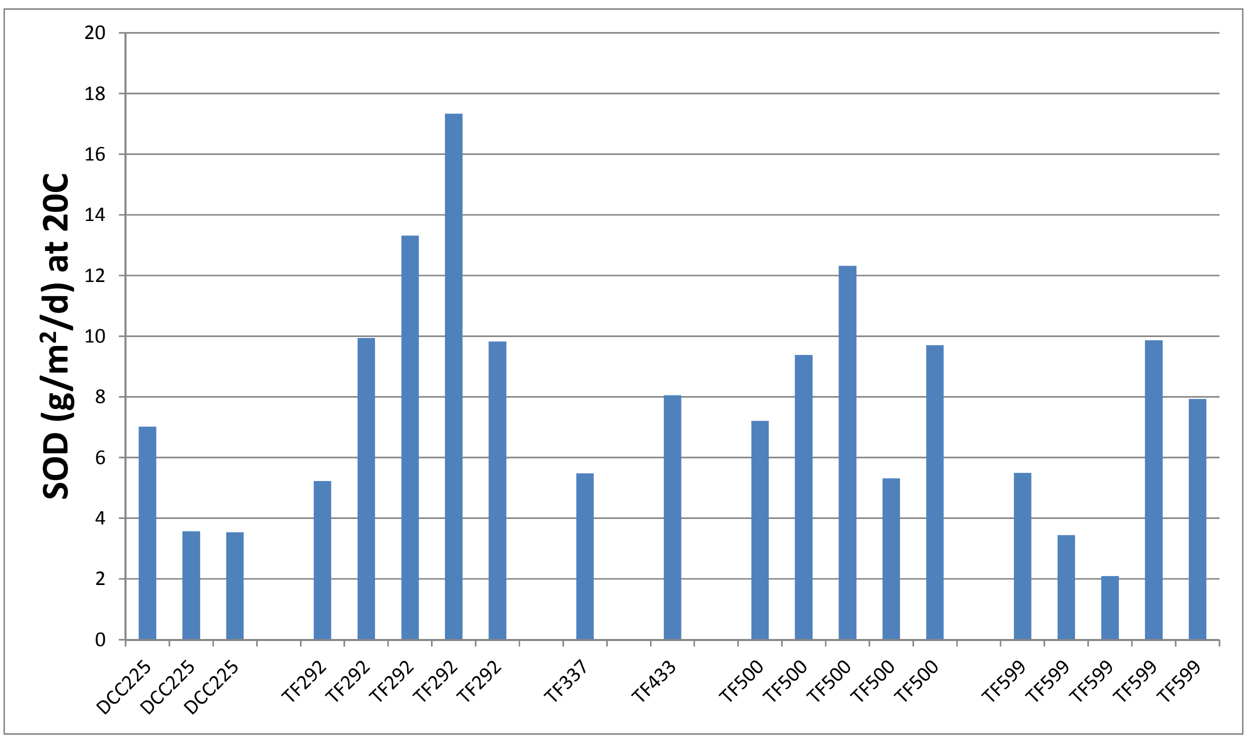

Figure 3-9: SOD Monitoring Results, 2011-2012 (n=20)

3.2.4 Reaeration

In 2009, USGS conducted a reaeration study in a 2 mile reach of TTF Creek, from just upstream of the T-8 outfall to the USGS gage 01467087 at Castor Avenue (Senior and Gyves, 2010) (Figures 3-10 and 3-11). Oxygen reaeration coefficients determined by a constant rate injection method using propane as the tracer gas were as low as 1.03/day at the impoundment behind the Juniata Golf Course dam (TF292). The highest reaeration coefficient was 55.04/day for a steep-gradient riffle reach between TF316 and the T14 CSO scour pool 0.12 miles upstream (TF328).

Reaeration coefficients determined from the field tracer-gas method were compared to values calculated by two other methods, one that is based on theoretical equations (Owens *et al.*, 1964; Tsivoglou and Neal, 1976) using physical properties (*e.g.*, velocity, depth, slope) of the stream as variables, and the other that is based on equations using the timing of measured daily maximum DO concentrations in the stream (McBride, 2002). Reaeration coefficients from the two alternate methods were most similar to values determined from the field tracer-gas method for the upstream portion of the study reach (sites TF375 to TF337), characterized by free-flowing riffle and pools. For the downstream portion of the study reach (Sites TF328 through TF280; T-14 scour pool to Castor Avenue) where sub-reaches have been more hydraulically affected by man-made structures than in the upstream portion, reaeration coefficients determined by the tracer-gas method were 2 to 10 times higher than coefficients determined by the two alternate methods (Table 3-1).

Figure 3-10: Dye Injection and Propane Gas Diffusion on September 3, 2009 in TTF Creek near US Route 1 (from Senior and Gyves, 2010)

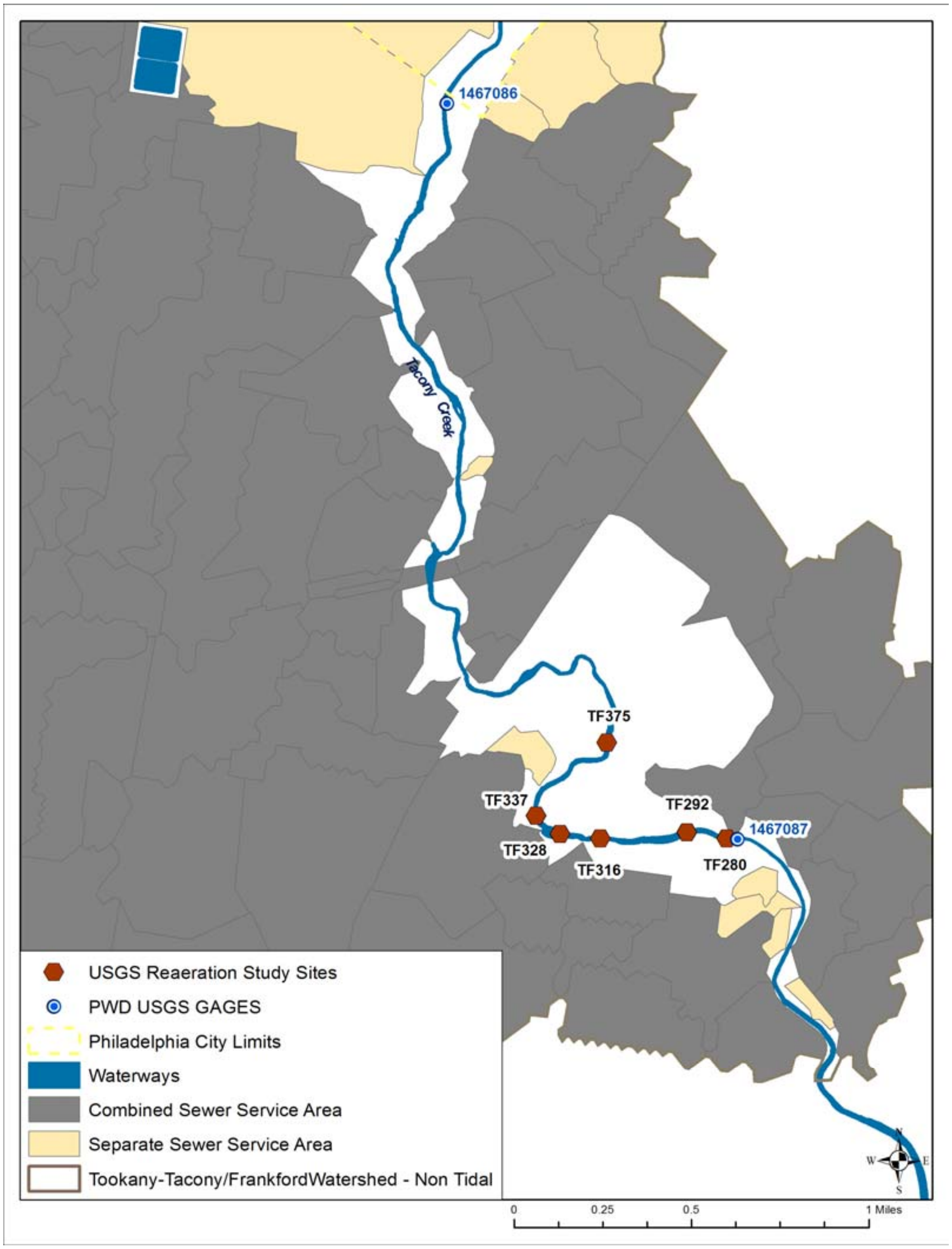

Figure 3-11: USGS Reaeration Study Sites in TTF Creek

Table 3-1: Measured and Calculated Reaeration Rates from USGS Study

Site	Model Segment	k2 measured at 20°C (1/day)	Date measured	k2 calculated method 1[a] at 20°C (1/day)	Percent difference, method 1 to measured	k2 calculated method 2[b] at 20°C (1/day)	Percent difference, method 2 to measured
TF375	17-22	7.75	9/3/09	6.65	-14.14	7.68	-0.81
TF337	23	2.80	9/3/09	2.52	-10.15	2.46	-12.13
TF328	24	3.25	8/18/09	0.62	-81.08	0.02	-99.29
TF316	25	55.04	8/18/09	13.20	-76.01	5.11	-90.72
TF292	26-28	1.03	9/1/09	0.57	-44.93	2.03	96.57
TF280	29-30	14.87	9/1/09	8.67	-41.72	3.87	-74.01

[a]Owens *et al.*, 1964; Tsivoglou and Neal, 1976

[b]McBride, 2002.

As discussed in Section 3.1.4, the Covar method (Covar, 1976) is used to calculate reaeration as a function of velocity and depth by one of three empirical formulas: Owens *et al.* (1964), Churchill *et al.* (1962), or O'Connor and Dobbins (1958). The Covar method was selected in this application of WASP. Information from the 2009 USGS study was used to test other methods of calculating reaeration to determine if there was a benefit to using a different reaeration equation in WASP. A set of reaeration equations summarized by Bowie *et al.* (1985) was selected for analysis. Variables in the equations included velocity, depth, slope, and/or travel time. The USGS study provided flow, depth, velocity, slope, and channel length information (Table 3-2) that was used to calculate a reaeration coefficient for each equation. This calculated reaeration coefficient was compared to observed values from the USGS study. Equations and calculated reaeration coefficients are included in Table 3-3.

Table 3-2: TTF Creek Reach Properties from USGS Reaeration Study

USGS Reach	Length (ft)	Flow (ft^3/s)	Velocity (ft/s)	Average Depth (ft)	Slope (ft/ft)
TF375	3915	15.2	0.234	1.17	0.003
TF337	2190	14.8	0.204	1.66	0.001
TF328	470	15.2	0.041	2.16	0.001
TF316	610	12.0	0.384	0.68	0.007
TF292	1310	14.6	0.089	2.98	0.001
TF280	680	16.4	0.171	1.6	0.011

Table 3-3: Calculated Reaeration Coefficients from Published Reaeration Equations

Source	Equation	Condition	Calculated k2 base e(1/day at 20 deg C) for USGS reach					
Summarized in Bowie *et al.* (1985)			TF375	TF337	TF328	TF316	TF292	TF280
O'Connor and Dobbins (1958)	$\frac{12.9v^{0.5}}{d^{1.5}}$		4.93	2.72	0.82	14.25	0.75	2.64
Owens *et al.* 1964 (1)	$\frac{21.7v^{0.67}}{d^{1.85}}$		6.13	2.93	0.62	23.31	0.57	2.79
Owens *et al.* 1964 (2)	$\frac{23.3v^{0.73}}{d^{1.75}}$		6.13	3.01	0.59	22.74	0.59	2.82
Langbein and Durum (1967)	$\frac{7.6v}{d^{1.33}}$		1.44	0.79	0.11	4.87	0.16	0.70
Cadwaller and McDonnell (1969)	$\frac{336(vS)^{0.5}}{d}$		7.61	2.89	1.00	25.61	1.06	9.11
Bansal (1973)	$\frac{4.67v^{0.6}}{d^{1.4}}$		1.57	0.88	0.23	4.51	0.24	0.84
Bennett and Rathbun (1972)	$\frac{106v^{0.413}S^{0.273}}{d^{1.408}}$		1.68	0.66	0.09	7.46	0.13	1.13
Long (1984)	$\frac{1.923v^{0.273}}{d^{0.894}}$		2.35	1.66	0.85	4.37	0.78	1.63
Grant (1976)	$0.09\left(\frac{\Delta h}{t}\right)$ at 25 deg C		4.84	1.41	0.28	18.54	0.61	12.98
Shindala and Truax (1980)	$0.08\left(\frac{\Delta h}{t}\right)$ at 25 deg C	Q <=10 ft^3/s	-	-	-	-	-	-
	$0.06\left(\frac{\Delta h}{t}\right)$ at 25 deg C	10 <=Q <=280 ft^3/s	3.23	0.94	0.19	12.36	0.41	8.65
USGS Study from Kilpatrick and Wilson (1989)			6.14	2.93	0.20	12.53	0.57	8.77
Owens *et al.* (1964)*	$\frac{0.906v^{0.67}}{d^{1.85}}$	S < 0.003 ft/ft	6.14	2.93	0.20	-	0.57	-
Tsivoglou and Neal (1976)*	$0.054\left(\frac{\Delta h}{t}\right)$	S > 0.003 ft/ft	-	-	-	12.53	-	8.77
WASP - Covar Method			6.14	2.93	0.82	23.34	0.75	2.79
Owens and Gibbs (1964)**	$\frac{5.349v^{0.67}}{d^{1.85}}$	d <2ft	6.14	2.93	-	23.34	-	2.79
Churchill (1962)**	$\frac{5.049v^{0.97}}{d^{1.67}}$	d >2 ft, fast velocity	-	-	-	-	-	-
O'Conner and Dobbins (1956)**	$\frac{3.93v^{0.5}}{d^{1.5}}$	d >2 ft, slow velocity	-	-	0.82	-	0.75	-
Observed in USGS study			7.68	2.81	3.25	55.04	1.03	14.87

For Table 3-3:
d = depth (ft)
Δ*h* = change in stream bed elevation (ft)
k2 = reaeration coefficient (/day)
Q = flow (ft^3/s)
v = velocity (ft/s)
S = slope (ft/ft)
t = travel time between two points where Δ*h* measured (days)
* *t* in hrs
** *v* in m/s, *d* in m

The results of the reaeration investigation indicate that, while the Cadwaller and McDonnell (1969) equation was the best overall fit for the USGS observed reaeration coefficient, there was not enough of a difference between the results of the equation and the Covar method used by WASP to necessitate using an alternate reaeration formula in the TTF and Cobbs DO Models. The closest calculated reaeration coefficient to the observed value for each USGS reach is highlighted in Table 3-3. None of the equations provided results that were near the highest reaeration coefficient measured at Site TF316. A scatter plot of the calculated versus observed reaeration coefficient is presented in Figure 3-12. For comparison, trend lines were included on the plot for the Cadwaller and McDonnell (1969) equation, the Covar method used in WASP, and the Kilpatrick and Wilson (1989) equations used in the USGS study.

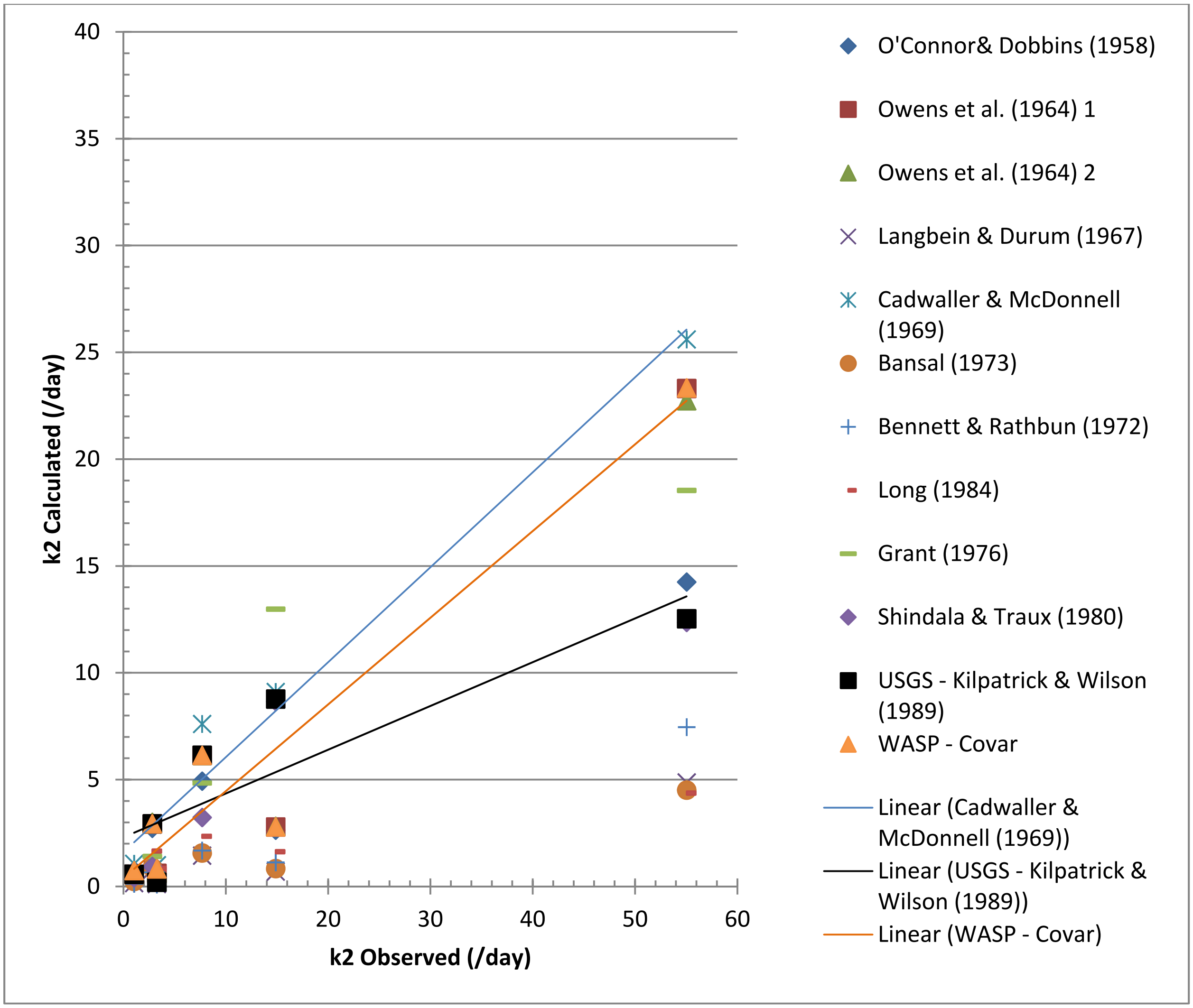

Figure 3-12: Calculated vs. Observed Reaeration Coefficient

3.2.5 Continuous Data

Since 2008, continuous DO, temperature, pH, conductivity, and turbidity have been observed every 30 minutes from March to December across a network of USGS gages in the City. Since 2010, two of the gages – 01467087 and 01474500 – have been equipped to measure photosynthetically active radiation (PAR). As described in annual Water Department reporting to the Pennsylvania Department of Environmental Protection (PADEP), all continuous water quality data undergo quality checks by Water Department staff. The full description of the QA/QC procedure is provided in Appendix B.

3.3 Model Validation Periods

Since WASP 7.5 cannot represent scouring of benthic algae, long term simulations of the benthic algae conditions were not possible. Therefore, event scale validation periods were chosen that collectively illustrate the main DO issues in these waterbodies:

- **Summer algal blooms concurrent with low DO**. These periods occur in extended summer dry weather. They are characterized by large diel DO fluctuations and low DO exacerbated by temperature effects.
- **Spring algal blooms**. These periods are marked by large diel DO fluctuations. Minimum DO concentrations are greater than in summer because of temperature effects.
- **Rapid, transient decreases in DO during CSO events**, especially small storms that yield combined sewer overflows with less stormwater dilution.

The 2009 USGS reaeration study period was also chosen for TTF DO Model validation.

Additional factors influencing the selection of validation periods were the availability of high quality data from the downstream USGS gage on each creek, and overlaps with benthic algae sampling data.

The model validation periods for each stream are summarized in Tables 3-4 and 3-5.

Table 3-4: TTF DO Model Validation Periods

Period	Dates	Features	Benthic algae sampling dates
T-1	Aug 18 - Aug 20, 2009	USGS reaeration rate study	None
T-2	Sep 1 - Sep 5, 2009	USGS reaeration rate study	None
T-3	Jun 20 - Jun 30, 2011	Extended dry weather summer algal bloom	June 20, 22, 24, 28
T-4	Jul 16 - Jul 25, 2011	Extended dry weather summer algal bloom	July 25
T-5	Mar 10 - Mar 30, 2012	Spring algal bloom; rapid transient DO decrease during small CSO event	March 12, 16, 20, 28

Table 3-5: Cobbs DO Model Validation Periods

Period	Dates	Features	Benthic algae sampling dates
C-1	Jul 30 - Aug 7, 2010	Extended dry weather summer algal bloom	None
C-2	Apr 20 - Apr 30, 2012	Spring algal bloom	April 16, 20, 23, 25, 26, 27, 30
C-3	Jul 23 - Jul 29, 2012	Algal regrowth; rapid transient DO decrease during small CSO event	July 23, 25, 26
C-4	Sep 9 - Sep 17, 2012	Algal regrowth	September 10, 11

3.4 Model Selection

During wet weather events, the rate of change in stage and discharge in TTF and Cobbs Creeks is large, a characteristic of highly urbanized streams. The flashiness of hydrographs in the urban stream environment results in the rapid transport of constituent discharges through the system. The applied H&H and water quality model must be able to compute numerical solutions of this highly dynamic environment.

Key criteria in water quality model selection were:

- Ability to handle rapid temporal changes in concentration common in urban stream environment
- Ability to simulate benthic algae and sediment oxygen demand
- Capability to receive output from US EPA SWMM5
- Model platform that is accepted by the modeling and regulatory communities
- Affordable for a public entity

Based on these criteria, WASP 7.5 was selected for this project (Wool *et al.*, 2003). The WASP model is a publicly available model administered by the US EPA Watershed and Water Quality Modeling Technical Support Center; Version 7.5 was released in 2011. Originally released in 1983, WASP is a dynamic compartment-modeling program for aquatic systems that simulates pollutants in a river network. This version, WASP 7.5, simulates benthic algae via its Advanced Eutro module.

The processes represented in the WASP 7.5 Advanced Eutro model are shown in the schematic in Figure 3-13. The fundamental WASP modeling equations, expressed in Wool *et al.* (2003) and Ambrose *et al.* (2006), govern the dynamic relationships between photosynthesis, respiration, growth and death of planktonic and attached algae, light and nutrients that limit growth (the latter according to Monod kinetics), temperature, and DO in the water column and/or benthos. Nutrients are partitioned into dissolved and particulate fractions, and organic and inorganic species. Detrital processes include settling, dissolution, and mineralization of organic matter.

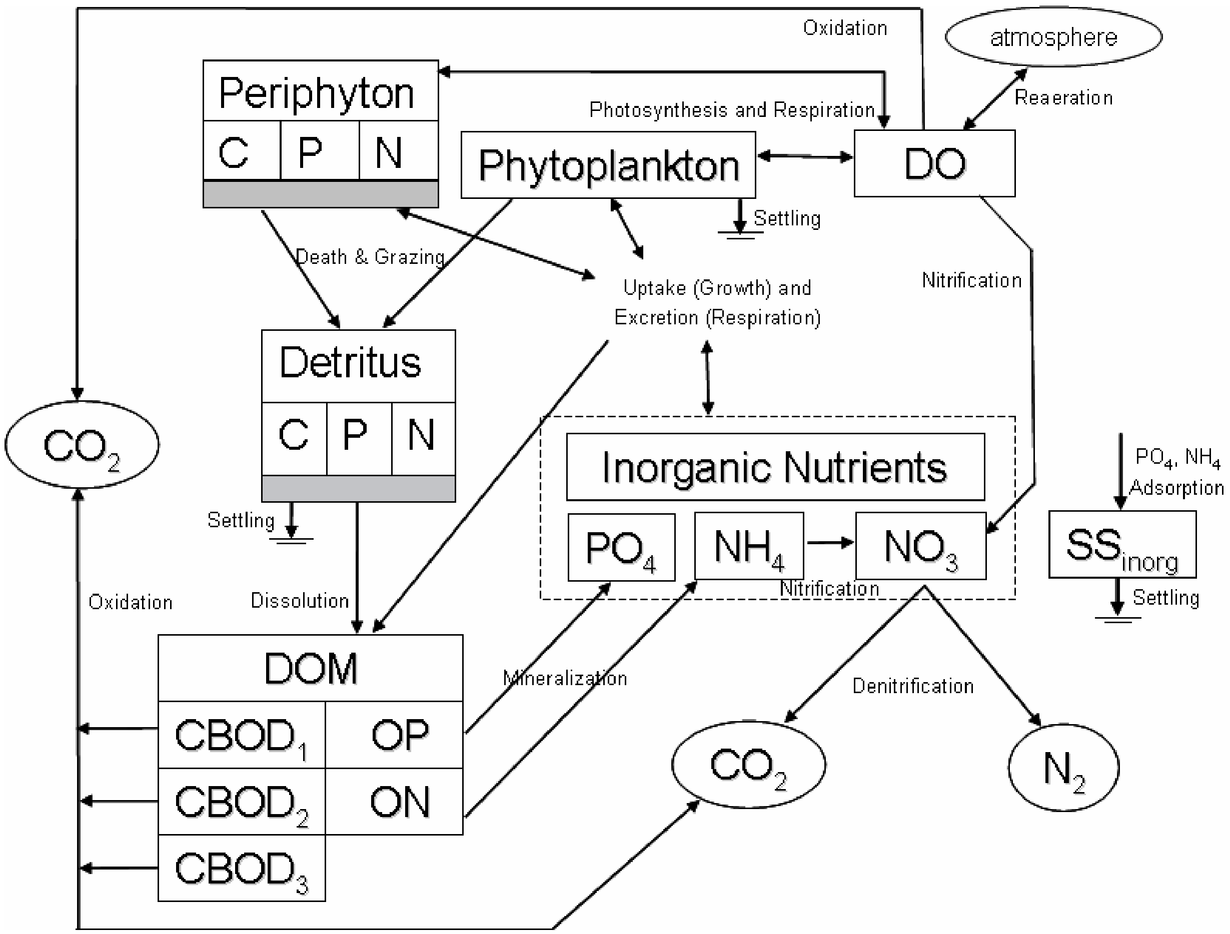

Figure 3-13: WASP7.5 Advanced Eutro Modeling Schematic (from Ambrose *et al.*, 2006)

Periphyton growth is impacted by temperature, light and nutrients. The growth of periphyton consumes nutrients and produces oxygen. Periphyton excrete cell contents and recycle dissolved and particulate organic matter to the stream water column carbon and nutrient pools. Sources and sinks for periphyton include growth, death, and respiration. Growth is computed from a maximum rate that is then modified based upon available light and internal nutrients. A key drawback is that WASP 7.5 does not simulate scouring of benthic algae.

Unlike phytoplankton, light reaching the stream bottom, rather than average amount of light in the water column, is used in the estimation of benthic algae growth. Rates of death and respiration are temperature dependent. Rates of growth, respiration, and death impact other model state variables including dissolved oxygen and nutrients. Nutrient limitation of the photosynthesis rate is dependent on intracellular nutrient concentrations. Light limitation is determined by the amount of PAR reaching the bottom of the water column. Incident light can be adjusted by spatially varying canopy cover.

Besides algal respiration, DO is also consumed by SOD, CBOD, and the nitrification of ammonium. DO is increased by algal photosynthesis and by reaeration from the atmosphere as a function of water depth and velocity.

The WASP model is widely accepted and has been used in numerous studies and total maximum daily loads (TMDLs), as described in Section 3.1. It has been coupled with SWMM output for Long Term Control Plan models of the Rouge River (Detroit), White River (Indianapolis), Merrimack River (Massachusetts), and Scioto and Olentangy Rivers (Columbus).
WASP can incorporate hydrodynamic output from other models, using a hydrodynamic linkage option. Since SWMM5 is not yet configured to generate the required ".hyd file", extensive work was performed by the Water Department to create software that generates the linkage file from SWMM5 output, as described in Philadelphia Water Department (2013).

3.5 Linkage from H&H Model to DO Model

As described in Philadelphia Water Department (2013), a software tool was developed by the Water Department to export output from SWMM5 to WASP. An updated version of this tool was used for the Tributary DO Models. The SWMM5 output was extracted at a 30 second interval to allow execution of WASP at a 30 second time step. Since WASP is limited to one boundary per segment, a composite flow-weighted concentration approach was used for each segment receiving multiple boundary inputs (Wool et al., 2003).

The TTF DO Model was divided into 37 segments, with an average segment length of 625 feet. The Cobbs DO Model was divided into 76 segments, including 18 segments for East and West Indian Creeks, and 7 segments for Naylors Run. Its average segment length is 1213 feet. Segmentation of each model is shown in Tables 3-6 and 3-7.

Table 3-6: TTF DO Model Segmentation

Segment	Length (ft)	Outfall
1	828	
2	1057	
3	135	
4	228	
5	326	
6	298	T-03
7	391	
8	499	
9	552	R-15
10	931	T-04, T-05

Segment	Length (ft)	Outfall
11	912	T-06
12	391	
13	842	T-07
14	962	T-08
15	956	T-09, T-10
16	258	T-11
17	393	
18	850	T-12, T-13
19	2010	
20	609	
21	273	
22	939	
23	1062	
24	241	T-14
25	373	
26	359	T-15
27	749	
28	489	
29	362	
30	301	
31	893	F-03
32	1371	F-04
33	375	F-05
34	494	R-18
35	728	
36	350	
37	356	F-06, F-07

Table 3-7: Cobbs DO Model Segmentation

	Segment	Length (ft)	Tributary	Outfall
Cobbs Creek	1	370		
	2	612		C31
	3	835		
	4	985		
	5	1044		
	6	714		
	7	450		C32
	8	727		

	Segment	Length (ft)	Tributary	Outfall
Cobbs Creek	9	750		
	10	600		
	11	572		
	12	550		
	13	60		C33
	14	493		
	15	616	East Indian Creek	
	16	2596		
	17	2413		C09, C10, R24, C37
	18	520		
	19	729		C11
	20	820		
	21	623		
	22	856		C12
	23	943		
	24	470		
	25	635		
	26	1262	Naylors Run	
	27	942		
	28	730		C13
	29	520		C14
	30	1431		
	31	995		R01
	32	405		C15, C16
	33	594		
	34	668		
	35	988		
	36	560		C17
	37	1500		C18
	38	579		
	39	431		
	40	387		C19
	41	630		
	42	876		
	43	852		
	44	460		
	45	887		C20
	46	741		C21

	Segment	Length (ft)	Tributary	Outfall
Cobbs Creek	47	445		
	48	957		C22
	49	329		
	50	704		
	51	917		C23
East Indian Creek	52	1773		
	53	2175		
	54	862		
	55	2128		
	56	492		
	57	376		
	58	2131		
	59	1822		C04, C05, C06, C36
	60	350		
	61	866	West Indian Creek	C07
	62	2428		
West Indian Creek	63	837		
	64	915		
	65	1225		
	66	1873		
	67	1350		
	68	4544		C01, C02
	69	1863		C34, C35
Naylors Run	70	5372		
	71	3475		
	72	1454		
	73	3850		
	74	5425		
	75	2430		
	76	2420		

3.6 Water Quality Model Input Data

3.6.1 Boundary Conditions

The TTF and Cobbs water quality models were designed so that a single WASP segment could receive up to four types of boundary inflows:

- Subcatchment runoff
- CSO discharges

- Baseflow
- Headwater inputs

3.6.1.1 Stormwater

Concentrations of chemical constituents in subcatchment runoff and CSO discharges were simulated in SWMM5, which has the capability to simulate surface runoff chemical and other constituent loadings through several functional approaches, including assigning constituent concentrations directly to a flow time series. Stormwater and sanitary wastewater physical and chemical constituents are carried through the collection system and discharged from the outfalls to the receiving waters during wet weather periods. These processes are represented in the Tributary H&H Models. Event mean concentrations (EMCs) were applied to subcatchments in the SWMM models to estimate runoff constituent loads. An EMC is defined as the mass load of a pollutant parameter yielded from a site during a storm divided by the total runoff volume discharged during the storm (Smullen and Cave, 2003). Estimates of EMCs derived from published national databases (Smullen and Cave, 2003; Smullen *et al.* 1999; Pitt, 2004) that were applicable to the DO models are listed in Table 3-8**.** Since the EMCs are pooled from a number of studies nationwide, and by definition represent averages, the same urban runoff EMC for each water quality parameter was assigned to all subcatchments.

WASP 7.5 Advanced Eutro accounts for a more comprehensive set of water quality parameters than listed in Table 3-8. Values for these parameters were derived from the published EMCs in Table 3-8 and are listed in Table 3-9. These derived values were assigned as EMCs to the modeled runoff to estimate runoff loads.

The National Stormwater Quality Database (NSQD) included measured DO values for stormwater, although they were not published by Pitt (2004). A median value for DO in runoff was calculated from the data in the NSQD and used as the EMC for DO. Organic nitrogen was calculated by subtracting ammonia from total Kjeldhal nitrogen. It was assumed that the organic nitrogen was 50 percent dissolved and 50 percent particulate, or detrital. This fractioning was applied to the calculated organic nitrogen to estimate EMC values for dissolved organic and detrital nitrogen. Preliminary analysis of these parameters concluded that model was not sensitive to the fractioning of organic nitrogen and that a 50/50 fraction was reasonable. Organic phosphorus was estimated by subtracting inorganic phosphate from total phosphorus. Similar to organic nitrogen, a 50/50 fraction of dissolved organic phosphorus to particulate, or detrital, phosphorus was assumed. WASP requires an ultimate value of CBOD, so the BOD5 values were converted to CBOD by applying a decay rate of 0.2/day (Chapra, 1997); $CBOD_{ult} = CBOD_5/(1\text{-}exp(-5*0.2)$ (Wool et l., 2003). Total organic carbon was calculated from CBOD via the 2.67 Oxygen: Carbon stoichiometric ratio. Half of the total organic carbon was assumed to be particulate and was the value used to define the detrital carbon EMC.

Table 3-8: National EMCs Derived from Published Sources

Parameter	EMC (mg/L)
Ammonia (NH_3)	0.44
Nitrite + Nitrate (NO_2 + NO_3)	0.60
Total Kjeldhal Nitrogen (TKN)	1.43
Inorganic Phosphate (PO_4)	0.10
Total Phosphorus (TP)	0.27
5 - day Biochemical Oxygen Demand (BOD_5)	9.50

Table 3-9: Water Quality Constituents Derived from EMCs as Required by WASP

WASP WQ Parameter	Derived From	EMC applied to runoff in SWMM (mg/L)
Ammonia	NH_3	0.44
Nitrate	NO_3	0.60
Dissolved Organic Nitrogen	TKN & NH_3	0.50
Inorganic Phosphate (orthophosphate)	PO_4	0.126
Dissolved Organic Phosphorus	TP & PO_4	0.07
CBOD	BOD_5	15.03
Dissolved oxygen	DO	8.2
Detrital carbon	BOD_5	2.81
Detrital nitrogen	TKN & NH_3	0.50
Detrital Phosphorus	TP & PO_4	0.07

3.6.1.2 Sanitary Base Wastewater

Loads from CSOs were calculated in SWMM by combining the modeled stormwater runoff and associated loads that enter the collection system with the estimated sanitary base wastewater flow and loads. A combination of these sources comprises the total flow and loads discharged from the outfall. The time varying proportion of runoff to sanitary components throughout a storm dictates the flow weighted composite pollutant concentrations of the discharge. Constant concentration values were assigned to base wastewater flow in the CSS domain of the Tributary H&H Models. These values were estimated from regulator sampling performed in dry weather by the Water Department at 69 locations in the collection system. The median values from the monitored data, shown in Table 3-10, formed the basis of pollutant concentrations assigned to the SWMM models. Similar to the approach taken for runoff EMCs, the water quality parameters for base wastewater flow were derived as needed to be compatible with WASP. Similar assumptions used in the EMC estimates were used to estimate dissolved and detrital organic nitrogen and phosphorus, ultimate CBOD, and detrital carbon concentrations in base wastewater. A DO concentration of 2.0 mg/L was assumed for the base wastewater. These values were applied to SWMM as a constant concentration on direct inflow at the nodes used to load base wastewater flow. Base wastewater loading values are shown in Table 3-11.

Table 3-10: Dry Weather Regulator Sampling Data of Base Wastewater

Parameter	Median (mg/L)	Mean (mg/L)	Standard Deviation (mg/L)
Ammonia (NH_3)	8.45	9.13	3.63
Nitrite + Nitrate (NO_2 + NO_3)	0.88	1.00	0.64
Total Kjeldhal Nitrogen (TKN)	19.98	20.58	6.40
Inorganic Phosphate (PO_4)	1.69	1.73	1.00
Total Phosphorus (TP)	3.44	5.50	4.53
5 - day Biochemical Oxygen Demand (BOD_5)	115	134	73

Table 3-11: Water Quality Constituents Derived from Base Wastewater as Required by WASP

WASP WQ Parameter	Derived From	Value applied to base wastewater in SWMM (mg/L)
Ammonia	NH_3	8.45
Nitrate	NO_3	0.88
Dissolved Organic Nitrogen	TKN & NH_3	5.78
Inorganic Phosphate (orthophosphate)	PO_4	1.69
Dissolved Organic Phosphorus	TP & PO_4	0.88
CBOD	BOD_5	182
Dissolved Oxygen	DO	2.0
Detrital Carbon	BOD_5	34
Detrital Nitrogen	TKN & NH_3	5.78
Detrital Phosphorus	TP & PO_4	0.88

3.6.1.3 Baseflow

The techniques used for baseflow separation were described in Section 2.0. To represent water quality loads, the baseflow was assigned constant constituent concentrations based on analyses of dry weather data from each watershed (Tables 3-12, 3-13 and 3-14). Data below the detection limit were assumed equal to half the method detection limit. The dry weather data were further categorized by location (*e.g.*, monitoring sites inside or outside the city). The median concentrations determined through these analyses were then applied to the corresponding segments in the model (Table 3-15).

For the TTF DO Model, continuous DO data were available for each validation period at USGS gage 01467086, and were used directly as the headwater boundary condition time series for DO.

Headwater boundary conditions for CBOD, nitrogen and phosphorus constituents were based on median concentrations of data collected near USGS gage 01467086 (Table 3-16).

For the Cobbs DO Model, continuous DO data were available for each validation period at USGS gage 01475530, and were used directly as the headwater boundary condition time series for DO at the uppermost Cobbs Creek segment.   Headwater boundary conditions for CBOD, nitrogen and phosphorus constituents for Cobbs Creek were based on median concentrations of data collected near USGS gage 01475530 (Table 3-16).   For East Indian and West Indian Creeks, and Naylors Run, which were each modeled to their full extents, the uppermost segment of each tributary was loaded with baseflow and subcatchment runoff concentrations listed in Tables 3-15 and 3-9, respectively.

DO in baseflow was set at 7.0 mg/L for all TTF and mainstem Cobbs Creeks model segments. For all tributary segments in the Cobbs Creek Model, DO in baseflow was set at 75% of saturation, calculated based on daily average temperature at USGS Gage 01475548.

Table 3-12: Summary of Dry Weather Water Quality Data for TTF Creek Inside City, March-September of 2000-2013

Parameter	Number of samples	Number of non-detects	Median	Std. dev.
Ammonia	47	17	0.11	0.26
TKN	20	2	0.55	0.50
Nitrate	52	2	1.77	0.78
Nitrite	42	21	0.03	0.05
Orthophosphate	52	46	0.05	0.02
Total P	37	3	0.08	0.09
BOD_{30}	13	0	6.86	3.47

Table 3-13: Summary of Dry Weather Water Quality Data for Cobbs and East/West Indian Creeks Inside City, March-September of 1999-2013

Parameter	Number of samples	Number of non-detects	Median	Std. dev.
Ammonia	32	16	0.05	0.06
TKN	20	0	0.61	0.19
Nitrate	38	0	2.10	0.49
Nitrite	27	12	0.03	0.02
Orthophosphate	38	38	0.04	0.01
Total P	15	0	0.08	0.03
BOD_{30}	20	1	4.11	2.51

Table 3-14: Summary of Dry Weather Water Quality Data for Cobbs Creek Watershed Outside City, January-December of 1999-2013

Parameter	Number of samples	Number of non-detects	Median	Std. dev.
Ammonia	21	18	0.05	0.04
TKN	11	4	0.36	0.23
Nitrate	30	0	2.92	0.38
Nitrite	15	13	0.03	0.01
Orthophosphate	30	30	0.03	0.01
Total P	8	5	0.03	0.02
BOD_{30}	11	2	3.71	1.41

Table 3-15: Water Quality Baseflow Concentrations Applied to TTF and Cobbs DO Models

WASP Water Quality Parameter	Baseflow conc. applied to TTF segments (mg/L)	Baseflow conc. applied to Cobbs segments inside City (mg/L)	Baseflow conc. applied to Cobbs segments outside City (mg/L)
Ammonia	0.11	0.05	0.05
Nitrate	1.77	2.12	2.95
Dissolved Organic Nitrogen	0.22	0.28	0.16
Inorganic Phosphate (orthophosphate)	0.05	0.05	0.05
Dissolved Organic Phosphorus	0.03	0.03	0.03
CBOD	6.86	4.11	3.71
Detrital carbon	1.28	0.76	0.69
Detrital nitrogen	0.22	0.28	0.16
Detrital Phosphorus	0.03	0.03	0.03

Table 3-16: Headwater Concentrations Applied to TTF and Cobbs DO Models

WASP Water Quality Parameter	Headwater conc. applied to TTF segment 1 (mg/L)	Headwater conc. applied to Cobbs segment 1 (mg/L)
Ammonia	0.10	0.05
Nitrate	2.14	2.66
Dissolved Organic Nitrogen	0.17	0.21
Inorganic Phosphate (orthophosphate)	0.05	0.05
Dissolved Organic Phosphorus	0.01	0.05
CBOD	5.47	3.85
Detrital carbon	1.02	0.71
Detrital nitrogen	0.17	0.21
Detrital Phosphorus	0.01	0.05

3.6.1.4 Water Temperature and PAR

Water temperature time series for all TTF and Cobbs DO Model segments were based on half-hourly water temperature data obtained from USGS Gages 01467087 and 01475548, respectively.

PAR time series for all TTF and Cobbs DO Model segments were based on half-hourly PAR data obtained from USGS Gages 01467087 and 01474500, respectively, for validation periods in 2010-2012. For 2009 validation periods in TTF Creek, the 2009 solar radiation time series was acquired from the National Renewable Energy Laboratory (NREL) National Solar Radiation Database for Philadelphia International Airport (NREL, 2012), and doubled to yield PAR values of the range observed in 2010-2012.

3.6.2 Model Parameterization

The WASP7.5 Advanced Eutro module has several global and spatially variable rate constants and input values that can be adjusted by the user. Global constants that were applied are listed in Table 3-17. Parameterization of global constants began with the default values listed in the WASP 7.5 user manual. These values were later adjusted during sensitivity analysis and calibration exercises to arrive at final validation values, as described in the next section.

Table 3-17: Global Constant Values Applied in Validation

Parameter	Validation Value
Nitrification Rate Constant at 20°C (1/day)	0.10
Nitrification Temperature Coefficient	1.07
Minimum Temperature for Nitrification Reaction (°C)	5.00
Denitrification Rate Constant 20°C (1/day)	0.09
Denitrification Temperature Coefficient	1.04
Half Saturation Constant for Denitrification Oxygen Limit (mg O2/L)	0.10
Detritus Dissolution Rate (1/day)	0.50
Temperature Correction for detritus dissolution	1.08
Dissolved Organic Nitrogen Mineralization Rate Constant 20°C (1/day)	0.02
Dissolved Organic Nitrogen Mineralization Temperature Coefficient	1.08
Dissolved Organic Phosphorus Mineralization Rate Constant 20°C (1/day)	0.20
Dissolved Organic Phosphorus Mineralization Temperature Coefficient	1.08
CBOD(1) Decay Rate Constant 20°C (1/day)	0.20
CBOD(1) Decay Rate Temperature Correction Coefficient	1.02
CBOD(1) Half Saturation Oxygen Limit (mg O2/L)	0.50
Fraction of Detritus Dissolution to CBOD(1)	0.75
Oxygen to Carbon Stoichiometric Ratio	2.69
Calculated Reaeration Option	Covar
Theta -- Reaeration Temperature Correction	1.03
Theta -- SOD Temperature Correction	1.02
Light Input Option	Input time series
Background Light Extinction Coefficient (1/m)	0.40
Benthic Algae D:C Ratio (mg D/mg C)	2.50
Benthic Algae N:C Ratio (mg N/mg C)	0.18
Benthic Algae P:C Ratio (mg P/mg C)	0.025
Benthic Algae Chl a:C Ratio (mg Chl/mg C)	0.025
Benthic Algae O2:C Production (mg O2/mg C)	2.69
Growth Model	Zero order
Max Growth Rate (gD/m^2-day, or 1/day)	30.00
Temp Coefficient for Benthic Algal Growth	1.05
Respiration Rate Constant (1/day)	0.20 in TTF; 0.75 in Cobbs
Temperature Coefficient for Benthic Algal Respiration	1.05
Internal Nutrient Excretion Rate Constant for Benthic Algae (1/day)	0.09
Temperature Coefficient for Benthic Algal Nutrient Excretion	1.08
Death Rate Constant (1/day)	0.15
Temperature Coefficient for Benthic Algal Death	1.05

Parameter	Validation Value
Half Saturation Uptake Constant for Extracellular Nitrogen (mg N/L)	0.02
Half Saturation Uptake Constant for Extracellular Phosphorus (mg P/L)	0.04
Light model option	Smith
Light Constant for growth (langleys/day)	135.00
Benthic Algae ammonia preference (mg N/L)	0.025
Minimum Cell Quota of Internal Nitrogen for Growth (mgN/gDW)	7.20
Minimum Cell Quota of Internal Phosphorus for Growth (mgP/gDW)	1.00
Maximum Nitrogen Uptake Rate for Benthic Algae (mgN/gDW-day)	720.00
Maximum Phosphorus Uptake Rate for Benthic Algae (mgP/gDW-day)	50.00
Half Saturation Uptake Constant for Intracellular Nitrogen (mgN/gDW)	9.00
Half Saturation Uptake Constant for Intracellular Phosphorus (mgP/gDW)	1.30

Spatially variable constants were derived as follows:

3.6.2.1 Canopy Cover

WASP allows the solar radiation input time series to be adjusted to account for tree canopy shading during “leaf-on” time periods when a greater amount of incident solar radiation is intercepted by deciduous trees and other leafy vegetation. This model parameter is called the Fraction of Light Intercepted by Tree Canopy (FLI), and works by reducing the solar radiation intensity reaching the water surface within a WASP segment. During model validation it was discovered that, despite the name, smaller values for FLI allow more light to reach the water surface. This parameter was also used to represent permanent structures providing shade, such as bridge decks.

Two datasets of FLI were used, one for leaf-on periods, and another for leaf-off time periods in each DO Model. FLI was not varied as a validation parameter. However, FLI was set to “leaf off” values for spring bloom simulation periods T-5 and C-2.

Unique FLI values were calculated for each WASP segment though a geographic information systems (GIS) analysis, by intersecting the locations of the corresponding dry weather flow channel area delineations with a high resolution Land Cover GIS Dataset.

The high resolution land cover dataset was developed as part of the Urban Tree Canopy (UTC) Assessment for Philadelphia (O’Neil-Dunne, 2011). It was created by the University of Vermont Spatial Analysis Laboratory. The primary sources used to derive this land cover layer were 2008 Orthophotography and 2008 LiDAR LAS data. Ancillary data sources included GIS data (building footprints, road polygons, and hydrography) provided by the City of Philadelphia (City). The minimum mapping unit for the delineation of features was set at ten square feet.

Some portions of the Cobbs DO Model domain were outside of the high resolution land use dataset coverage. In these portions, an assortment of lower resolution orthophotography was used to estimate the shaded fraction of the channel area.

Both approaches were based on a fractional area analysis of either 0% or 100% shaded zones within an orthographic snapshot. Vegetation density, vegetation type, and stream orientations relative to solar arc were not accounted for.

3.6.2.2 Sediment Oxygen Demand

As stated in the Available Data Summary Section of this report, in-stream SOD values were measured in the Cobbs and Tacony creeks. This parameter was applied to individual WASP segments.

Cobbs

Based on SOD measurements at Site DCC225, one baseline SOD value of 5 $g/m^2/day$ was assigned to all Cobbs Model segments located within the City of Philadelphia, and one baseline SOD value of 2 $g/m^2/day$ was assigned to all Cobbs Model segments outside of the city.

TTF

Within the TTF DO Model unique baseline SOD values were estimated for each WASP segment. Within this model domain high spatial resolution in-stream survey data was available for a significant portion of the stream length and bottom area. This survey data was indirectly leveraged to estimate baseline SOD values.

As part of a separate effort within the Water Department, high spatial resolution in-stream survey data was collected by the Water Department's Ecological Restoration Group for the purpose of assessing stream restoration activities. At each survey point, bed material type was also recorded. Correlations between bed material type and SOD were assigned from average SOD measured values. These relationships formed the basis of a Geographic Information System (GIS) analysis of numerous survey points and correlated SOD values within corresponding WASP segment dry weather channel area delineations. An inverse distance weighted method was used to interpolate between survey points and correlated SOD values. Area weighted averages within WASP segment boundaries were used to estimate baseline SOD values within the survey zone.

The survey data was further exploited by developing correlations for predicted SOD to stream sinuosity, and predicted SOD to dry weather flow depth. These relationships and other best engineering judgments were used to estimate baseline SOD values for WASP segments outside of the survey zone.

3.6.2.3 Algae Habitat

One of the parameters in the WASP Advanced Eutrophication module that controls the amount of benthic algae biomass within a WASP segment is the Fraction of Bottom Area in Each Segment Providing Suitable Substrate for Growth (FAS). For example, a WASP segment with an FAS value of 0.33 would have benthic algae growth limited to one third of its channel bottom area.

As stated in Section 3.2, benthic algal densities were sampled in the Cobbs and Tacony Creeks. These measurements were related to FAS, but the sampling areas were much smaller than their corresponding WASP segments.

Cobbs

All WASP segments within the Cobbs DO Model domain were assigned a uniform baseline FAS value of 0.5. Subsequently, FAS values were adjusted during validation of the Cobbs DO Model.

TTF

Within the TTF DO Model, unique baseline FAS values were estimated for each WASP segment. Within this model domain high spatial resolution in-stream survey data was available for a significant portion of the stream length and bottom area. This survey data was indirectly used to estimate baseline FAS values.

As stated in the previous section, high spatial resolution fluvial geomorphological survey data was collected by the Water Department. At each survey point, bed material type was also recorded. Correlations between bed material type and suitable benthic algae habitat were inferred, forming a basis of a GIS analysis of suitable benthic algae habitat areas within corresponding WASP segment dry weather channel area delineations. These area fractions were used to estimate baseline FAS values within the survey zone.

The survey data was further leveraged by developing correlations for predicted FAS to stream sinuosity, and predicted FAS to dry weather flow depth. These relationships and other judgments were used to estimate baseline FAS values outside of the survey zone.

After the baseline values were estimated, FAS values in the entire water quality domain were adjusted during validation of the TTF DO Model.

3.6.2.4 Dam Reaeration

Dam reaeration inputs were entered according to Butts and Evans (1983), as mentioned in Section 3.1.

A list of model segments and spatially variable parameter values is shown in Tables 3-18 and 3-19.

Table 3-18: Spatially Variable Parameters in Cobbs DO Model

	Segment	SOD ($g/m^2/d$)	FLI	FAS	Dam elevation (m)	Dam Pool WQ Coefficient	Dam Type Coefficient
Cobbs Creek	1	5	0.39	0.6			
	2	5	0.43	0.5			
	3	5	0.30	0.5			
	4	5	0.53	0.5			
	5	5	0.74	0.5			

	Segment	SOD ($g/m^2/d$)	FLI	FAS	Dam Elevation(m)	Dam Pool WQ Coefficient	Dam Type Coefficient
Cobbs Creek	6	5	0.55	0.5			
	7	5	0.40	0.5			
	8	5	0.59	0.5			
	9	5	0.44	0.5			
	10	5	0.44	0.5			
	11	5	0.29	0.5			
	12	5	0.16	0.5			
	13	5	0.30	0.5			
	14	5	0.38	0.5			
	15	5	0.39	0.5			
	16	5	0.60	0.5			
	17	5	0.45	0.5	3.05	0.65	0.80
	18	5	0.20	0.5			
	19	5	0.29	0.5			
	20	5	0.50	0.5			
	21	5	0.50	0.5			
	22	5	0.45	0.5			
	23	5	0.57	0.5			
	24	5	0.59	0.5			
	25	5	0.59	0.5			
	26	5	0.46	0.5			
	27	5	0.24	0.5			
	28	5	0.20	0.5			
	29	5	0.30	0.5			
	30	5	0.48	0.5			
	31	5	0.48	0.5			
	32	5	0.61	0.5			
	33	5	0.59	0.5			
	34	5	0.65	0.5			
	35	5	0.56	0.6			
	36	5	0.69	0.6			
	37	5	0.43	0.6			
	38	5	0.28	0.6			
	39	5	0.52	0.6			
	40	5	0.38	0.6			
	41	5	0.16	0.5			
	42	5	0.40	0.5			
	43	5	0.67	0.5			

	Segment	SOD ($g/m^2/d$)	FLI	FAS	Dam Elevation(m)	Dam Pool WQ Coefficient	Dam Type Coefficient
Cobbs Creek	44	5	0.58	0.5			
	45	5	0.65	0.5			
	46	5	0.66	0.5			
	47	5	0.41	0.5			
	48	5	0.65	0.5			
	49	5	0.40	0.5			
	50	5	0.60	0.5			
	51	5	0.64	0.5			
East Indian Creek	52	2	0.55	0.5			
	53	2	0.20	0.5			
	54	2	0.10	0.5			
	55	2	0.06	0.5			
	56	5	0.09	0.5			
	57	5	0.12	0.5			
	58	5	0.16	0.5			
	59	5	0.17	0.5			
	60	5	0.00	0.5			
	61	5	0.43	0.5			
	62	5	0.32	0.5			
West Indian Creek	63	2	0.01	0.5			
	64	2	0.13	0.5			
	65	2	0.09	0.5			
	66	2	0.14	0.5			
	67	2	0.03	0.5			
	68	5	0.13	0.5			
	69	5	0.17	0.5			
Naylors Run	70	2	0.19	0.5			
	71	2	0.12	0.5			
	72	2	0.40	0.5			
	73	2	0.20	0.5			
	74	2	0.56	0.5			
	75	2	0.06	0.5			
	76	2	0.04	0.5			

Table 3-19: Spatially Variable Parameters in TTF DO Model

Segment	SOD ($g/m^2/d$)	FLI	FAS	Dam elevation (m)	Dam Pool WQ Coefficient	Dam Type Coefficient
1	5.50	0.46	0.30			
2	6.20	0.61	0.18			
3	5.25	0.85	0.56	1.22	1.00	0.60
4	5.10	0.70	0.39			
5	5.00	0.70	0.41			
6	5.00	0.48	0.40			
7	5.07	0.31	0.37			
8	7.00	0.72	0.20			
9	5.40	0.55	0.33	0.91	1.00	0.80
10	5.20	0.66	0.38			
11	5.50	0.44	0.32			
12	5.00	0.35	0.57			
13	6.00	0.36	0.37			
14	4.99	0.41	0.58			
15	4.40	0.43	0.75			
16	4.70	0.45	0.71			
17	4.80	0.16	0.74			
18	3.60	0.45	0.89			
19	3.80	0.61	0.84			
20	6.10	0.53	0.31			
21	6.60	0.24	0.14			
22	5.70	0.37	0.41			
23	5.70	0.58	0.68			
24	5.20	0.89	0.86			
25	4.00	0.71	1.00			
26	7.90	0.80	0.75			
27	10.10	0.70	0.50			
28	11.10	0.86	0.50			
29	5.80	0.87	0.88	2.13	0.65	0.75
30	5.80	0.86	0.95			
31	1.00	0.57	0.90	0.61	0.65	0.75
32	1.00	0.61	0.90			
33	1.00	0.50	0.90			
34	1.00	0.01	0.90			
35	1.00	0.69	0.90			
36	1.00	0.53	0.90			
37	7.00	0.97	0.20			

It should be noted that for validation of the 2009 USGS study period in TTF Creek (validation periods T-1 and T-2), measured reaeration rates were applied to their corresponding segments (Table 3-1). For segments not sampled, the calculated rate obtained from the Covar method at baseflow conditions was applied.

USGS measured reaeration rates were not applied to other TTF DO Model validation periods because the data is applicable only to the flow condition at which it was measured, and not to conditions of unsteady-state flow as was observed in the other periods.

3.7 Water Quality Model Sensitivity Analysis

A sensitivity analysis was performed to determine the effect of various rate constants on model output. Parameters were varied one at a time on the full DO model extents at unsteady flow conditions. In addition to the standard WASP output state variables (*e.g.*, DO, benthic algae, orthophosphate, etc.), additional process terms such as nutrient uptake rates, photosynthesis rate, light attenuation coefficient, etc. were also analyzed via a custom post-processor developed by the Water Department that utilized equations described in the WASP 7.5 user manual. This allowed additional insight into the effect of input terms on model output.
It was found that the most sensitive global constants were:

- Maximum growth rate
- Temperature coefficients for growth rate and SOD
- Background light extinction coefficient
- Minimum cell quotas for internal N and P for growth
- Benthic algae stoichiometric ratios

Other global constants that were sensitive to a lesser degree were:

- CBOD decay rate
- Respiration rate
- Death rate
- Temperature coefficients for CBOD decay, respiration, and death rates
- Half-saturation uptake constant for extracellular phosphorus
- Light constant for growth

An example of the effect of varying maximum growth rate is shown in Figures 3-14 through 3-18. As growth rate is increased, biomass increases and diel DO fluctuations increase. Nutrient uptake and photosynthesis rates also increase with a greater maximum growth rate.

Temperature coefficients are used to adjust a kinetic rate when the water temperature deviates from 20°C. SOD is very sensitive to this coefficient as shown in Figure 3-19.

Sensitivity to benthic algae stoichiometric ratios is shown in Figures 3-20 and 3-21. The measured ratio yields similar biomass density but less diel DO fluctuation than the Redfield ratio. This is because with the oxygen to carbon ratio held constant between the two scenarios, much less oxygen is consumed and produced using the measured ratios which have less carbon per unit of chl-a.

The importance of including spatially variable terms such as dam reaeration and SOD are demonstrated in Figures 3-22 and 3-23, respectively.

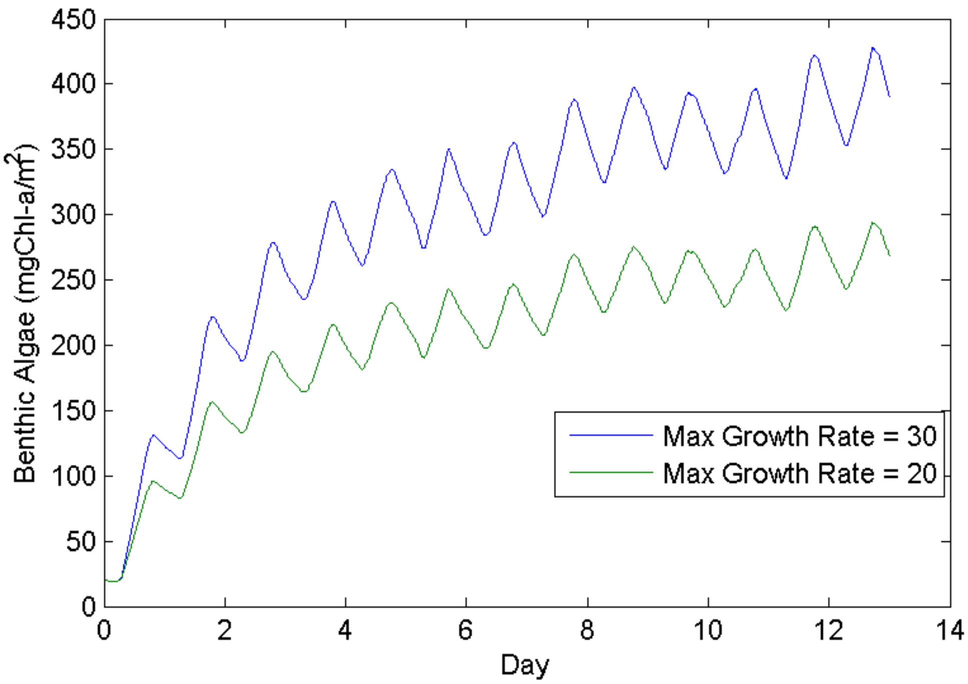

Figure 3-14: Sensitivity of Benthic Algal Density to Maximum Growth Rate

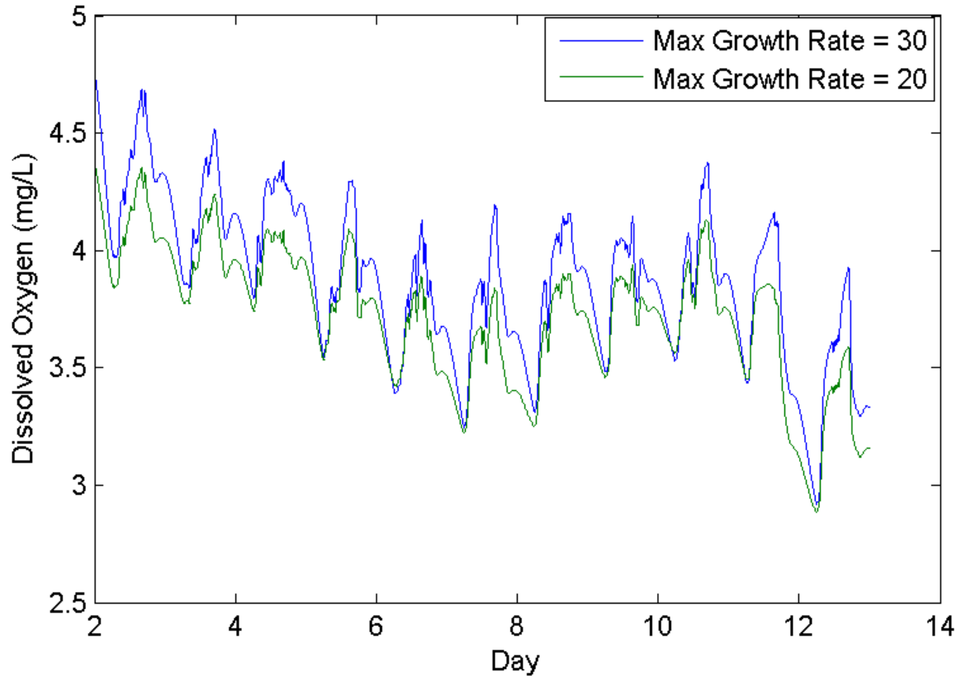

Figure 3-15: Sensitivity of DO to Maximum Growth Rate

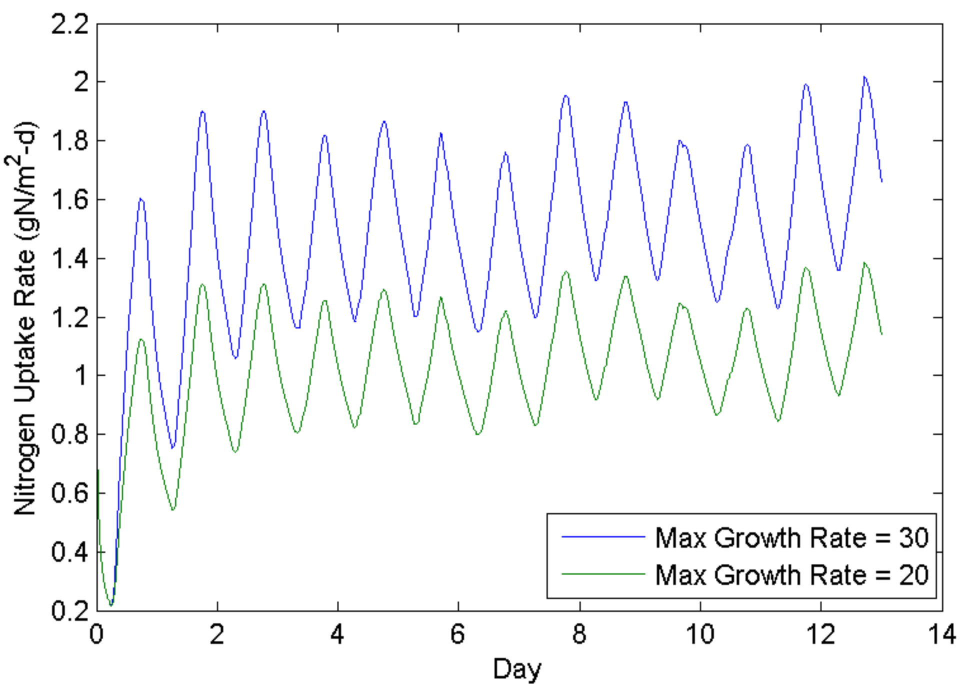

Figure 3-16: Sensitivity of Nitrogen Uptake Rate to Maximum Growth Rate

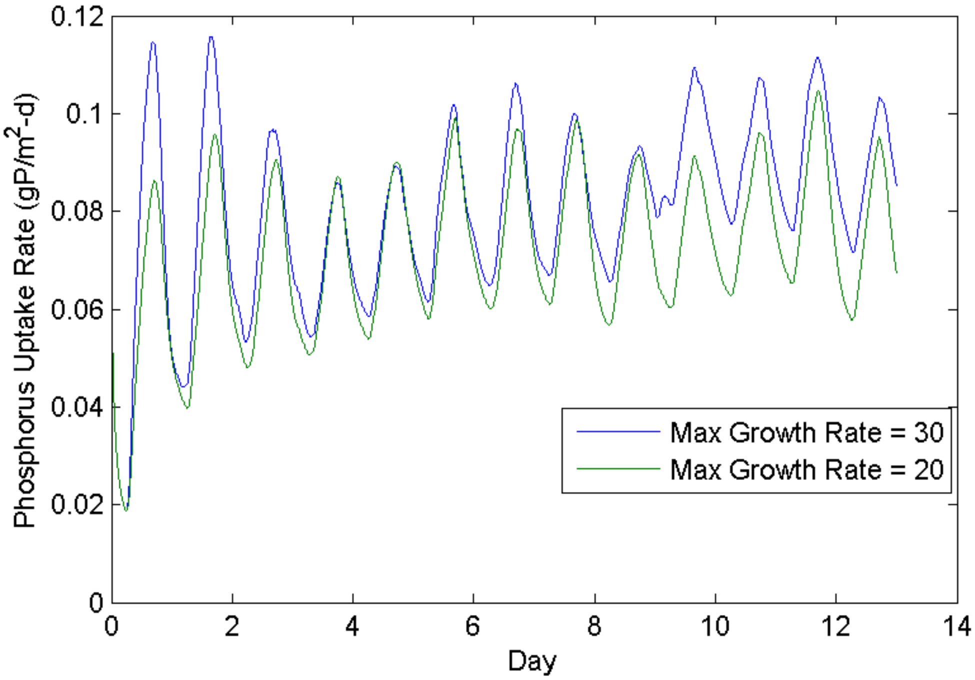

Figure 3-17: Sensitivity of Phosphorus Uptake Rate to Maximum Growth Rate

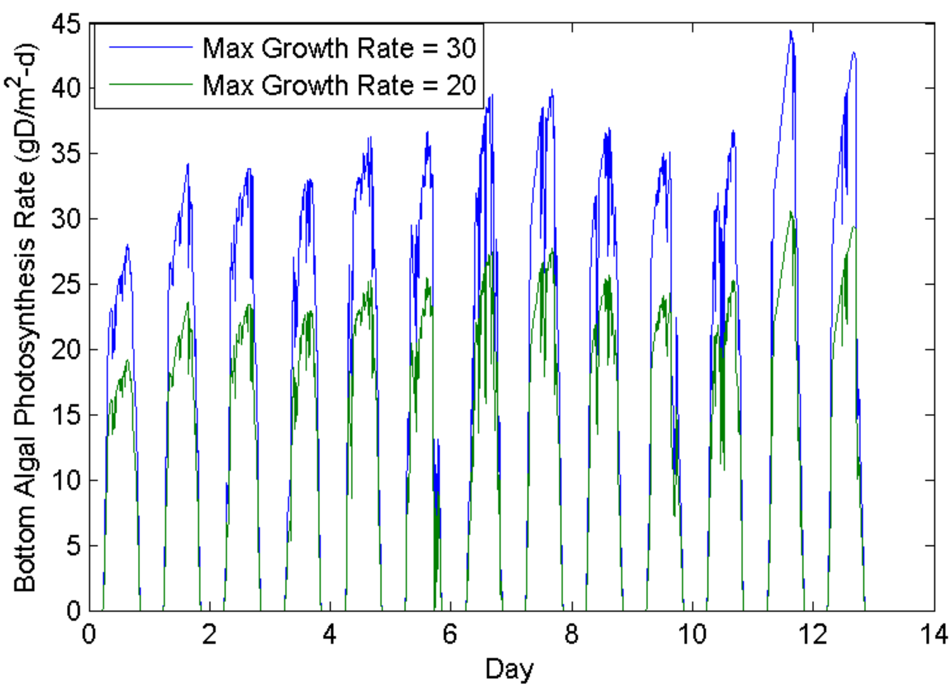

Figure 3-18: Sensitivity of Photosynthesis Rate to Maximum Growth Rate

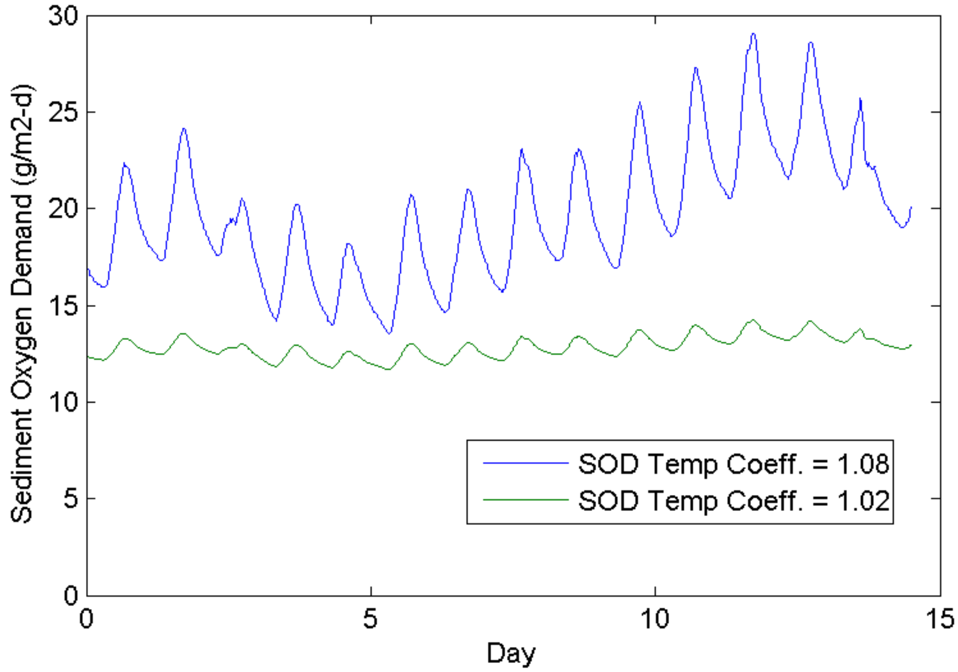

Figure 3-19: Sensitivity of SOD to SOD Temperature Coefficient

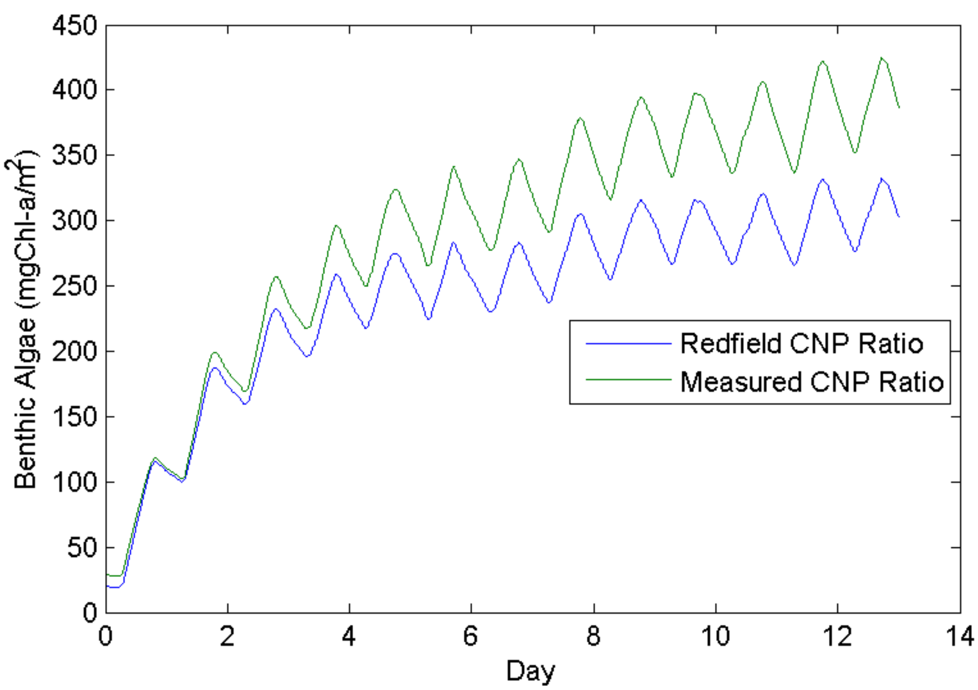

Figure 3-20: Sensitivity of Benthic Algal Density to CNP Ratio

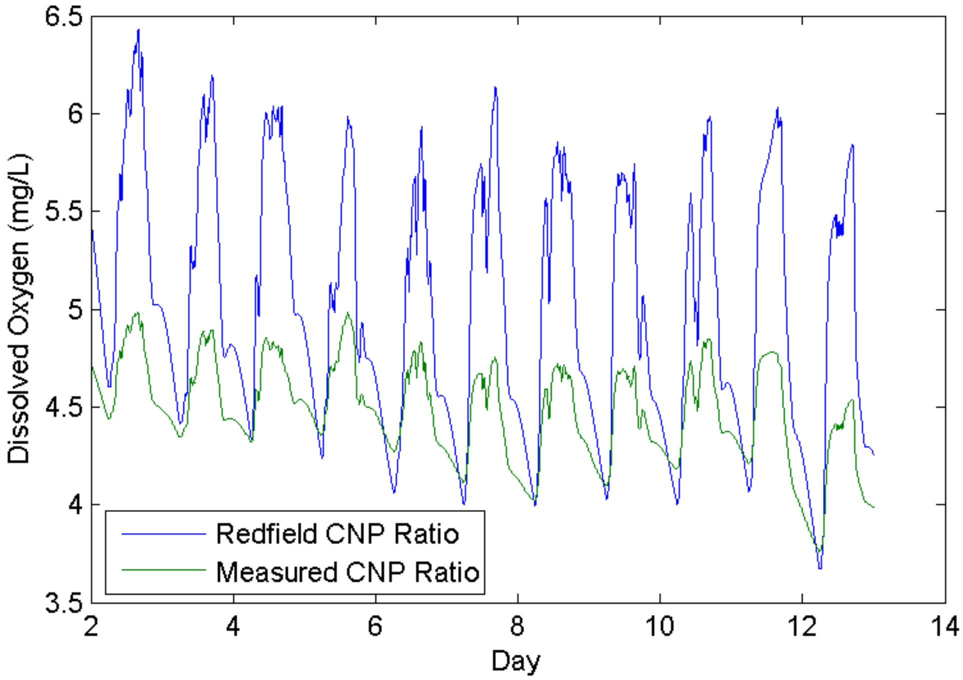

Figure 3-21: Sensitivity of DO to CNP Ratio

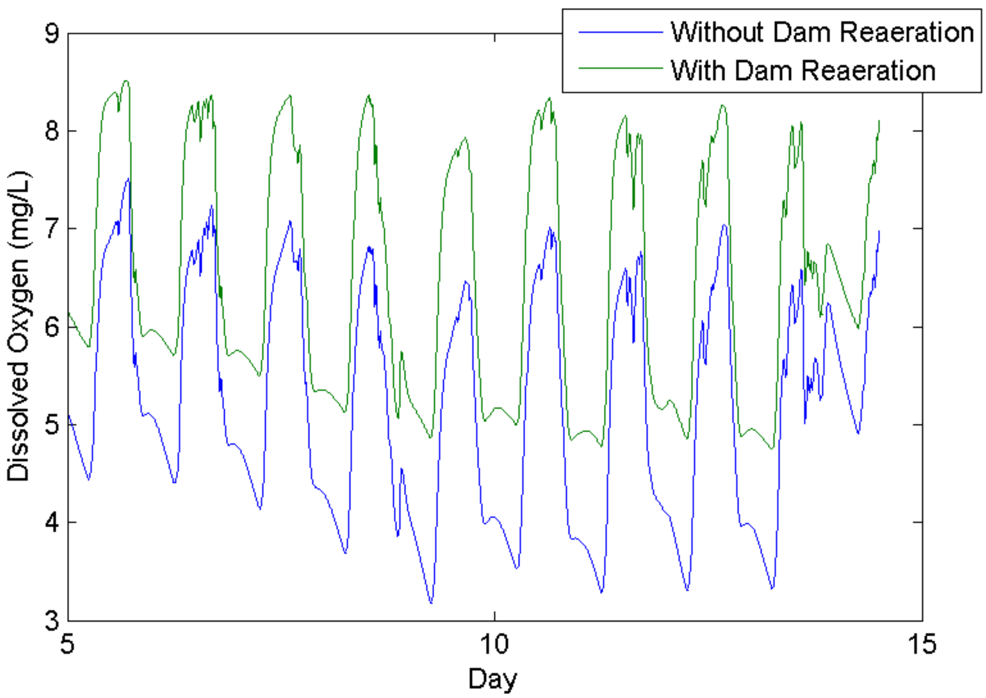

Figure 3-22: Sensitivity of DO to Dam Reaeration

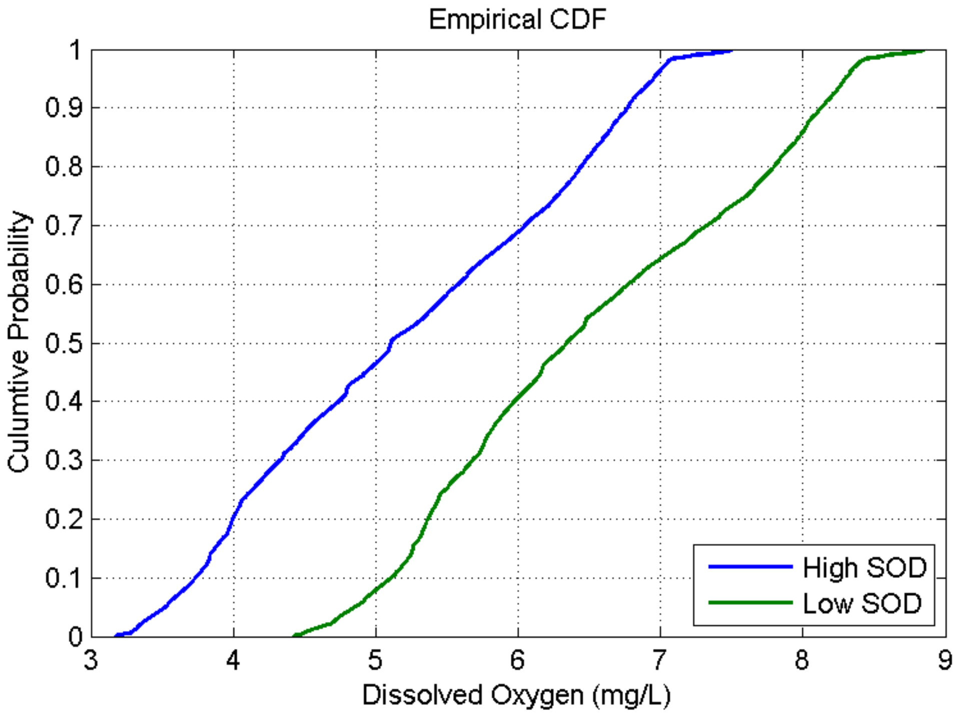

Figure 3-23: Sensitivity of DO to SOD

3.8 Model Validation

Observed and simulated results for DO concentrations were compared for individual periods at the downstream USGS gage on each creek. Time series plots and right-continuous cumulative distribution function (CDF) plots were used to evaluate model performance. Model evaluation statistics of observed and predicted DO concentrations were tabulated for each validation period (Tables 3-19 and 3-20); mean absolute error (MAE) and root mean square error (RMSE) are defined in Tetra Tech (2007). Time series plots of observed and simulated benthic algal density were produced for periods when observed data was available. Plots are shown in Sections 3.8.1 and 3.8.2.

3.8.1 TTF Creek

The observed data from the 5 periods totaling 53 days in 2009-2012 were used to validate the TTF DO model. Half-hourly DO concentration data at USGS Gage 01467087 (n=2544), and benthic algal density samples (n=27) were used to compare predicted and observed data. Based on results of the sensitivity analysis, the rate constants in Tables 3-16 and 3-18 were applied to all TTF DO model validation periods.

Results and discussion

Benthic algal density was measured by collecting three replicate samples per sampling event at each site. The average, minimum and maximum values are plotted in Figures 3-24 through 3-26. Overall, predictions of benthic algal density at Site TF316 (model segment 26) were generally within the range of observed data, indicating that the model is reliably simulating benthic algae kinetics in the spring and summer seasons represented by Validation Periods T-3 and T-5. The increase in benthic algae in the spring 2012 bloom (T-5) is particularly well represented. In T-3, the increase in benthic algae from June 20 to June 24, 2011 is well represented; however, the decrease in benthic algae in T-3 observed on 6/28/11 is not reflected in the model or in the observed DO data at USGS Gage 01467087 (Figure 3-27). This underscores the challenges inherent in understanding benthic algae growth and loss processes. In T-4, only one set of benthic algae samples was collected within the period modeled, and it was well represented by the model.

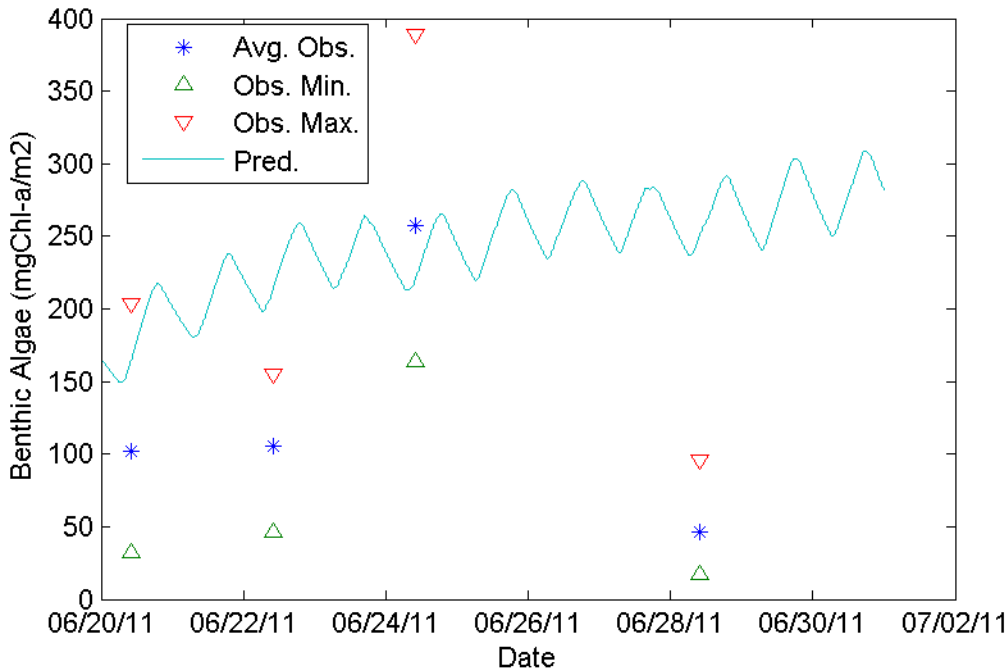

Figure 3-24: Observed and Simulated Benthic Algal Density at Site TF316, Validation Period T-3

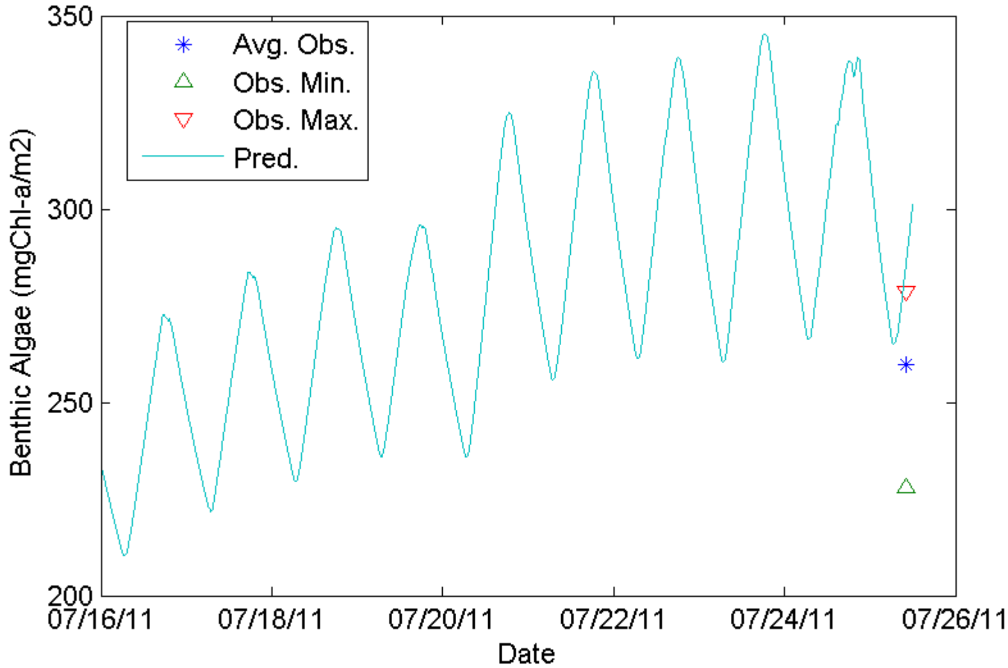

Figure 3-25: Observed and Simulated Benthic Algal Density at Site TF316, Validation Period T-4

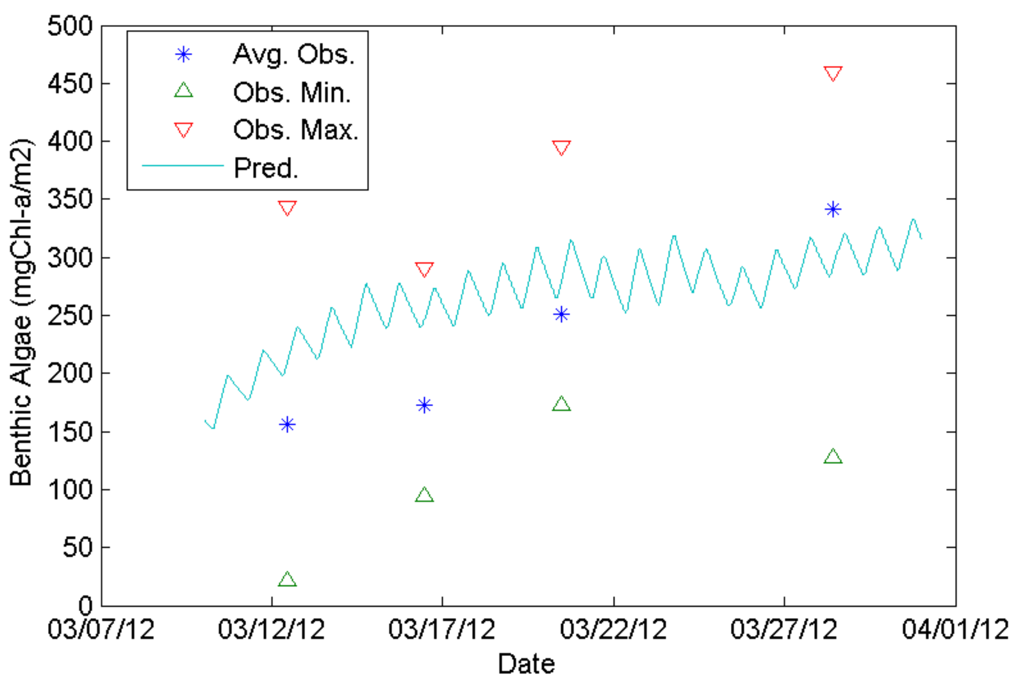

Figure 3-26: Observed and Simulated Benthic Algal Density at Site TF316, Validation Period T-5

Simulations of DO at Site TF280 (USGS Gage 01467087; Segment 30) were made using calculated reaeration rates for validation periods T-3, T-4 and T-5, and measured reaeration rates in Segments 17-30 for T-1 and T-2. Periods T-1 through T-4 occurred in summer, and T-5 occurred in the spring. Plots are shown in Figures 3-27 through 3-41 and evaluation statistics are listed in Table 3-20. Half-hourly observed DO concentration data was smoothed with a 2 hour moving average for T-2 and T-3 to eliminate signal noise.

In general, the results indicate good performance across all the summer validation periods. The similarities in variance in the CDF plot of observed and simulated DO for T-3 (Figure 3-30) indicate benthic algal processes were well simulated. Similarities in medians in the CDF plot indicate the balance between SOD, BOD, reaearation, photosynthesis and respiration were well simulated in T-3; RMSE for the full DO time series was 0.65 mg/L. In T-4, daily DO fluctuation was underpredicted with a MAE of 1.88 mg/L, although the MAE for the full time series was 1.09 mg/L.

During the USGS 2009 study period, daily DO fluctuations were slightly overpredicted for T-1 (MAE = 0.76 mg/L), and daily DO minima were slightly underpredicted (MAE = 0.50 mg/L). Simulation of T-2 yielded slightly better error statistics than T-1; T-2 error statistics were all less than 1 mg/L.

Daily minimum DO concentrations were predicted with MAE of 0.36 to 0.59 mg/L for the summer season validation periods T-1 through T-4. Minimum DO concentrations were generally underpredicted in validation periods T-1 through T-4.

The results for the spring 2012 bloom (T-5) were mixed. Two minor storms, each yielding peak flows less than 75 cfs at USGS Gage 01467087, caused rapid transient decreases in DO, particularly the 3/25/12 storm in which DO decreased from 5.0 to 1.4 mg/L in 4 hours and exceeded the minimum standard (Figure 3-33). These were presumably caused by CSOs with minimal dilution of stormwater. The DO model did not reproduce either one of the two rapid transient DO decreases in T-5, which in this case was due to H&H Model underprediction of CSO flows and loading. However, a similar result occurred in the Cobbs DO Model during a period with accurate H&H Model prediction, therefore other factors such as loading concentrations or CBOD decay rate require investigation and improvement. Prior to and after the storms in T-5, DO was well simulated. The effect of benthic algae on daily DO fluctuations across the whole period was well simulated (MAE = 0.86 mg/L).

Overall, MAE and RMSE across all validation periods were less than 1 mg/L in 32 of 40 outcomes, and ranged from 0.38 to 1.97. These results indicate adequate model performance in representing eutrophication kinetics and the effects of SOD and reaeration in TTF Creek. The effect of CBOD during small CSO events is the main simulation flaw that requires future improvement.

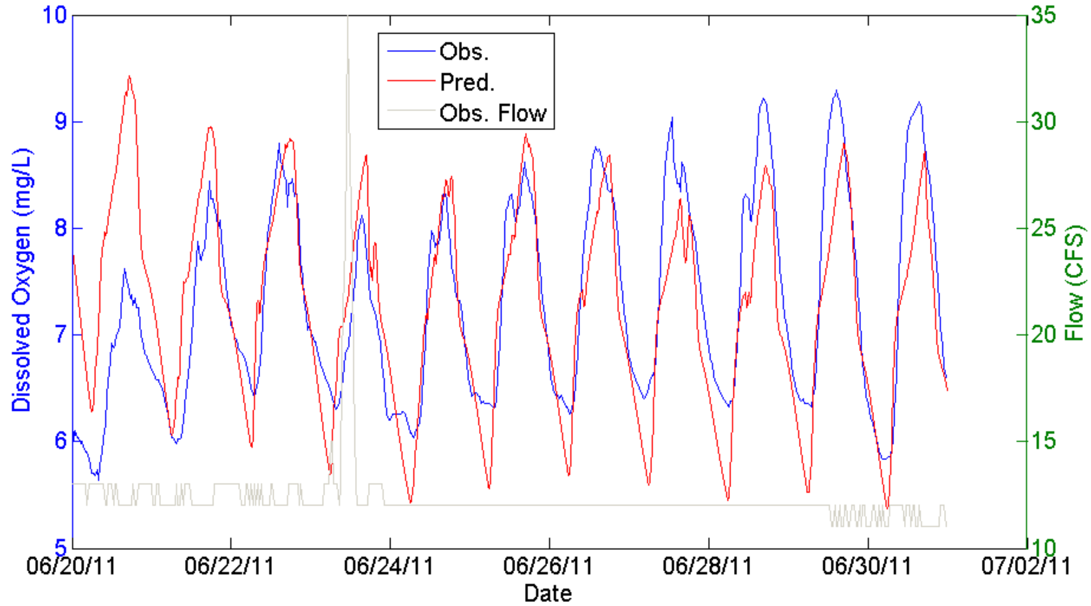

Figure 3-27: Observed and Simulated DO Concentration at Site TF280, Validation Period T-3

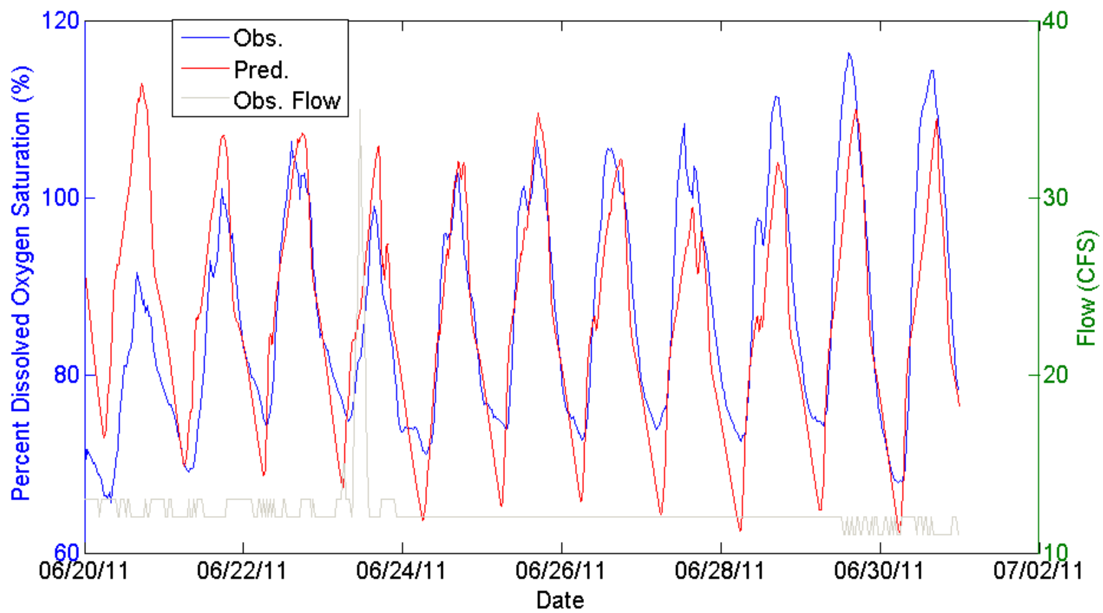

Figure 3-28: Observed and Simulated DO Percent Saturation at Site TF280, Validation Period T-3

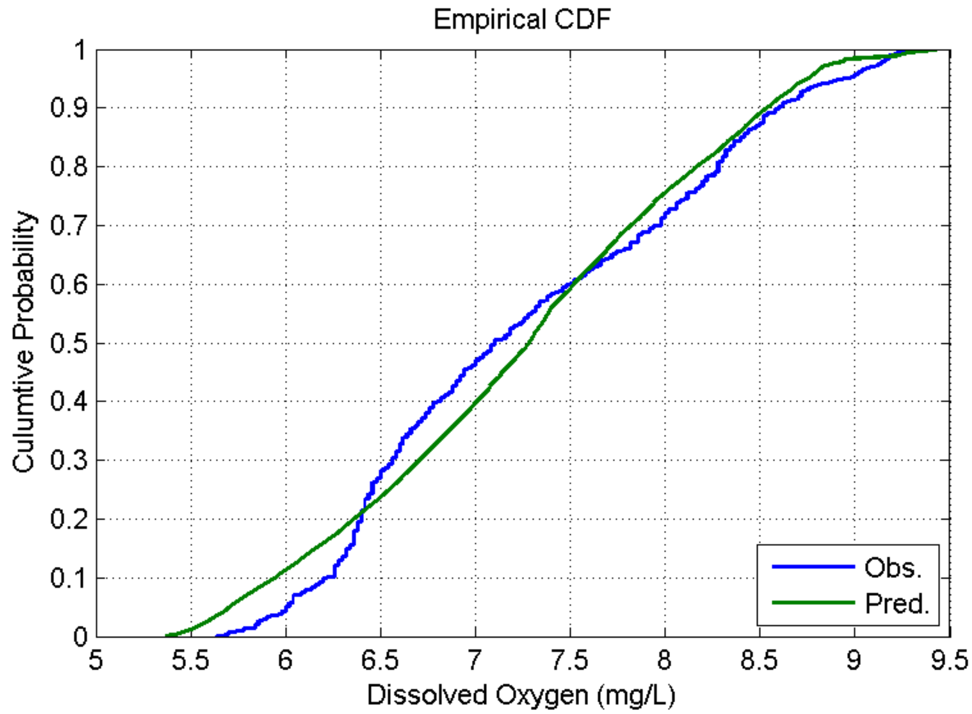

Figure 3-29: Observed and Simulated CDF of DO Concentration at Site TF280, Validation Period T-3

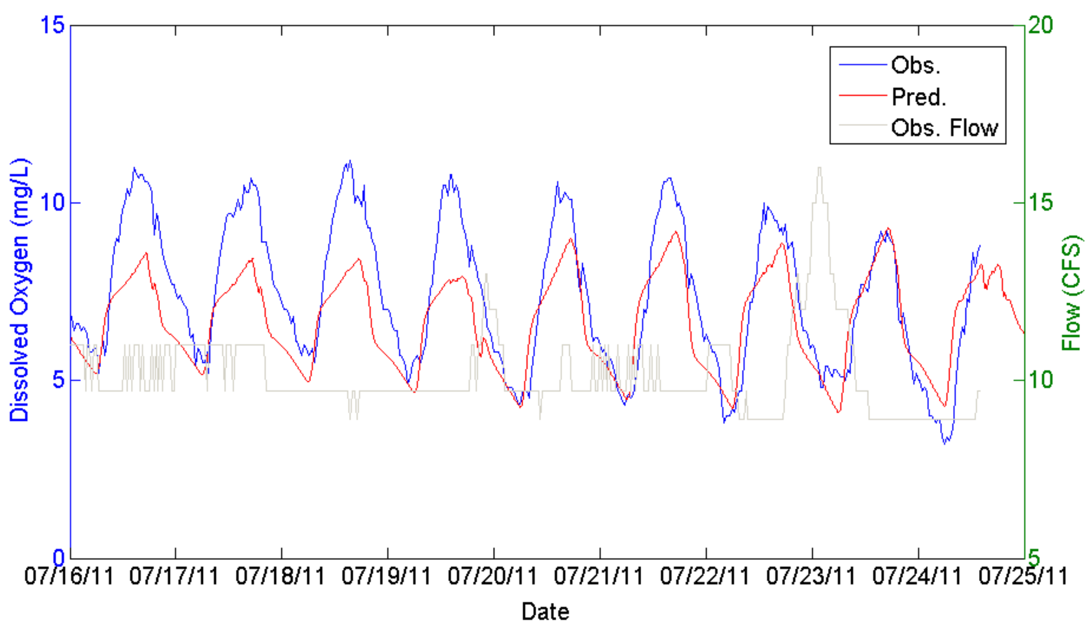

Figure 3-30: Observed and Simulated DO Concentration at Site TF280, Validation Period T-4

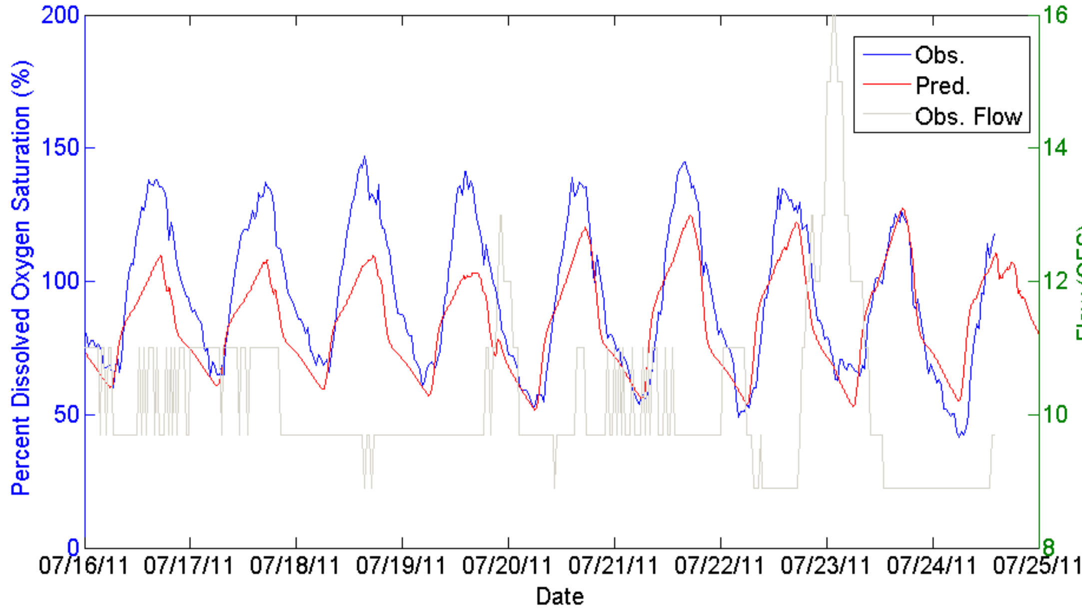

Figure 3-31: Observed and Simulated DO Percent Saturation at Site TF280, Validation Period T-4

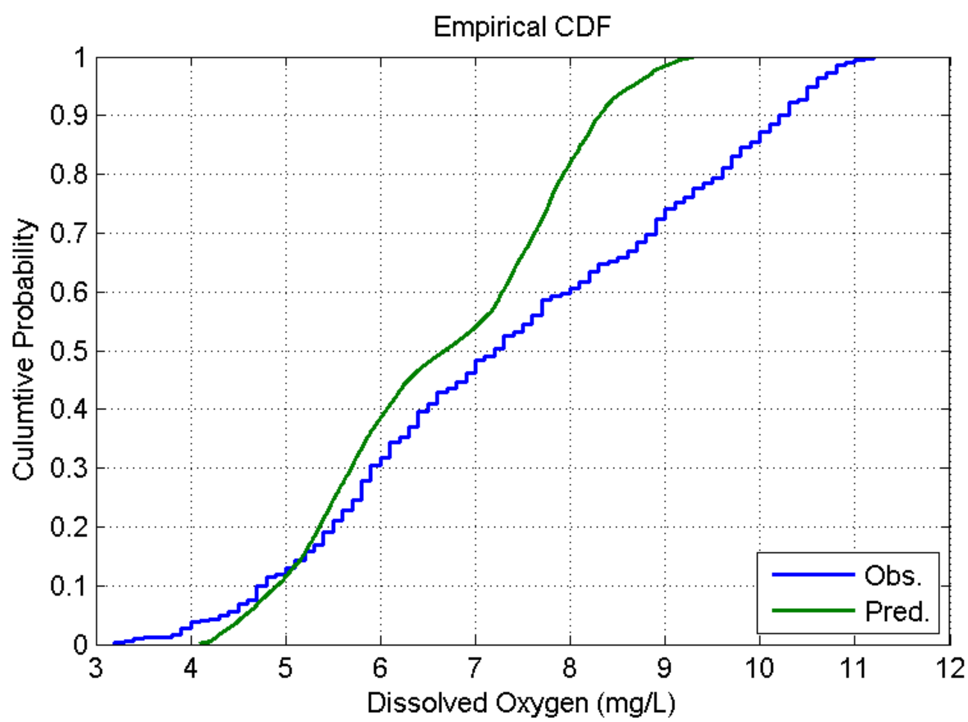

Figure 3-32: Observed and Simulated CDF of DO Concentration at Site TF280, Validation Period T-4

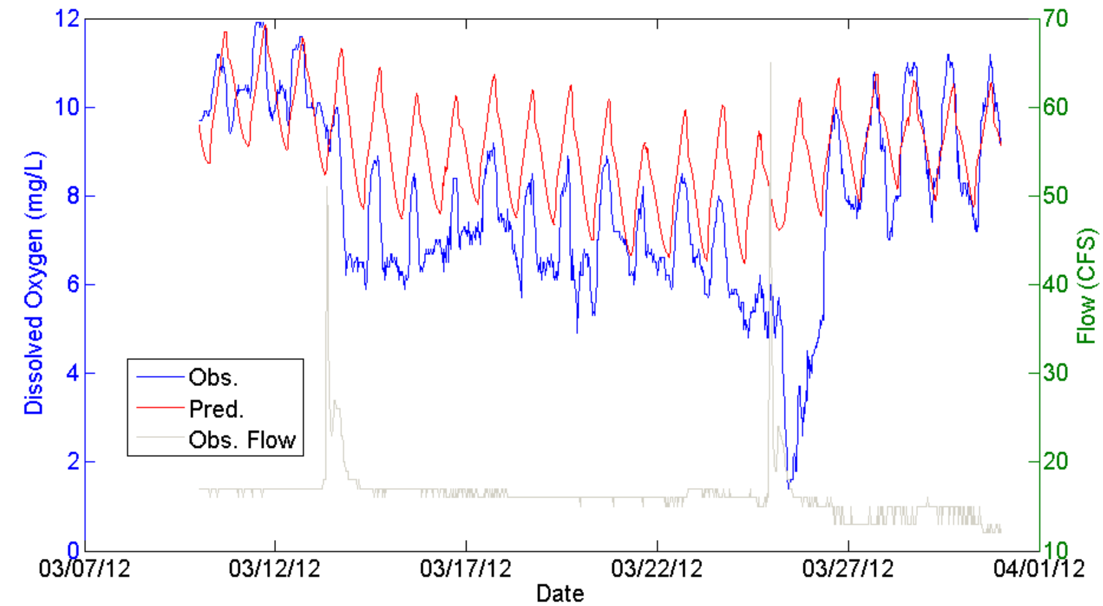

Figure 3-33: Observed and Simulated DO Concentration at Site TF280, Validation Period T-5

A rapid decrease in DO occurred 3/25/12.

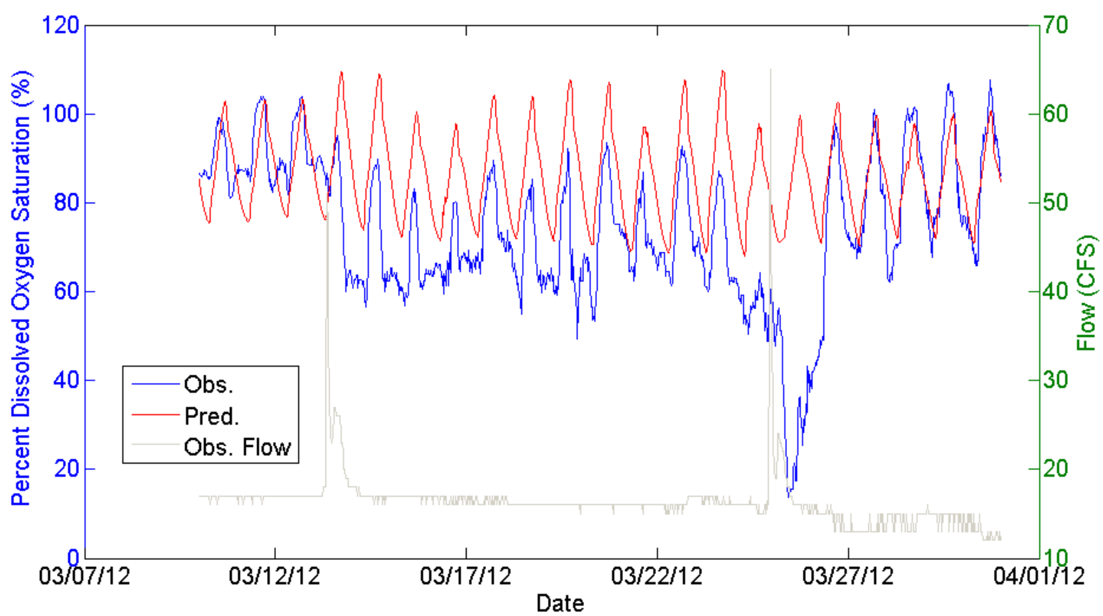

Figure 3-34: Observed and Simulated DO Percent Saturation at Site TF280, Validation Period T-5

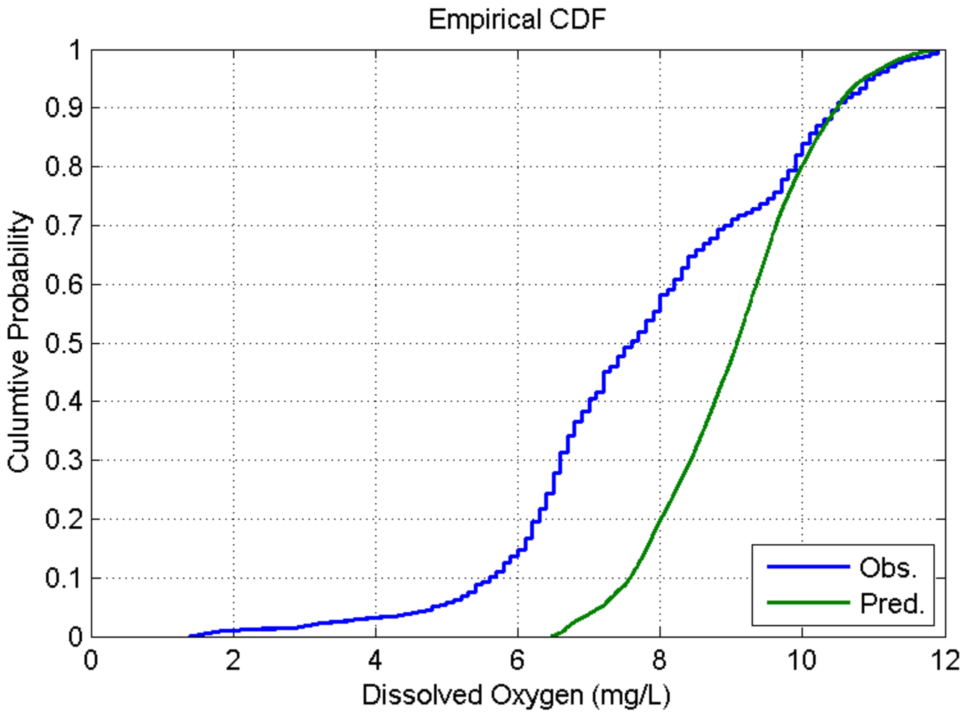

Figure 3-35: Observed and Simulated CDF of DO Concentration at Site TF280, Validation Period T-5

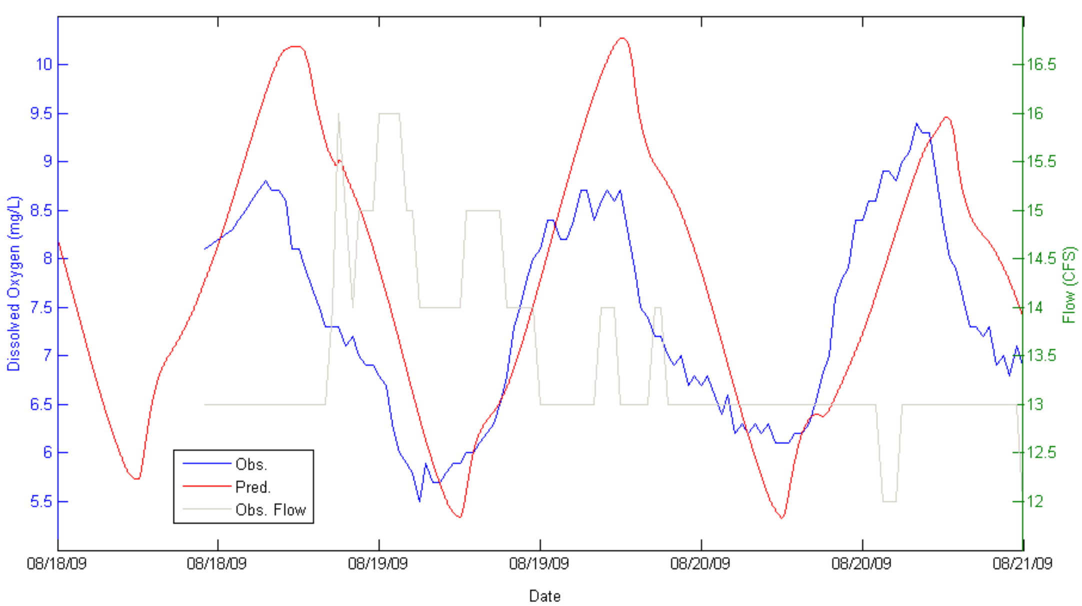

Figure 3-36: Observed and Simulated DO Concentration at Site TF280, Validation Period T-1

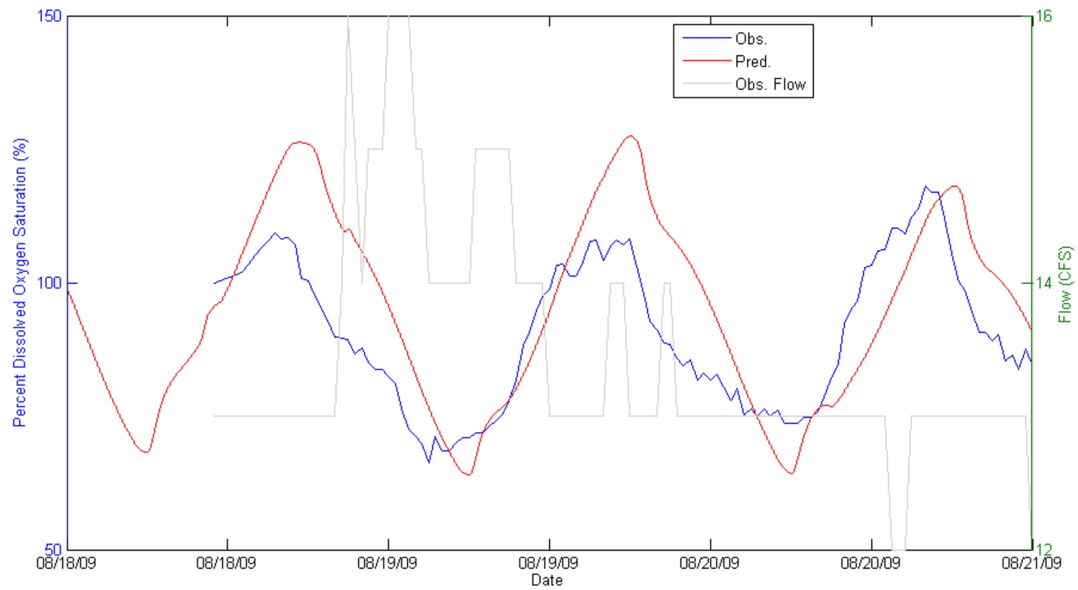

Figure 3-37: Observed and Simulated DO Percent Saturation at Site TF280, Validation Period T-1

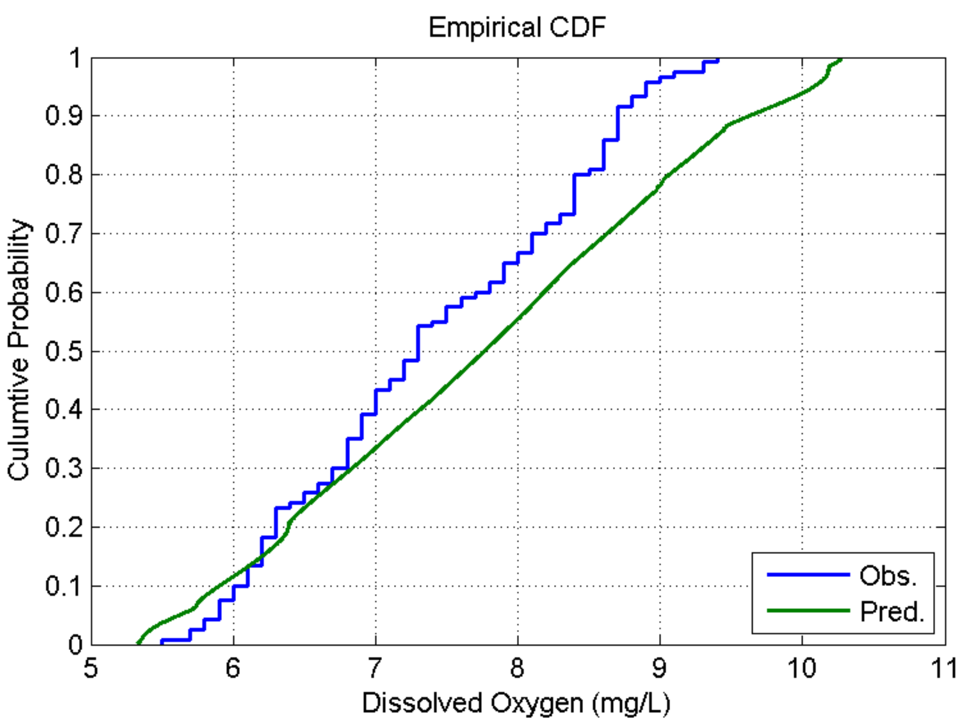

Figure 3-38: Observed and Simulated CDF of DO Concentration at Site TF280, Validation Period T-1

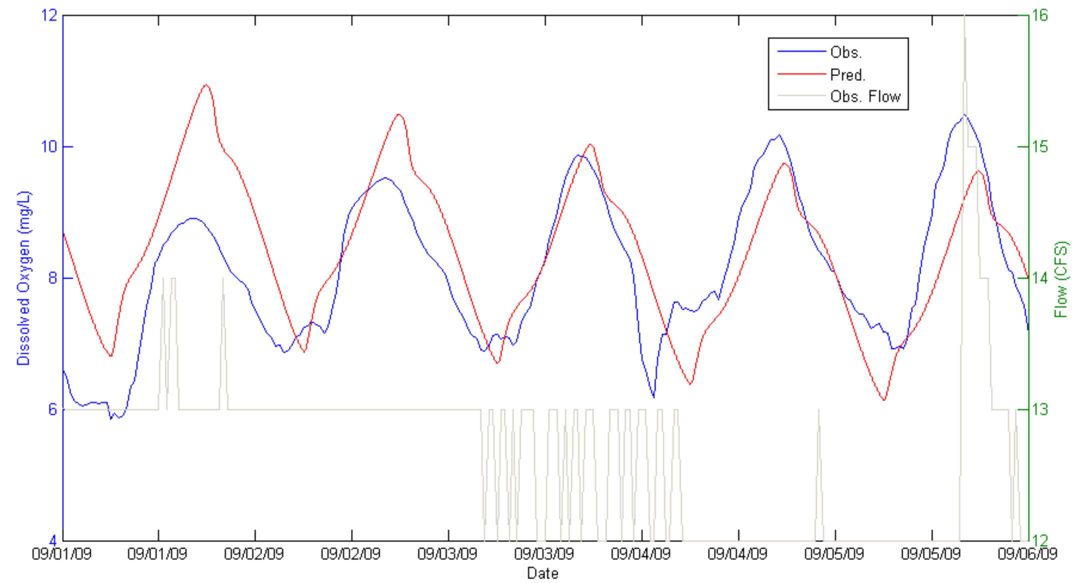

Figure 3-39: Observed and Simulated DO Concentration at Site TF280, Validation Period T-2

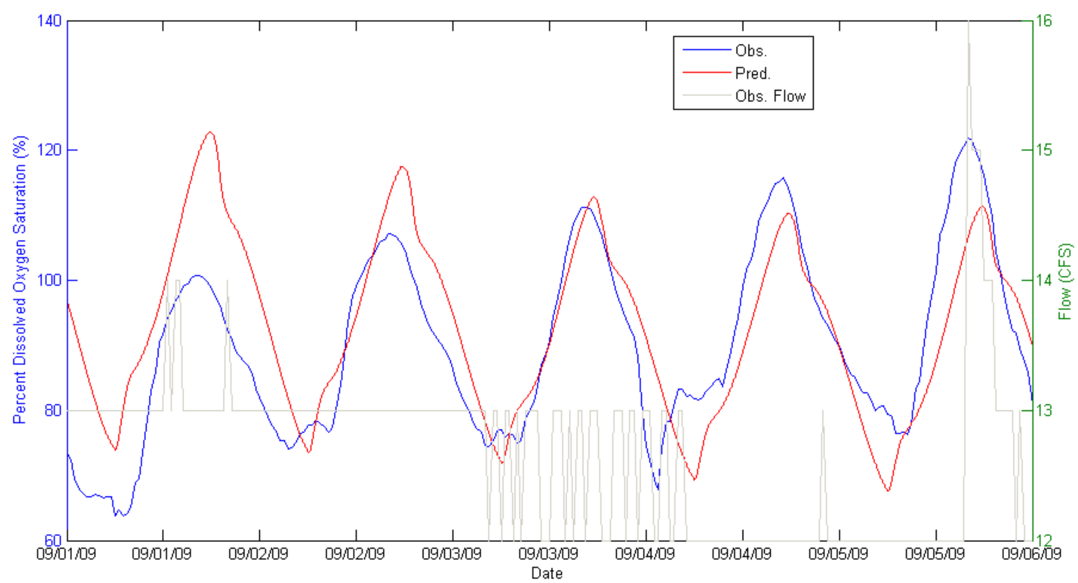

Figure 3-40: Observed and Simulated DO Percent Saturation at Site TF280, Validation Period T-2

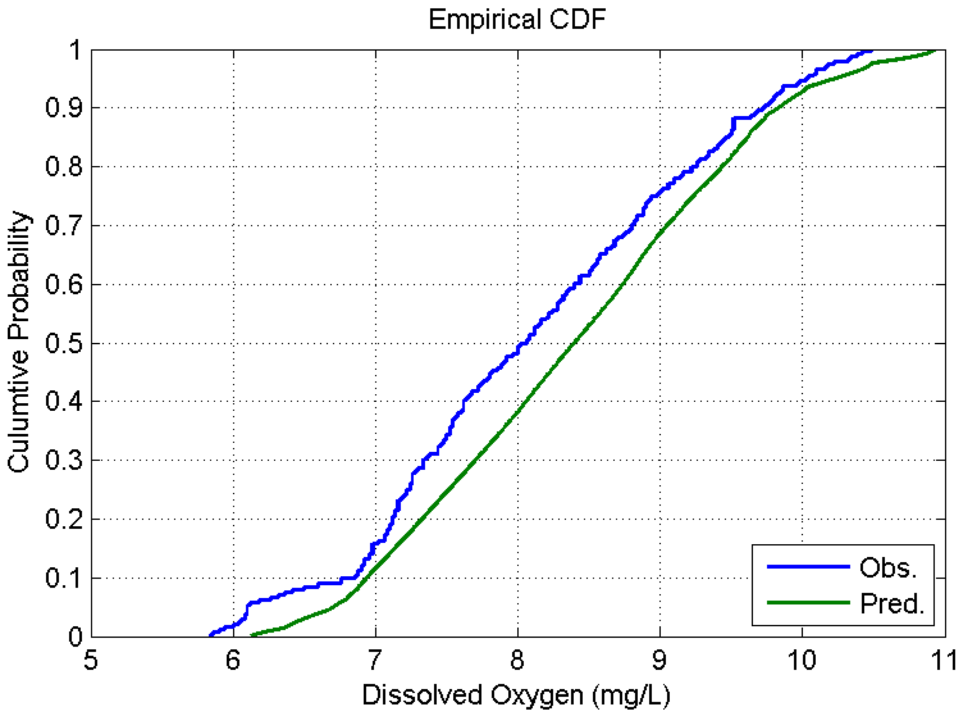

Figure 3-41: Observed and Simulated CDF of DO Concentration at Site TF280, Validation Period T-2

Table 3-20: TTF DO Model Evaluation Statistics for Validation Periods T-1 through T-5

All values are in mg/L.

	T-1		T-2		T-3		T-4		T-5	
	MAE	RMSE	MAE	RMSE	MAE	RMSE	MAE	RMSE	MAE	RMSE
DO: all timesteps	0.89	1.07	0.75	0.93	0.50	0.65	1.09	1.33	1.51	1.97
Daily Mean DO	0.63	0.78	0.64	0.76	0.38	0.52	0.87	0.52	1.26	0.52
Daily Min. DO	0.57	0.64	0.50	0.62	0.59	0.63	0.36	0.63	1.44	0.63
Daily DO Fluctuation	0.76	0.99	0.51	0.66	0.54	0.66	1.88	0.66	0.86	0.66

3.8.2 Cobbs Creek

The observed data from 4 periods totaling 36 days in 2010-2012 were used to validate the Cobbs Creek DO Model. Half-hourly DO concentration data at USGS Gage 01475548 (n=1728), and benthic algal density samples (n=72), were used to compare predicted and observed data. Based on results of the sensitivity analysis, the rate constants in Tables 3-17 and 3-18 were applied to all Cobbs DO Model validation periods.

Results and discussion

Benthic algal density was measured by collecting three replicate samples per sampling event at each site. The average, minimum and maximum values are plotted in Figures 3-42 through 3-47. Overall, predictions of benthic algal density at Sites DCC770 and DCC251 (model segments 1 and 39) were generally within the range of observed data, indicating that the model is reliably simulating benthic algae kinetics in the spring and summer seasons represented by Validation Periods C-2, C-3 and C-4. In C-2, the scour of benthic algae on 4/23/12 (Figure 3-6) could not be simulated in WASP 7.5, likely leading to modeled overprediction of algae during the immediate 3 day post-storm period. Four days after the storm, sufficient regrowth had occurred such that measured densities were more in agreement with model simulations. Simulations of C-3 and C-4 show predicted benthic algal densities falling within the range of observed data at both sites.

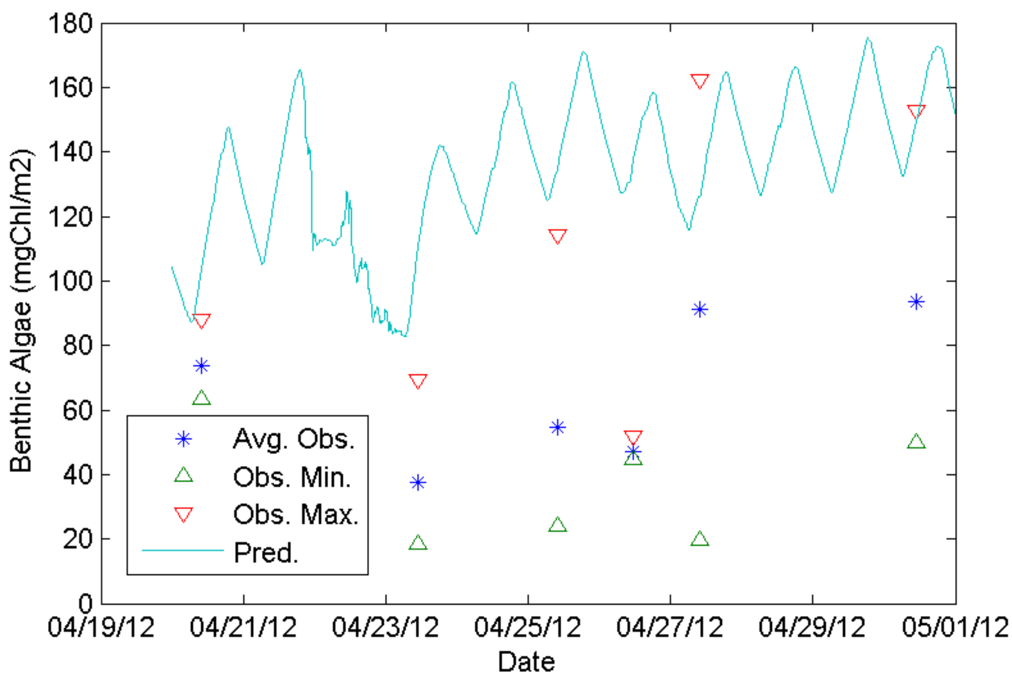

Figure 3-42: Observed and Simulated Benthic Algal Density at Site DCC770, Validation Period C-2. A scouring event occurred 4/23/12.

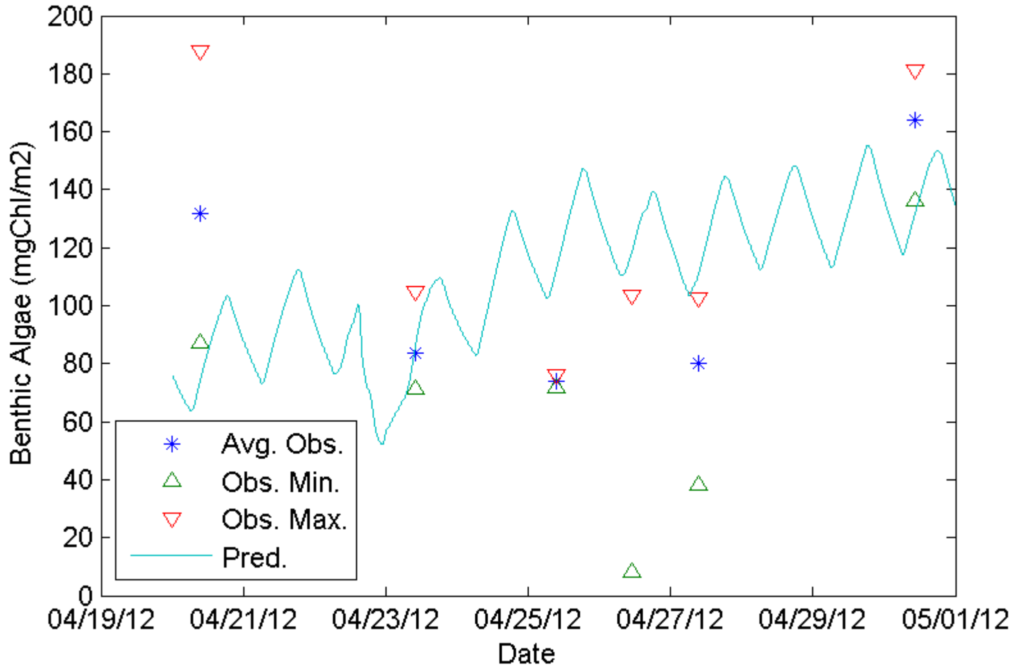

Figure 3-43: Observed and Simulated Benthic Algal Density at Site DCC251, Validation Period C-2. A scouring event occurred 4/23/12.

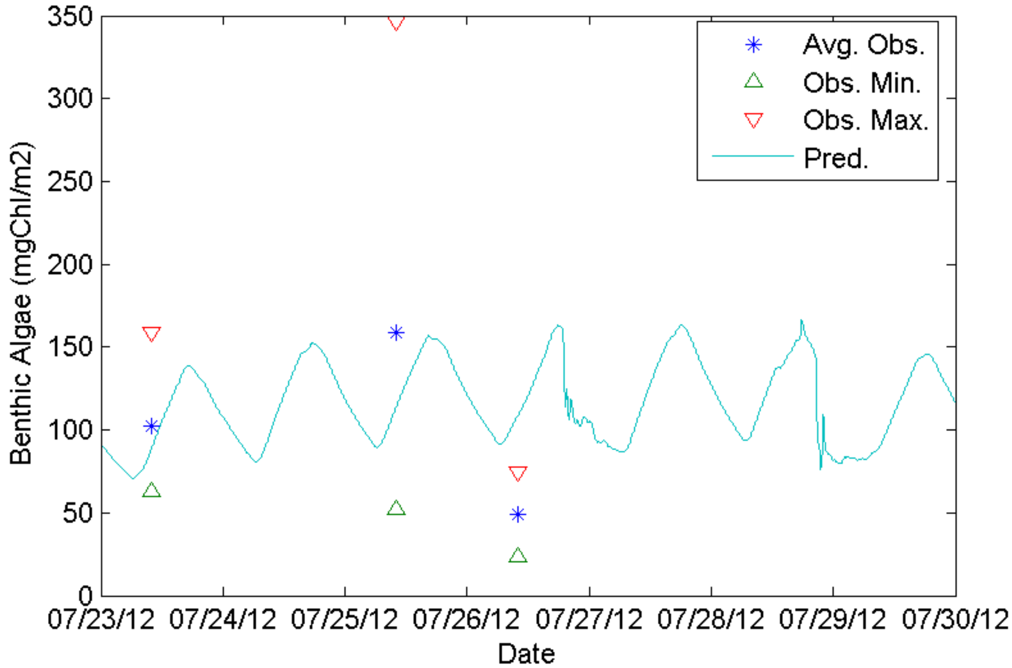

Figure 3-44: Observed and Simulated Benthic Algal Density at Site DCC770, Validation Period C-3

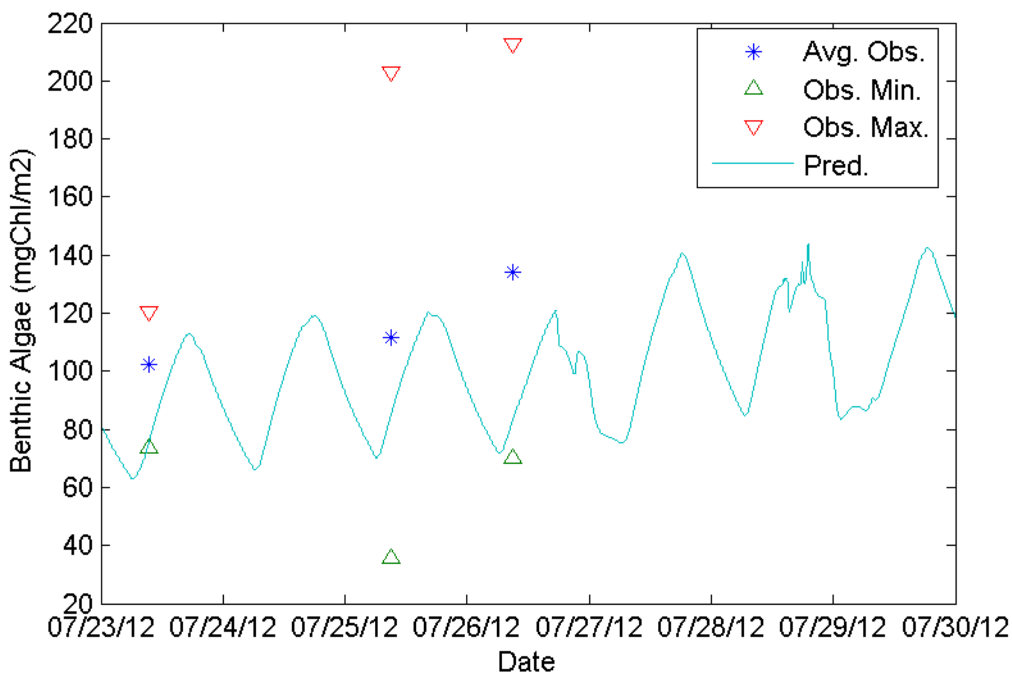

Figure 3-45: Observed and Simulated Benthic Algal Density at Site DCC251, Validation Period C-3

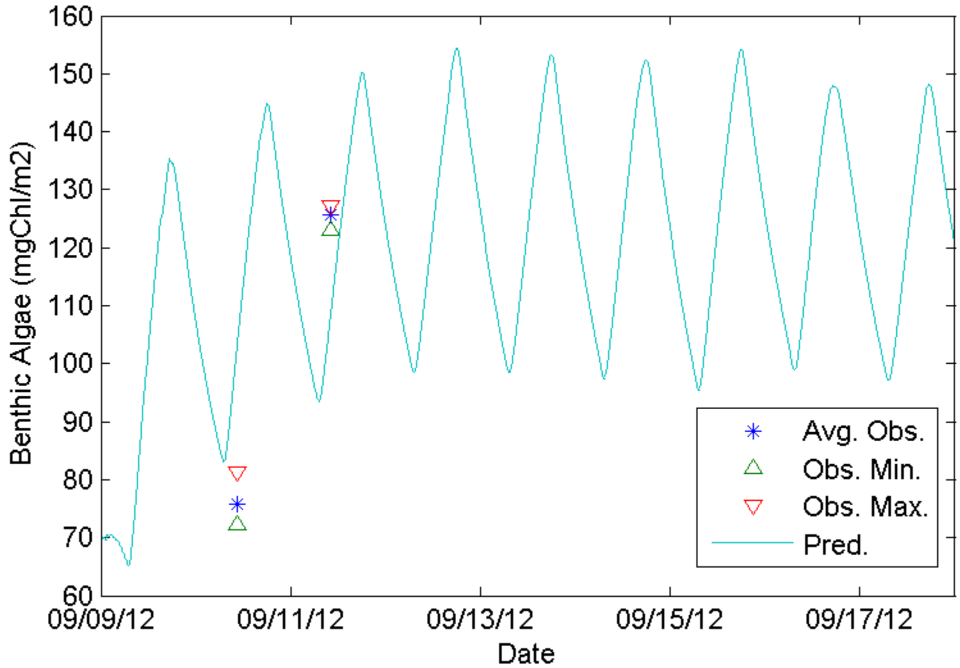

Figure 3-46: Observed and Simulated Benthic Algal Density at Site DCC770, Validation Period C-4

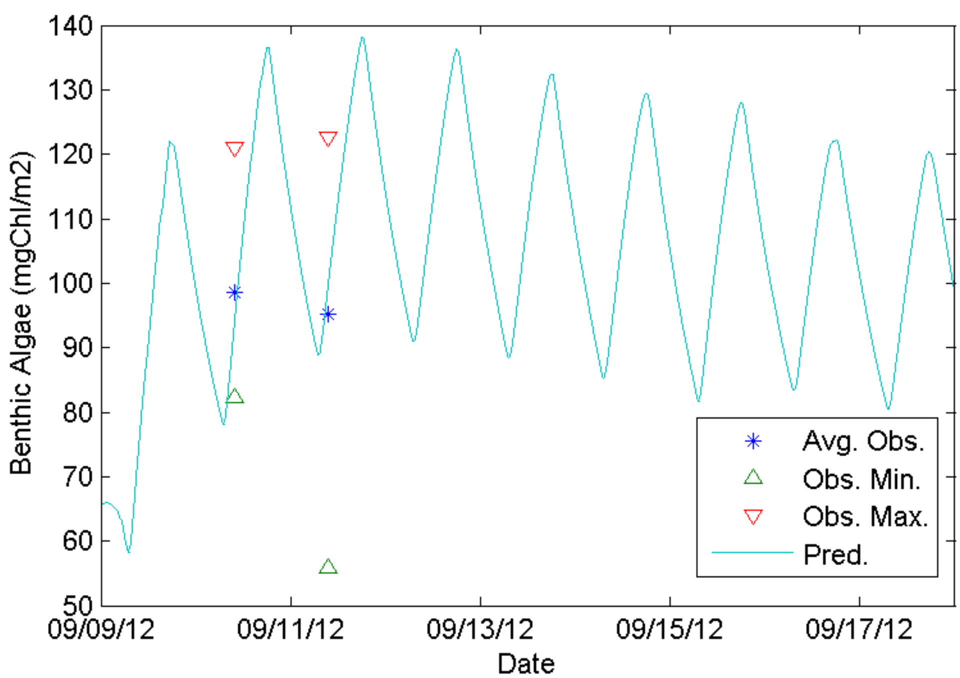

Figure 3-47: Observed and Simulated Benthic Algal Density at Site DCC251, Validation Period C-4

Simulations of DO at Site DCC251 (USGS Gage 01475548; Segment 40) were made using rate constants in Tables 3-17 and 3-18. All global constants were set to the same values as the TTF DO Model except for the benthic algae respiration rate. Considering that the taxonomic analysis of the two streams found moderately different benthic algal communities, it is reasonable to have some differences in benthic algae kinetic rate constants. Validation period C-1 occurred in spring and C-2 through C-5 occurred in summer. Plots are shown in Figures 3-48 through 59 and evaluation statistics are listed in Table 3-21.

In general, the results indicate adequate model simulation performance, except for the two limitations described earlier. The first is the lack of a scour algorithm in WASP 7.5. Scour and regrowth were apparent in C-2; DO is well simulated in C-2 except during the immediate 3 day post-storm period (Figure 3-51). Prior to the storm, and following sufficient regrowth after the storm, DO is well simulated. The second limitation is the failure to simulate the rapid transient decrease in DO during the small storm in C-3 (Figure 3-54). The H&H Model performed well during C-3 indicating CSO flows were well predicted. A more nuanced approach to CSO loading such as applying multiple CBOD constituents, one for stormwater and another for base wastewater, should be explored as a future improvement.

The similarities in variance of observed and simulated DO for C-1 (Figure 3-50), indicate benthic algal processes were well simulated with a daily DO concentration fluctuation MAE of 0.66 mg/L. Similarities in medians indicate the balance between SOD, BOD, reaearation, photosynthesis and respiration were well simulated in C-1 and C-4 (Figures 3-50 and 3-53); daily mean DO concentration MAE was 0.70 and 1.26 mg/L, respectively.

Daily minimum DO concentrations were predicted with MAE of 0.65 to 1.10 mg/L for the three periods without a rapid transient DO decrease, i.e, C-1, C-2 and C-4.

Overall, MAE and RMSE across all validation periods were less than or equal to 1 mg/L in 10 of 32 outcomes, and less than 1.5 mg/L in 19 of 32 outcomes, ranging from 0.65 to 3.11 mg/L. There was adequate model performance in representing the effects of SOD and reaeration in Cobbs Creek, and eutrophication kinetics outside of the immediate period of scouring and initial regrowth. The effects of CBOD during small CSO events and the ability to simulate scour and initial regrowth are the main issues that require future improvement.

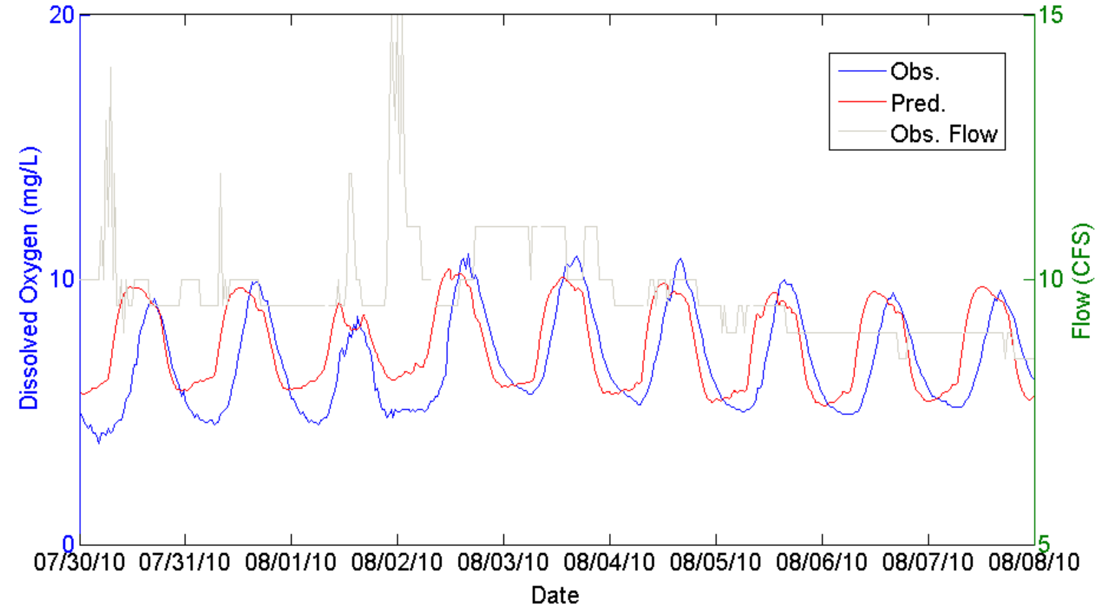

Figure 3-48: Observed and Simulated DO Concentration at Site DCC251, Validation Period C-1

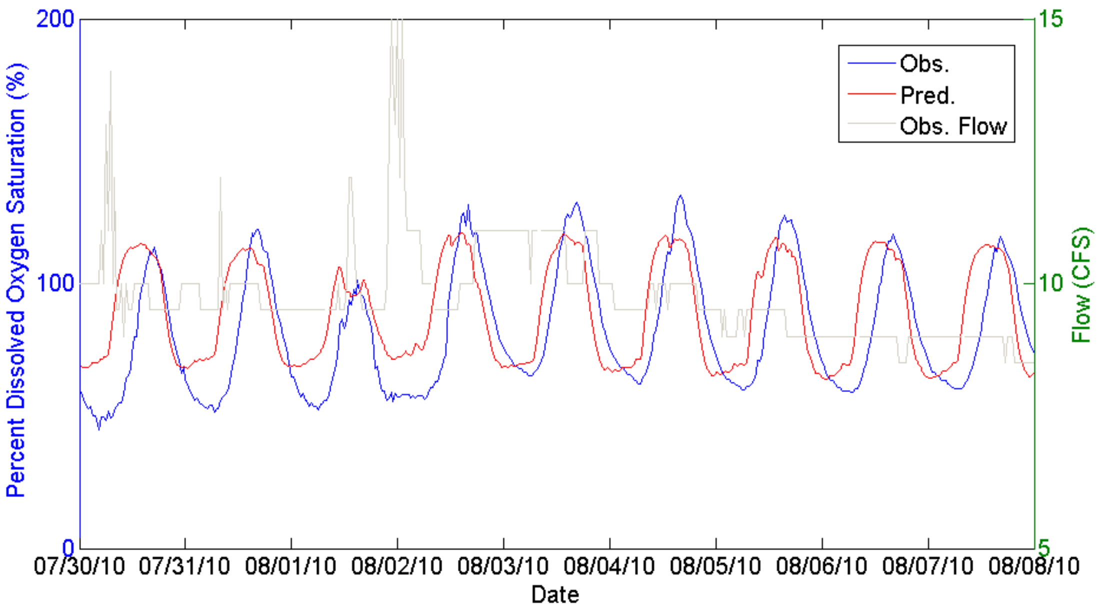

Figure 3-49: Observed and Simulated DO Percent Saturation at Site DCC251, Validation Period C-1

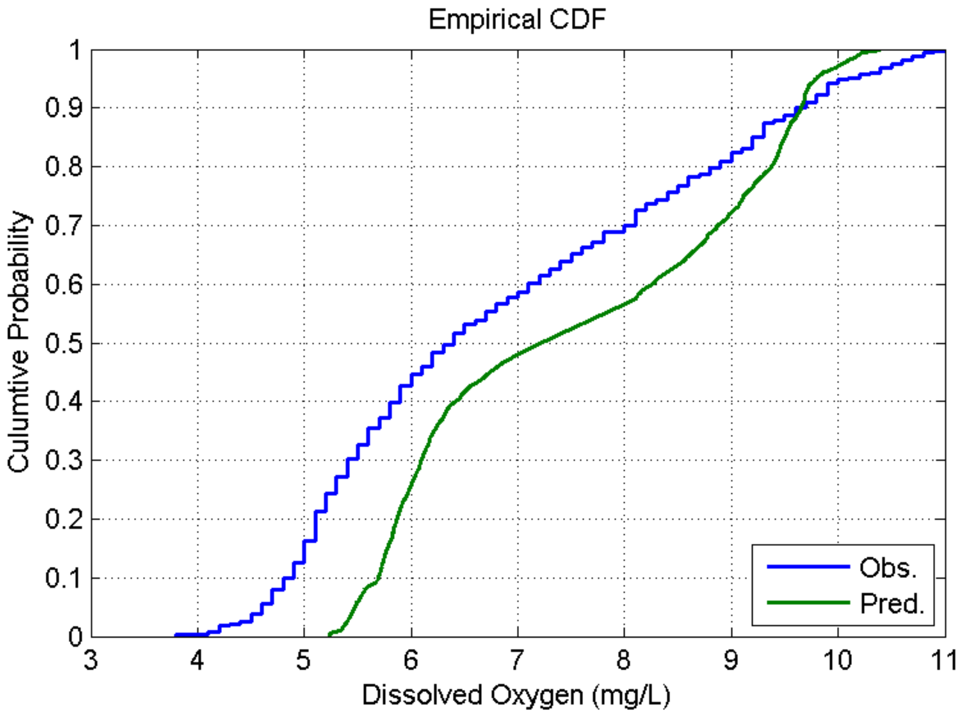

Figure 3-50: Observed and Simulated CDF of DO Concentration at Site DCC251, Validation Period C-1

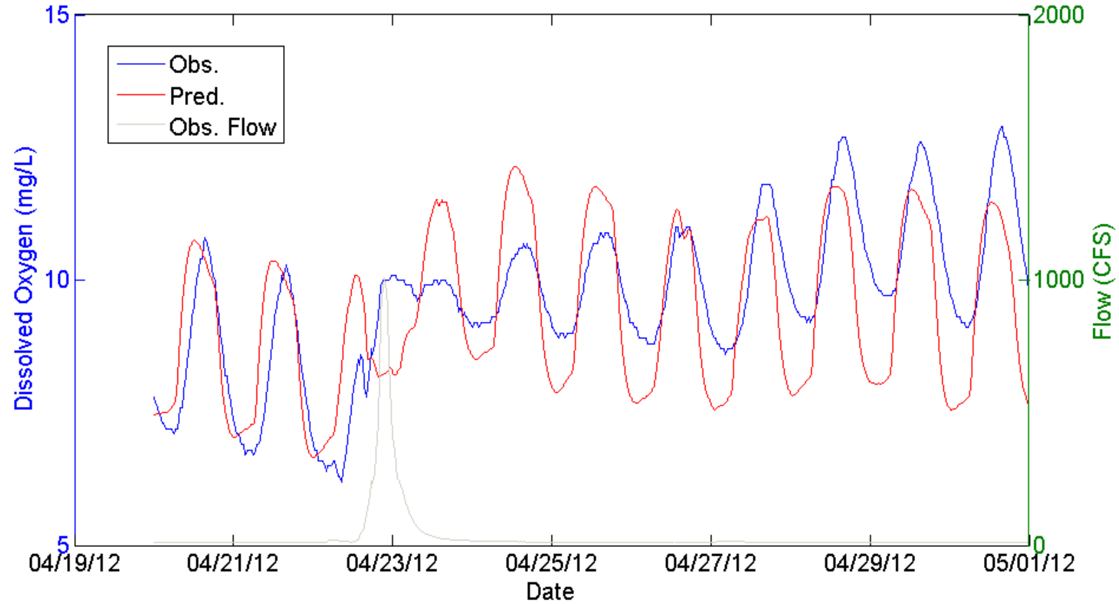

Figure 3-51: Observed and Simulated DO Concentration at Site DCC251, Validation Period C-2

A scouring event occurred on 4/23/12.

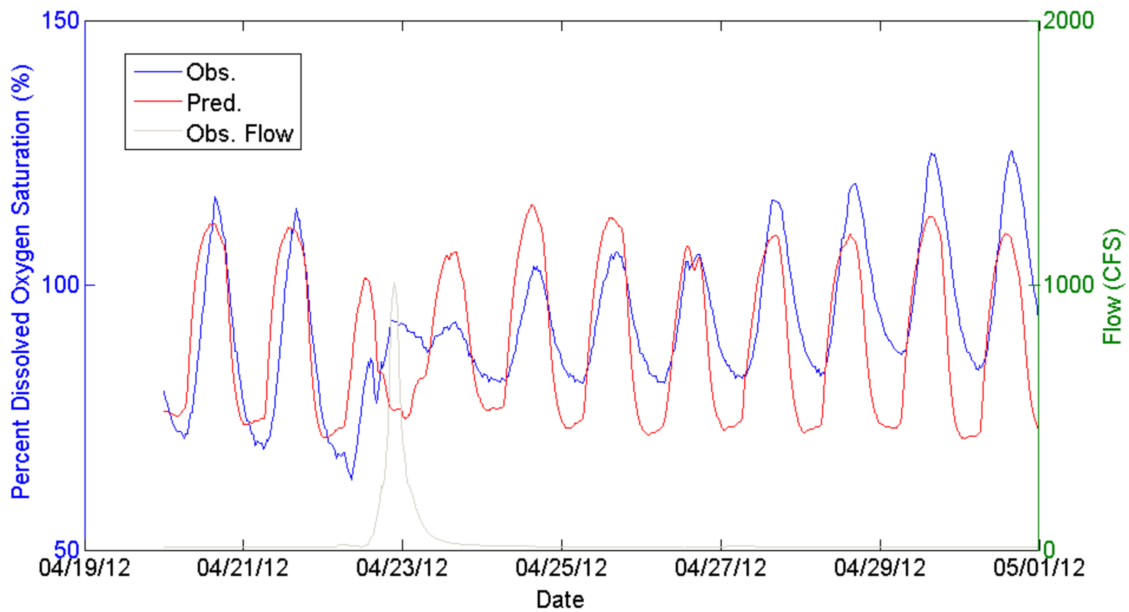

Figure 3-52: Observed and Simulated DO Percent Saturation at Site DCC251, Validation Period C-2

A scouring event occurred on 4/23/12.

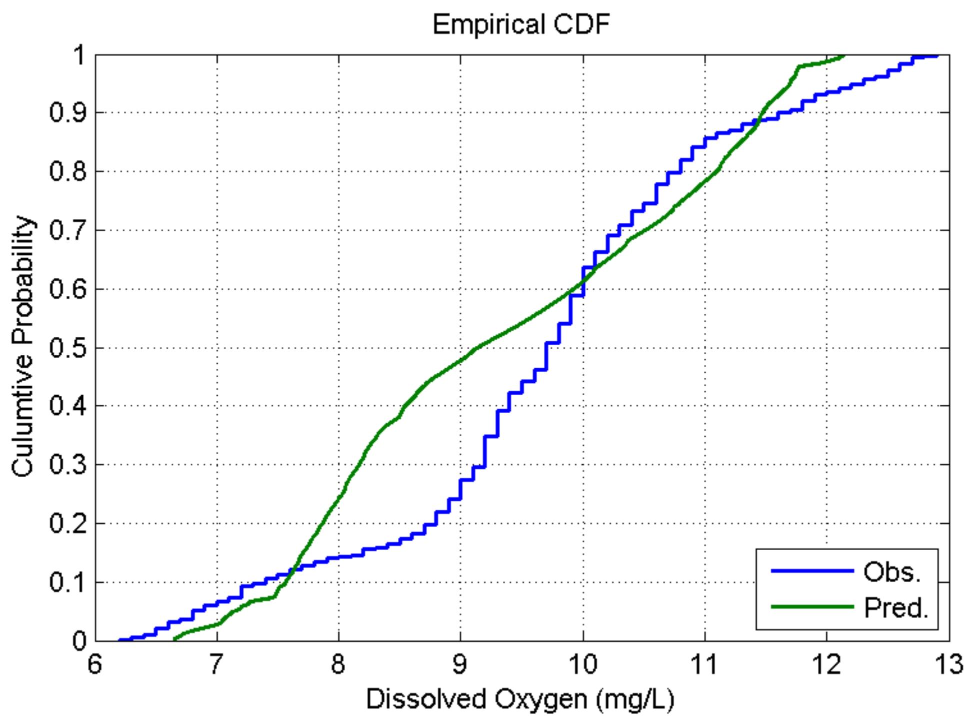

Figure 3-53: Observed and Simulated CDF of DO Concentration at Site DCC251, Validation Period C-2

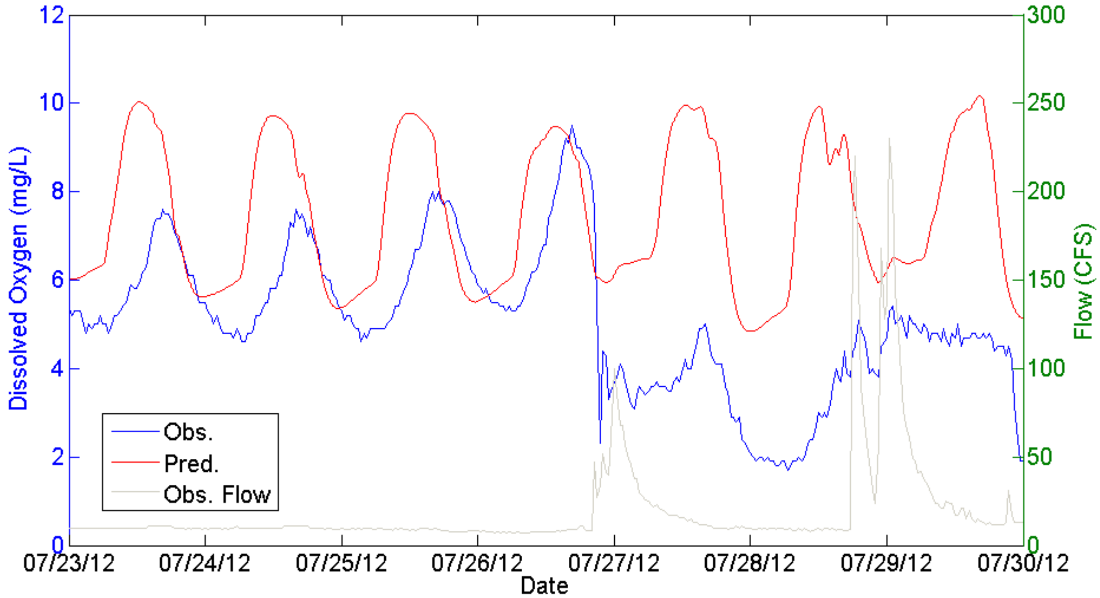

Figure 3-54: Observed and Simulated DO Concentration at Site DCC251, Validation Period C-3

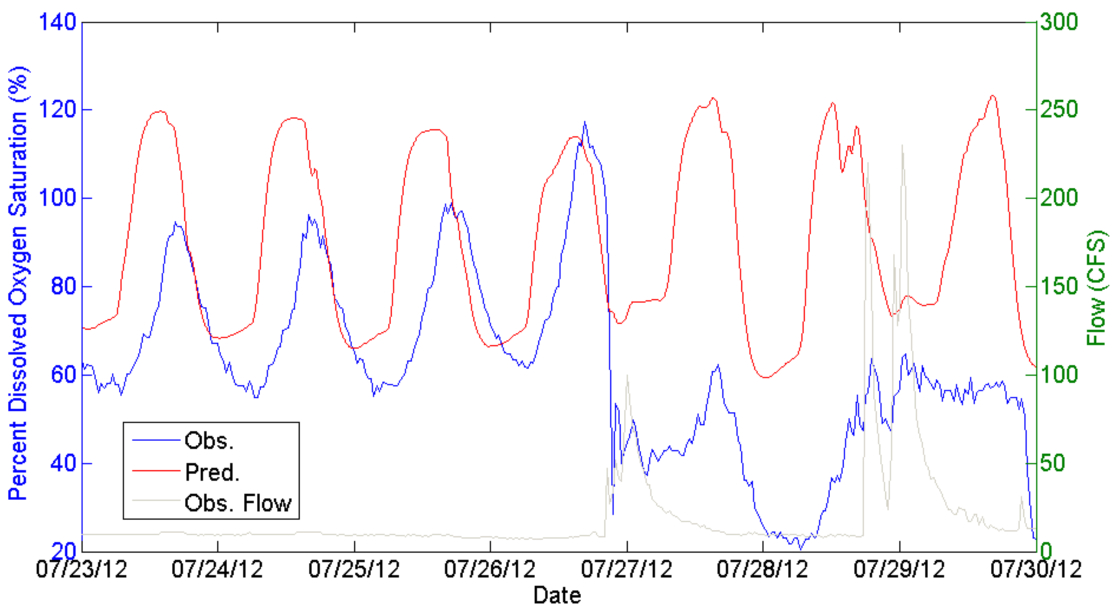

Figure 3-55: Observed and Simulated DO Percent Saturation at Site DCC251, Validation Period C-3

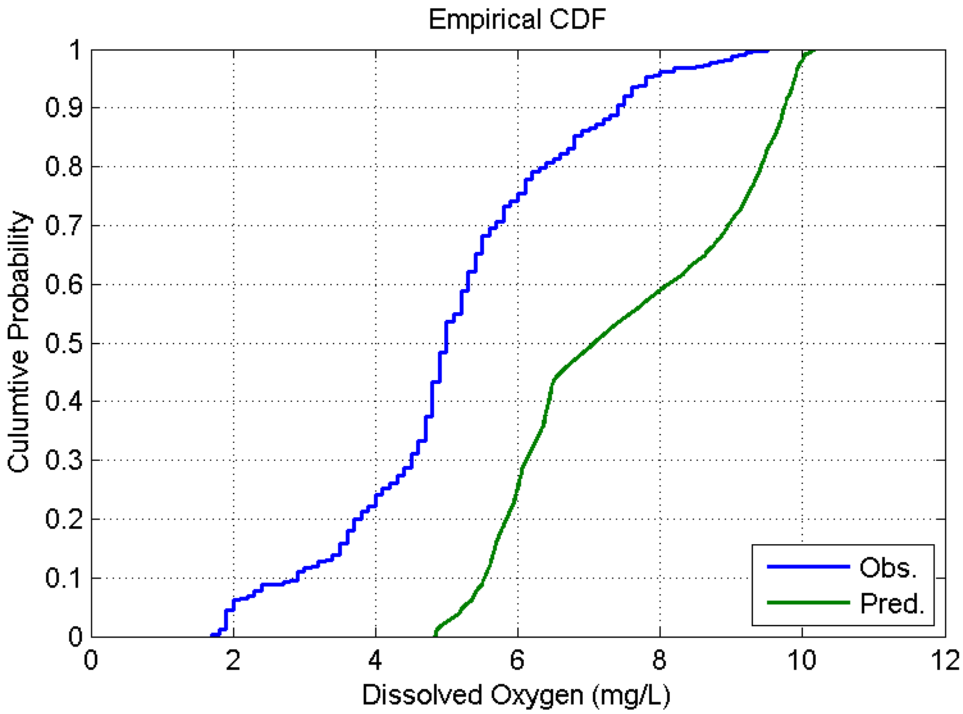

Figure 3-56: Observed and Simulated CDF of DO Concentration at Site DCC251, Validation Period C-3

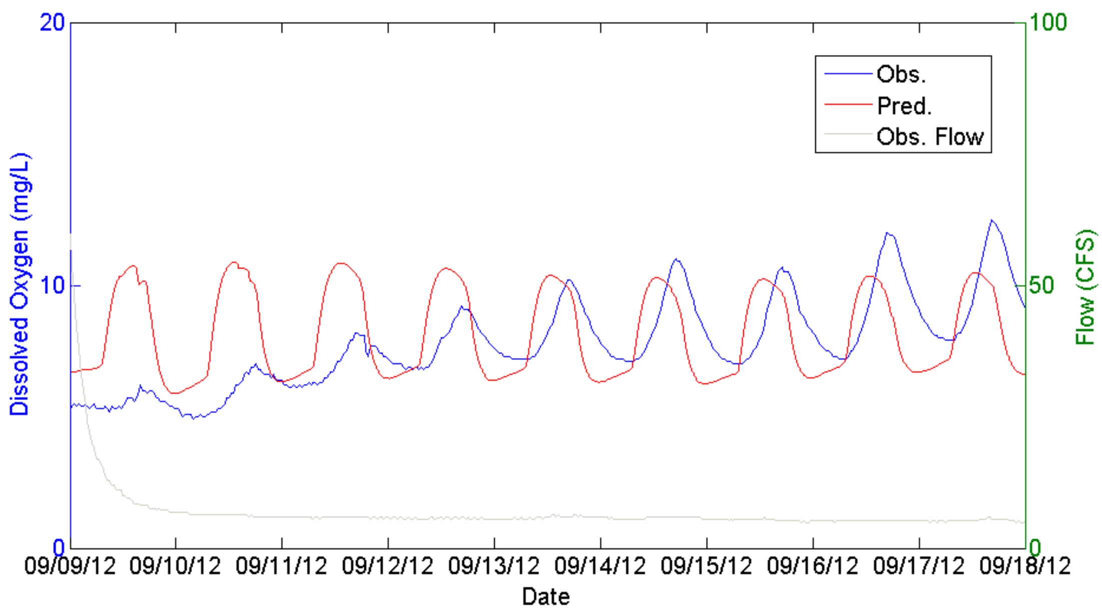

Figure 3-57: Observed and Simulated DO Concentration at Site DCC251, Validation Period C-4

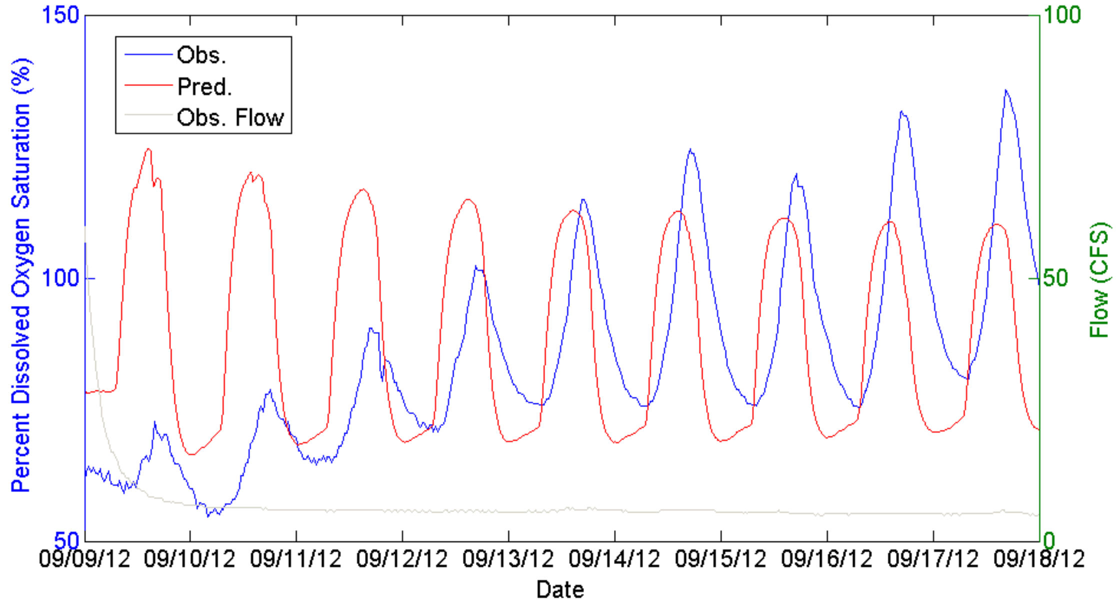

Figure 3-58: Observed and Simulated DO Percent Saturation at Site DCC251, Validation Period C-4

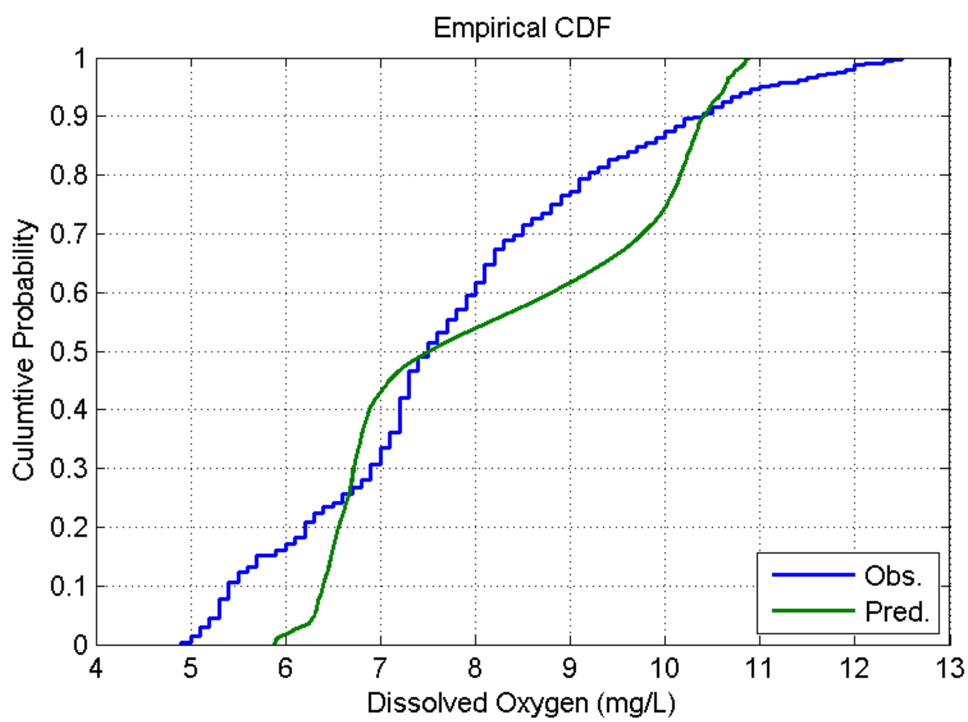

Figure 3-59: Observed and Simulated CDF of DO Concentration at Site DCC251, Validation Period C-4

Table 3-21: Cobbs DO Model Evaluation Statistics for Validation Periods C-1 through C-4

	C-1		C-2		C-3		C-4	
	MAE	RMSE	MAE	RMSE	MAE	RMSE	MAE	RMSE
DO: all time steps	1.26	1.62	1.02	1.23	2.54	3.11	1.72	2.13
Daily Mean DO	0.70	0.83	0.74	0.94	2.52	2.77	1.26	1.56
Daily Min. DO	0.65	0.87	1.10	1.28	2.16	2.45	0.97	1.15
Daily DO Fluctuation	0.66	0.81	1.00	1.31	1.70	1.87	1.48	1.95

All values are in mg/L.

3.9 Dissolved Oxygen Model Limitations

The TTF and Cobbs DO Models are limited by many factors. Chief among them, as evidenced in these applications, is the lack of a benthic algae scour algorithm in WASP 7.5. This prevents long term simulations which are desirable to model the stream response to runoff from the typical year precipitation. The Water Department has begun a dialogue with the WASP 7.5 developers at US EPA to address this, and it is hoped that a future release of WASP will add a scour algorithm.

The WASP 7.5 version of the model also contains a limit in the input file of 10,000 entries per boundary, so that at a 30 second time step, ~3.5 days of wet weather can be simulated in full temporal resolution. The Water Department obtained a software update from US EPA that expanded the limit to 50,000. An even greater limit would be needed for continuous simulation of the typical year.

Furthermore, the WASP 7.5 version represents the benthic algal community as one group with a single set of rate constants, but in the stream there are multiple groups each with different growth and loss rates. Competition among algal species throughout the spring, summer and fall seasons can bring a change in the dominant group and its particular set of kinetic rates. Any effects on overall biomass density are lost when representing the entire community as one group.

Other possible limitations relate to modeling decisions made by the Water Department, and are not directly attributable to WASP. Settling of particulate carbon, organic nitrogen and organic phosphorus were not modeled. Instead, a simpler approach was used that exclusively transformed particulate organic matter via dissolution. Adsorption of orthophosphate and ammonia were not modeled. Light extinction was modeled as a global rather than spatially variable constant, without additional effects from dissolved organic carbon or suspended solids. The assignments of spatially variable SOD and FAS were limited by available sampling and channel survey data, respectively.

3.10 Potential Areas for Improvement

The development of the DO Models followed an approach of continuous improvement and validation. The selected versions of the models presented in this report represent a snapshot in time, and does not limit the development of future updates, which may include more detailed and accurate information, additional simplifications, changes to a different model platform version, or even the selection of a different model platform. Model development flexibility is paramount to achieving models that best fit a variety of applications and analysis goals.

As with all models, the TTF and Cobbs DO Models are limited by the quality of the monitored validation data, both flow and water quality, as well as the accuracy of the information used to construct the models. While an effort was made to use the best available data, future improvements to GIS data sets, additional bathymetry data, additional flow monitoring data, and additional water quality monitoring data could be used to improve the predictive ability of these models.

Specific areas for potential model improvement are listed below.

- **Rapid transient DO decreases during storms.** In their present form, the DO Models do not adequately simulate this phenomenon. Two main avenues will be explored to rectify this – improvements in the H&H Model during small storms, and the use of multiple CBOD species, for stormwater and sanitary baseflow, that each have their own decay rate. For example, if a higher decay rate were assigned to CBOD that exclusively represents sanitary wastewater, rapid transient DO decreases from small CSO events might be better simulated.
- **Long term simulation**. This capability is a precursor to simulating the typical year for precipitation and long term forecasts of future scenarios. Because of the frequency of disturbance and algal losses due to scouring in both creeks, a benthic algae scour algorithm is needed to conduct meaningful long term simulations. When this capability is established, the Water Department would transition to using a first order rather than zero order growth model.
- **Benthic algae data.** Better use could be made of the locally measured intracellular CNP ratios. Attempts to date have failed to replicate the degree of diel DO fluctuation typically observed in the TTF and Cobbs Creeks. To date, the observed trend is better achieved by applying the Redfield ratio in the model. Further efforts will be carried out to explore using the local CNP data. Also, more pre- and post-storm sampling could be performed to characterize algal scour and regrowth.
- **SOD data.** Sampling efforts in 2012 yielded only one viable location in Cobbs Creek. Other locations in Cobbs Creek as well as the East and West Indian Creeks and Naylors Run tributaries could be explored to provide additional SOD data in the Cobbs Creek Watershed.
- **Stream restoration updates to the H&H Model.** The Water Department is in the midst of restoring several miles of stream-way in the TTF and Cobbs Creeks Watersheds.

Changes to channel morphology need to be incorporated in the H&H Model to provide updated estimates of flow, depth and velocity, which in turn affect simulations of pollutant transport and reaeration. For example, stream daylighting in a section of Indian Creek was recently completed and needs to be reflected in the Cobbs Creek H&H Model when simulating post-construction time periods.

- **Additional methods for DO model validation.** In addition to comparing observed and simulated DO and benthic algal density, comparisons could also be made of observed and simulated stream metabolism as a method for model validation. Continuous DO data from the USGS gages could be used to derive estimates of observed community productivity and respiration. Uehlinger and Naegeli (1998), Uehlinger *et al.* (2003), and Srivastra outline approaches to calculating stream metabolism that could be applied to these data.
- **Uncertainty analysis.** Water quality models are imperfect representations of natural systems, and are subject to uncertainties. For the TTF and Cobbs Creeks DO models, a computationally efficient method such as Latin Hypercube Sampling could be explored using WASP input parameter probability distributions from literature (*e.g.*, Lindenschmidt, 2006) and from local sampling data. This would provide a probabilistic range of model output, rather than a single-value fixed model output.

3.11 Conclusions

DO water quality models were developed and validated for the TTF and Cobbs Creek. Water quality simulations were performed with a model (WASP 7.5) that simulated coupled benthic algae, SOD, BOD, nitrification, and reaeration processes. A total of nine validation periods were selected to represent the key phenomena impacting DO in TTF and Cobbs Creeks – eutrophic algal blooms, high sediment oxygen demand, and rapid transient decreases in DO during CSO events. Loading of CBOD and nutrients from stormwater runoff, combined sewer system outfalls, secondary tributaries and baseflow were each considered in model development. A sensitivity analysis was conducted to identify the key global and spatially variable rate constants and coefficients. Spatially variable constants were parameterized with the aid of extensive SOD measurements and high resolution stream surveys of bed material.

Time series plots, CDF plots, and statistical summaries were used to evaluate water quality model performance. Analyses indicate adequate water quality model performance, particularly for TTF Creek. Future areas of improvement have been identified and can be pursued to enhance model performance for both TTF and Cobbs Creeks.

References

Alp, E. and C.S. Melching, 2006. Calibration of a Model for Simulations of Water Quality During Unsteady Flow in the Chicago Waterway System and Application to Evaluate Use Attainability Analysis Remedial Actions; Technical Report #18. Submitted to the Metropolitan Water Reclamation District of Greater Chicago.

Ambrose, R.B., Martin, J.L., Wool, T.A., 2006. WASP7 Benthic Algae – Model Theory and User's Guide. EPA 600/R-06/106. USEPA Office of Research and Development, Washington, DC.

Biggs, B. J. F, 2000. Eutrophication of Streams and Rivers: Dissolved Nutrient-Chlorophyll Relationships for Benthic Algae. Journal of the North American Benthological Society 19: 17-31.

Biggs, B. J. F. and M. E. Close, 1989. Periphyton Biomass Dynamics in a Gravel Bed River: The Relative Effect of Flow and Nutrients. Freshwater Biology 22: 209-231.

Borchardt, M. A, 1996. Nutrients. Pages 183-227 in: Algal Ecology (R. J. Stevenson, M. L. Bothwell, and R. L. Lowe, eds.), Academic Press, San Diego.

Bott, T.L. and J.D. Newbold, 2000. Effects of Water Velocity on Jackson River Periphyton Biomass and Nutrient Uptake. Submitted by Stroud Water Research Center. Publication No. 2000005.

Bowie, G., Mills, W., Porcella, D., Campbell, C., Pagenkopf, J., Rupp, G., Johnson, K., Chan, P., Gherini, S., and Chamberlin, C., 1985. Rates, Constants and Kinetics Formulations in Surface Water Quality Modeling (2nd edition). EPA-600/3-85/040, Athens, Georgia.

Butts, T.A. and Evans, R.L., 1983. Effects of Channel Dams on Dissolved Oxygen Concentrations in Northeastern Illinois Streams, Circular 132, State of Illinois, Dept. of Reg. and Educ., Illinois Water Survey, Urbana, IL.

Cadwallader, T. E. and A. J. McDonnell, 1969. A Multivariate Analysis of Reaeration Data, *Water Res.*, 3, 731–742.

Camp Dresser & McKee, 2004. Indianapolis CSO LTCP Hydraulic and Water Quality Modeling Report. Prepared for the City of Indianapolis.

Chapra, S.C., 1997. *Surface Water-Quality Modeling*. New York: McGraw Hill.

Chetelat, J., F. R. Pick, A. Morin, and P. B. Hamilton, 1999. Periphyton Biomass and Community Composition in Rivers of Different Nutrient Status. Canadian Journal of Fisheries and Aquatic Sciences 56: 560-569.

Churchill, M.A., Elmore, H.L., and Buckingham, R.A., 1962. Prediction of Stream Reaeration Rates. J. San. Engr. Div. ASCE SA4:1, Proc. Paper 3199.

Commonwealth of Pennsylvania Department of Environmental Protection, 2013. Pennsylvania Code Title 25. Environmental Protection. Chapter 93. Water Quality Standards.

Covar, A.P. 1976. Selecting the Proper Reaeration Coefficient for Use in Water Quality Models. Presented at the USEPA Conference on Environmental Simulation and Modeling, April 19-22, Cincinnati, OH.

Cronin, G., McCutchan, J.H., Pitlick, J., and Lewis, W.M., 2007. Use of Shields Stress to Reconstruct and Forecast Changes in River Metabolism. Freshwater Biology 52:1587-1601.

Davis, J.F., 2002. Factors Affecting Photosynthetic Rates of Periphyton in Shallow Streams of Southeastern Pennsylvania. Water Environment Research 74:370-376.

Di Toro, D.M., P.R. Paquin, K. Subburamu, and D.A. Gruber, 1990. Sediment Oxygen Demand Model: Methane and Ammonia Oxidation. Journal of Environmental Engineering 116(5):945-986.

Eckhardt, K., 2005. How to construct Recursive Digital Filters for Baseflow Separation. Hydrological Processes 19(2):507-515.

Elder, J.W., 1959. The Dispersion Of Marked Fluid In Turbulent Shear Flow. J. Fluid Mech 5 (4), 544–560.

Faulkner, G., F. Horner, and W. Simonis. 1980. The Regulation of the Energy-Dependent Phosphate Uptake by the Blue-green Alga Anacystis nidulans. Planta 149: 138-143.

Flinders, C.A. and D.D. Hart, 2009. Effects of Pulsed Flows on Nuisance Periphyton Growths in Rivers: A Mesocosm Study. River Research and Applications 25:1320-1330.

Francouer, S. N, 2001. Meta-analysis of Lotic Nutrient Amendment Experiments: Detecting and Quantifying Subtle Responses. Journal of the North American Benthological Society 20: 358-368.

Giga, J.V., 1985. Sediment Oxygen Demand: A Comparison of Laboratory and In Situ Methods for a Passaic River Case Study. PhD Dissertation, Rutgers, The State University of New Jersey, New Brunswick, New Jersey.

Goldman, J. C, 1979. Temperature Effects on Steady-state Growth, Phosphorus Uptake, and the Chemical Composition of a Marine Phytoplankter. Microbial Ecology 5: 153-166.

Hantush, M.M., 2007. Modeling Nitrogen-Carbon Cycling and Oxygen Consumption in Bottom Sediments. Advances in Water Resources 30:59-79.

Higashino, M., C.J. Gantzer, and H.G. Stefan, 2004. Unsteady Diffusional Mass Transfer at the Sediment/Water Interface: Theory and Significance for SOD Measurement. Water Research 38:1-12.

Jones, J. R., M. M. Smart, and J. N. Burroughs, 1984. Factors Related to Algal Biomass in Missouri Ozark Streams. Verh. Int. Ver. Limnol (International Association of Theoretical and Applied Limnology) 22: 1867-1875.

Kilpatrick, F.A., and Wilson, J.F., Jr. 1989. Measurement of Time of Travel in Streams by Dye Tracing: U.S. Geological Survey Techniques of Water-Resources Investigations, book 3, chap. A9, 27 p.

Kjeldsen, K., 1994. The Relationship between Phosphorus and Peak Biomass of Benthic Algae in Small Lowland Streams. Verh. Int. Ver. Limnol. Limnol (International Association of Theoretical and Applied Limnology) 25: 1530-1533.

Kluitenberg, E.H., Mercer, G.W., and Kaunelis, V., 1999. Water Quality Modeling to Support the Rouge River Restoration. *Proc. National Conf. on Retrofit Opport. for Water Rec. Protect. in Urban Environ.,*Chicago, IL, EPA/625/C-99/001, U.S. EPA, Washington, D.C., 160 p.

Lim, K. J., B. A. Engel, Z. Tang, J. Choi, K. Kim, S. Muthukrishnan, and D. Tripathy, 2005. Automated Web GIS Based Hydrograph Analysis Tool, WHAT. Journal of the American Water Resources Association 41(6):1407-1416.

Lindenschmidt, K-E, 2006. The Effect of Complexity on Parameter Sensitivity and Model Uncertainty in River Water Quality Modelling. Ecological Modelling 190:72-86.

Lohman, K., J. R. Jones, and B. D. Perkins, 1992. Effects of Nutrient Enrichment and Flood Frequency on Periphyton Biomass in Northern Ozark Streams. Canadian Journal of Fisheries and Aquatic Sciences 49: 1198-1205.

Louis Berger Group, 2010. Benthic TMDL Development for the Jackson River, Virginia. Submitted to Virginia Department of Environmental Quality.

Lyne, V.D. and M. Hollick, 1979. Stochastic Time-Variable Rainfall-Runoff Modeling. *In:* Hydro. and Water Resour. Symp. Institution of Engineers Australia, Perth, Australia, pp. 89-92.

McBride, G.B., 2002. Calculating Stream Reaeration Coefficients from Oxygen Profiles. Journal of Environmental Engineering 128:384-386.

Miskewitz, R., Francisco, K. and Uchrin, C., 2010. Comparison of a Novel Profile Method to Standard Chamber Methods for Measurement of Sediment Oxygen Demand. Journal of Environmental Science and Health 45:795-802.

Miskewitz, R., 2011. Sediment Oxygen Demand Measurements Collected in the Tacony Creek, Philadelphia, Pennsylvania. Data Report submitted to Philadelphia Water Department.

Miskewitz, R., 2012. Sediment Oxygen Demand Measurements Collected in Tacony and Cobbs Creeks, Philadelphia, Pennsylvania. Data Report submitted to Philadelphia Water Department.

Nakamura, Y. and H.G. Stefan, 1994. Effect of Flow Velocity on Sediment Oxygen Demand: Theory. Journal of Environmental Engineering 120(5):996-1016.

National Renewable Energy Laboratory, 2012. National Solar Radiation Data Base 1991-2010 Update. <http://rredc.nrel.gov/solar/old_data/nsrdb/1991-2010/targzs/targzs_by_state.html#P>

O'Connor, D.J. and Dobbins, 1958. Mechanism of Reaeration in Natural Streams. Trans. Am. Soc. Civil Engin. 123:641-666.

Odum, H. T., 1956. Primary Production in Flowing Waters. Limnology and Oceanography 1:102-117.

O'Neil-Dunne, J., 2011. A Report on the City of Philadelphia's Existing and Possible Tree Canopy. Prepared for the US Forest Service. <http://www.fs.fed.us/nrs/utc/reports/UTC_Report_Philadelphia.pdf>

Owens, M., Edwards, R., and Gibbs, J., 1964. Some Reaeration Studies in Streams. Int. J. Air Water Poll. 8:469-486.

Philadelphia Water Department, 2004. Darby-Cobbs Watershed Comprehensive Characterization Report. Philadelphia, PA. 190 pp. <http://www.phillywatersheds.org/doc/DarbyCobbs_CCR.pdf>

Philadelphia Water Department, 2005. Tookany-Tacony/Frankford Watershed Comprehensive Characterization Report. Philadelphia, PA. 313 pp. <http://www.phillywatersheds.org/doc/Tacony_Frankford_CCR.pdf>

Philadelphia Water Department, 2011. Green City Clean Waters. Philadelphia, PA. 719 pp. <http://www.phillywatersheds.org/ltcpu/LTCPU_Complete.pdf>

Philadelphia Water Department, 2013. Tributary Water Quality Model for Bacteria; Consent Order & Agreement Deliverable VI. Philadelphia, PA. 239 pp. <http://phillywatersheds.org/doc/Tributary%20Water%20Quality%20Model%20for%20Bacteria%20Report.pdf>

Pitt, R., A. Maestre, R. Morquecho, D. Williamson, 2004. Collection and Examination of a Municipal Separate Storm Sewer System Database. Stormwater and Urban Systems Modeling Conference. In: Models and Applications to Urban Water Systems, Vol. 12 (edited by W. James). CHI. Guelph, Ontario, pp. 257-294.

Redfield, A.C., B.H. Ketchum, and F.A. Richards, 1963. The Influence of Organisms on the Composition of Seawater, in *The Sea*, M.N. Hill, ed. Vol. 2, pp. 27-46, Wiley-Interscience, NY.

Rhee, G. Y. and I. J. Gotham, 1981a. The Effect of Environmental Factors on Phytoplankton Growth: Temperature and the Interactions of Temperature with Nutrient Limitation. Limnology and Oceanography 26: 635-648.

Rhee, G. Y. and I. J. Gotham, 1981b. The Effect of Environmental Factors on Phytoplankton Growth: Light and the Interactions of Light with Nitrate Limitation. Limnology and Oceanography 26: 649-659.

Rutherford, J.C. and S.M. Cuddy, 2005. Modelling Periphyton Biomass, Photosynthesis and Respiration in Streams. CSIRO Land and Water Technical Report 23/05.

Senior, L.A. and M.C. Gyves, 2010. Determination of Time-of-Travel, Dispersion Characteristics, and Oxygen Reaeration Coefficients During Low Streamflows – Lower Tacony/Frankford Creek, Philadelphia, Pennsylvania: U.S. Geological Survey Scientific Investigations Report 2010-5195, 90 p.

Smith, K. and J. Hothem, 2006. Continuous Modeling of Wet Weather Strategies; Annual Water Quality Results Support a Municipality's Decision-Making Process. Proceedings from WEFTEC 2006.

Smullen, J.T., A.L. Shallcross , and K.A. Cave, 1999. Updating the U.S. Nationwide Urban Runoff Quality Database. Water Science and Technology 39(12):9-16.

Smullen J.T., and K.A. Cave, 2003. National Stormwater Runoff Pollutant Database. In: Wet-Weather Flow in the Urban Watershed, edited by R. Field and D. Sullivan. Lewis Publishers. Boca Raton, pgs 67-78.

Srivastra, R. Dissolved Oxygen in Streams: Parameter Estimation for the Delta Method. <http://home.iitk.ac.in/~rajeshs/DO.pdf>

Tetra Tech, 2007. The Environmental Fluid Dynamics Code: Theory and Computation; Volume 3: Water Quality Module. 90 pp.

Thomann, R.V. and J.A. Mueller, 1987. *Principles of Surface Water Quality Modeling and Control*. New York: Harper Collins Publishers.

Tsivoglou, E.C. and L.A. Neal, 1976. Tracer Measurements of Reaeration: III. Predicting the Reaeration Capacity of Inland Streams. J. Water Poll. Control Fed. 48:2669-2689.

Uehlinger, U. and M.W. Naegeli, 1998. Ecosystem Metabolism, Disturbance, and Stability in a Prealpine Gravel Bed River. J. N. Am. Benthol. Soc. 17:165-178.

Uehlinger, U., Kawecka, Robinson, C.T., 2003. Effects of Experimental Floods on Periphyton and Stream Metabolism Below a High Dam in the Swiss Alps (River Spol). Aquatic Sciences 65:199-209.

van Donk, E. and S. S. Kilham, 1990. Temperature Effects on Silicon- and Phosphorus-limited Growth and Competitive Interactions among Three Diatoms. Journal of Phycology 26: 40-50.

Welch, E. B., J. M. Jacoby, R. R. Horner, and M. R. Seeley, 1988. Nuisance Biomass Levels of Periphytic Algae in Streams. Hydrobiologia 157: 161-168.

Wool, A.T., Ambrose, R.B., Martin, J.L. and Corner, E.A., 2003. Water Quality Analysis Simulation Program (WASP), Version 6: Draft Users Manual. Retrieved from http://www.epa.gov/athens/wwqtsc/html/wasp.html.

Wynne, D. and G.-Y. Rhee, 1986. Effects of Light Intensity and Quality on the Relative N and P Requirement (the optimum N:P ratio) of Marine Phytoplanktonic Algae. Journal of Plankton Research 8: 91-108.

Wynne, D. and G.-Y. Rhee, 1988. Changes in Alkaline Phosphotase Activity and Phosphate Uptake in P-limited Phytoplankton, Induced by Light Intensity and Spectral Quality. Hydrobiologia 160: 173-178.

Ziadat, A.H. and B.W. Berdanier, 2004. Stream Depth Significance During In-Situ Sediment Oxygen Demand Measurements in Shallow Streams. Journal of the American Water Resources Association 40(3):631-638.

Appendix A1

Sediment Oxygen Demand Measurements Collected in the Tacony Creek, Philadelphia, Pennsylvania

Sediment Oxygen Demand Measurements Collected in the Tacony Creek, Philadelphia, Pennsylvania

Data Report
October 20, 2011

Robert Miskewitz Ph.D.
Rutgers University
Department of Environmental Sciences
14 College Farm Road
New Brunswick, New Jersey 08901

Rutgers was contracted by the Philadelphia Water Department (PWD) to calculate SOD fluxes from field measurements collected by PWD personnel. The data included five days of measurements in August 2011 at five locations with multiple measurements collected at three sites (site map shown in Figure 1). All data was stored by PWD personnel on an ftp site and access was given to Rutgers. Data consisted of pre and post deployment dissolved oxygen (DO) offset tests, DO gradient measurements, ADV velocity measurements, and depth measurements at each location. These data were used to calculate the flux of oxygen through the water column. The method used calculates the SOD flux as the product of the eddy viscosity and the vertical gradient of dissolved oxygen (Miskewitz et al. 2010).

DO offset values: DO measurements were collected before and after each deployment to ensure consistent readings between sensors. In-Situ RDO probes were used for all measurements. Pre and post deployment tests consisted of placing all three DO probes in a bucket and allowing the readings to settle to constant values. Once the readings were constant, the mean and standard deviation of each offset was calculated for period of at least two minutes (Table 1). The offsets used for DO gradient measurements were calculated from only the pre-test data (except at TF599 on 8/3/2011 because the DO gradients never settled to a constant value) because the conditions in the bucket for the pre-test were consistently closer to the ambient conditions in the stream in terms of actual DO concentration and temperature. The procedure was such that the same sample of stream water used for the pre-test offset remained in the test bucket and was used also for the post-test. During the time between pre- and post-tests, the temperature and DO concentrations in the test bucket equalized with the ambient air rather than the conditions in the river, and thus the post-test measured offset was for conditions other than those present in the stream. Future data collection should instead use fresh stream water for both pre- and post-tests, rather than just the former.

The standard deviation of these readings represents the repeatability error of the DO differential between sensors (Table 2). This was used later to calculate the confidence interval for the DO gradient measurements. Offsets were calculated for both the analog and SDI-12 (digital) measurements. All data was checked for outliers via the Modified Z-score method (Iglewicz and Hoaglin 1993); this data was identified and removed. Outliers were only found in the SDI-12 and appeared to be due to incomplete or broken transmission of data. Nevertheless, final calculations based on SDI-12 are recommended as more reliable since the analog data was subject to a correction for signal resistance, which varied for each deployment.

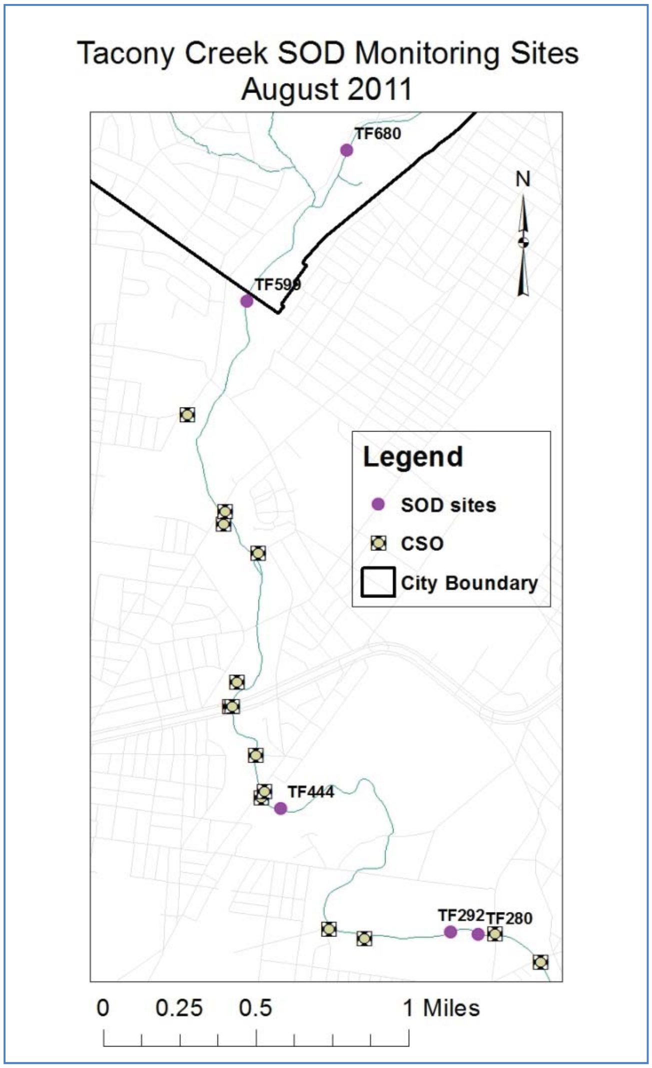

Figure 1. SOD monitoring site map

Table 1. Analog Output Offset Summary Sheet

Site	Date	Offset (mg/L Relative to Probe #1)			Calculated Repeatability Error (mg/L)		
		Probe 1	Probe 2	Probe 3	Probe 1 to Probe 2	Probe 1 to Probe 3	Probe 2 to Probe 3
TF599	8/2/2011	0.000	0.176	0.273	0.009	0.009	0.007
TF680	8/2/2011	0.000	0.179	0.317	0.007	0.011	0.008
TF444	8/3/2011	0.000	0.151	0.256	0.009	0.010	0.007
TF599	8/3/2011	0.000	0.166	0.290	0.008	0.003	0.010
TF280	8/5/2011	0.000	0.142	0.284	0.003	0.007	0.007
TF292	8/5/2011	0.000	0.228	0.351	0.009	0.010	0.009
TF599	8/11/2011	0.000	0.328	0.459	0.007	0.011	0.008
TF292	8/18/2011	0.000	0.170	0.329	0.005	0.007	0.006

Table 2. SDI-12 Output Offset Summary Sheet

Site	Date	Offset (Relative to Probe #1)			Calculated Repeatability Error		
		Probe 1	Probe 2	Probe 3	Probe 1 to Probe 2	Probe 1 to Probe 3	Probe 2 to Probe 3
TF599	8/2/2011	0.000	0.164	0.280	0.009	0.010	0.008
TF680	8/2/2011	0.000	0.152	0.292	0.010	0.012	0.014
TF444	8/3/2011	0.000	0.158	0.286	0.003	0.004	0.002
TF599	8/3/2011	0.000	0.166	0.124	0.008	0.018	0.014
TF280	8/5/2011	0.000	0.165	0.317	0.004	0.005	0.003
TF292	8/5/2011	0.000	0.221	0.346	0.021	0.011	0.023
TF599	8/11/2011	0.000	0.149	0.272	0.007	0.010	0.008
TF292	8/18/2011	0.000	0.134	0.305	0.002	0.003	0.004

DO gradient measurements: DO at three elevations above the stream bed was measured at 10 second intervals for the extent of the deployment at each location. The appropriate offset values were applied to each measurement to correct the value relative to DO probe 1, with probe 1 positioned closest to the surface, probe 3 closest to the sediment, and probe 2 in the center (Figure 2). A figure illustrating the DO concentration during one sampling interval is present as Figure 3.

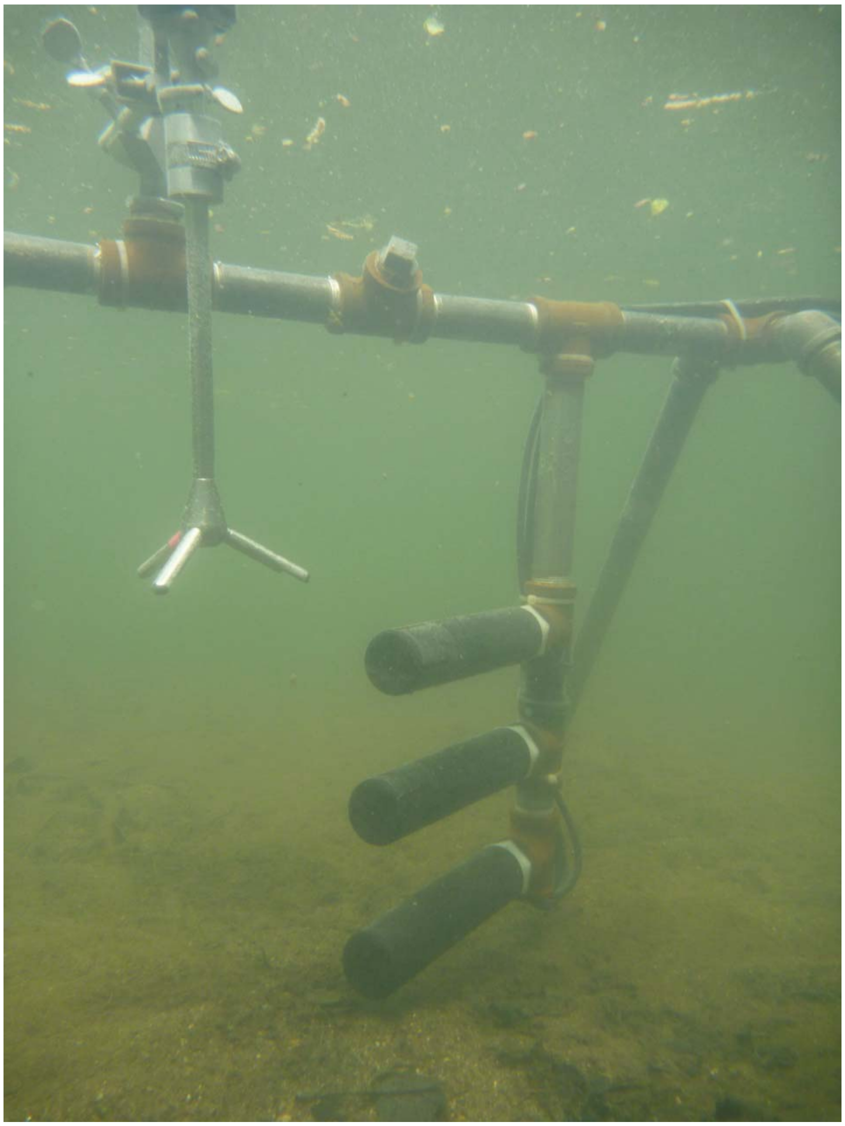

Figure 2. SOD sampling apparatus. DO probes 1, 2, and 3 are positioned at top, center and bottom, respectively. The ADV sensor is on the left.

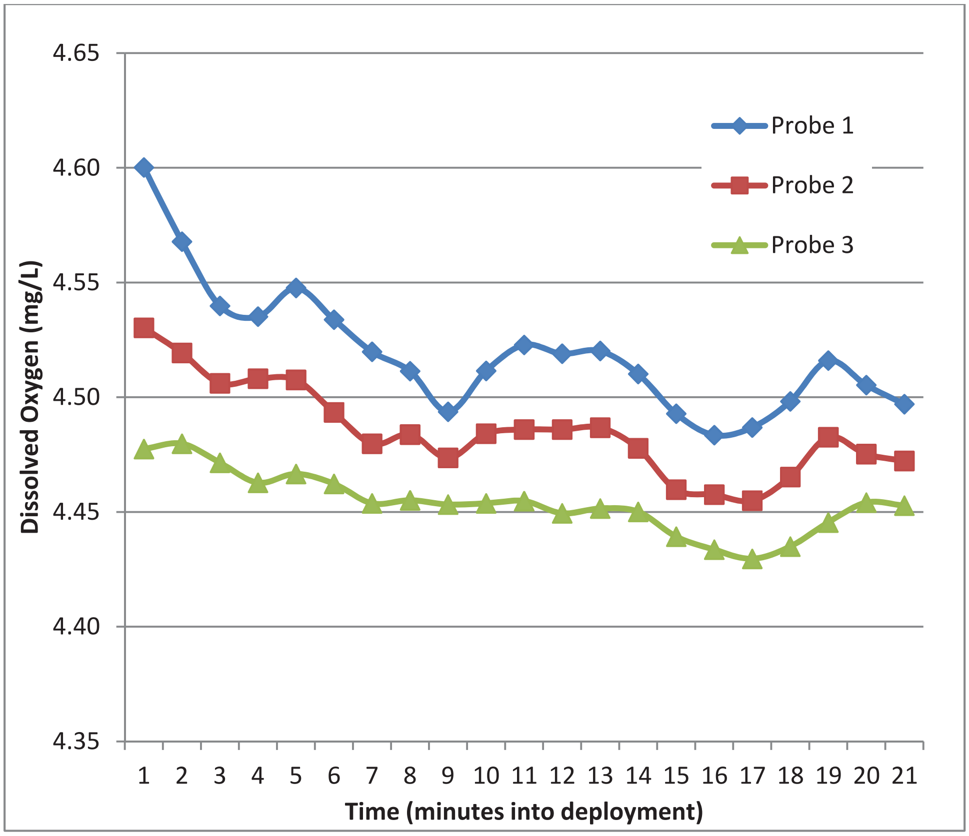

Figure 3. One Minute Average Dissolved Oxygen Measurements Collected at TF444 on 8/3/2011

It is important to note here that the absolute DO measurement is not used; rather the difference between probes is what is required for gradient calculation. The Modified Z-score method was employed to determine the presence of outliers in the measurement record. The only difference in the procedure was that the outlier test was completed for two minute intervals in order to account for fluctuations in the ambient DO concentration. Statistically significant gradients were observed during six of the eight sampling intervals (Table 3).

Table 3. Deployment Mean Concentration Difference Summary

		DO Concentration Difference (mg/L)						
		Analog			SDI-12			
		Probe 1 to Probe 3	Probe 1 to Probe 2	Probe 2 to Probe 3	Probe 1 to Probe 3	Probe 1 to Probe 2	Probe 2 to Probe 3	Notes:
TF599	8/2/2011	0.033	0.038	-0.005	0.047	0.036	0.012	
TF680	8/2/2011	-0.013	-0.004	-0.009	0.000	0.002	-0.002	NS
TF444	8/3/2011	0.033	0.023	0.010	0.067	0.035	0.032	
TF599	8/3/2011	0.021	0.008	0.014	0.026	0.028	-0.002	
TF280	8/5/2011	-0.001	-0.002	0.001	0.000	0.000	0.000	NS
TF292	8/5/2011	0.031	0.004	0.027	0.024	0.013	0.011	
TF599	8/11/2011	-0.007	0.011	-0.018	0.001	0.016	-0.015	
TF292	8/18/2011	0.089	0.020	0.069	0.060	0.017	0.044	

NS= No Significant Gradient observed

ADV Measurements: The ADV package measures velocity in 3 dimensions at a rate of 10 Hz. The output from the sensor includes a measure of signal quality. This measure was used to identify error in the velocity record. Errors typically arise from bubbles or elevated sediment concentrations that cause attenuation of the acoustic signal. All periods containing errors identified in this manner were simply excluded from the analysis. The remaining record was used to calculate the friction velocity. The manufacturer specified accuracy of the ADV is 1% of the measured velocity. Since the vertical and horizontal velocities are used to calculate the friction velocity, a sum of squares was calculated for both signals. The result is a combined uncertainty of 1.4% which was applied to the calculated value. This represents a fairly conservative approach however; the uncertainty from the velocity measurements are minor compared to the uncertainty associated with the DO gradient measurements.

Flux calculations: Fluxes were calculated for one minute intervals for each deployment. The uncertainty associated with the DO concentration gradient was calculated from the calculated standard deviations of the offset values. Using these values, a 90% confidence interval was calculated for the one minute mean gradient value. The product of the DO gradient uncertainty and the ADV uncertainty was then calculated and this value is presented in Appendix 1 alongside the calculated SOD flux values. Table 4 is a summary of the SOD flux data for each of the deployments. The standard deviation presented in this table is a measure of the variation of the measured values and is not a measure of the combined uncertainty of each measurement. The values presented were calculated excluding data points that appeared questionable. The mean flux and standard deviation values for the entire deployment (including questionable values) are presented in parentheses. The data that was excluded was identified as values that resulted from stream bed disturbance due to placement of the sampler, sharp changes in the stream DO concentration due to rainfall or other environmental conditions, and what appeared to be a section of water with depressed DO passing the instrumentation during the middle of the deployment.

Table 4. Dissolved Oxygen Flux Summary Sheet

				SDI-12		Analog	
		Mean Stream Velocity (cm/s)	St. Dev. Stream Velocity (cm/s)	Mean Vertical Dissolved Oxygen Flux (g/m2/day)	Std. Dev. Vertical Dissolved Oxygen Flux (g/m2/day)	Mean Vertical Dissolved Oxygen Flux (g/m2/day)	Std. Dev. Vertical Dissolved Oxygen Flux (g/m2/day)
TF599	8/2/2011	1.93	0.32	6.95	4.65	4.88	4.19
TF680	8/2/2011	15.71	0.76	NS	NS	NS	NS
TF444	8/3/2011	3.55	0.18	10.47	4.24	5.22	3.24
TF599	8/3/2011	1.53	0.28	4.40 (4.14)	2.75 (4.35)	3.63 (3.44)	2.39 (4.02)
TF280	8/5/2011	9.34	0.55	NS	NS	NS	NS
TF292	8/5/2011	1.91	0.29	6.29 (3.66)	3.42 (4.70)	7.29 (4.76)	4.05 (4.80)
TF599	8/11/2011	1.99	0.39	2.50 (0.62)	1.56 (2.58)	1.65 (-0.21)	1.37 (2.50)
TF292	8/18/2011	1.65	0.14	12.22 (7.13)	12.10 (11.94)	15.39 (10.15)	12.45 (12.23)

NS indicates no significant gradient

The DO and SOD flux values vary greatly between the analog and SDI measurements. This difference is directly due to procedure that is used to transmit the results to the datalogger. The analog measurements produce a current between 4 and 20 mAmps. A known resistance is connected into the circuit and the voltage drop across the resistor is measured and converted to a DO concentration. Although the magnitude of each resistor was measured before and after each deployment these measurements vary. The resistors used in the study had a +/- 5% accuracy tolerance which may have been a large source of error in the field measurements. The SDI-12 measurements are transmitted as digital numbers. Although there is more chance for incomplete or missed transmission, these errors are typically easily identifiable though outlier tests. Thus the use of the SDI-12 calculated fluxes is recommended.

References:

Boris Iglewicz and David Hoaglin (1993), "Volume 16: How to Detect and Handle Outliers", The ASQC Basic References in Quality Control: Statistical Techniques, Edward F. Mykytka, Ph.D., Editor.

Miskewitz, R., Francisco, K. and Uchrin, C. (2010) Comparison of a novel profile method to standard chamber methods for measurement of Sediment Oxygen Demand, *Journal of Environmental Science and Health,* Vol. 45 No. 7.

Appendix A2

Sediment Oxygen Demand Measurements Collected in Tacony and Cobbs Creeks, Philadelphia, Pennsylvania

Sediment Oxygen Demand Measurements Collected in Tacony and Cobbs Creeks, Philadelphia, Pennsylvania

Data Report
October 24, 2012

Robert Miskewitz Ph.D.
Rutgers University
Department of Environmental Sciences
14 College Farm Road
New Brunswick, New Jersey 08901

Rutgers was contracted by the Philadelphia Water Department (PWD) to calculate SOD fluxes from field measurements collected by PWD personnel. The data included 29 measurements collected at seven locations in the Tacony and Cobbs Creeks in the City of Philadelphia (site map shown in Figures 1a and 1b). All data was stored by PWD personnel on an ftp site and access was given to Rutgers. Data consisted of pre and post deployment dissolved oxygen (DO) offset tests, DO gradient measurements, Acoustic Doppler Velocimeter (ADV) velocity measurements, and depth measurements at each location. These data were used to calculate the flux of oxygen through the water column. The DO profile method used calculates the SOD flux as the product of the vertical gradient of dissolved oxygen and the eddy viscosity (Miskewitz et al. 2010).

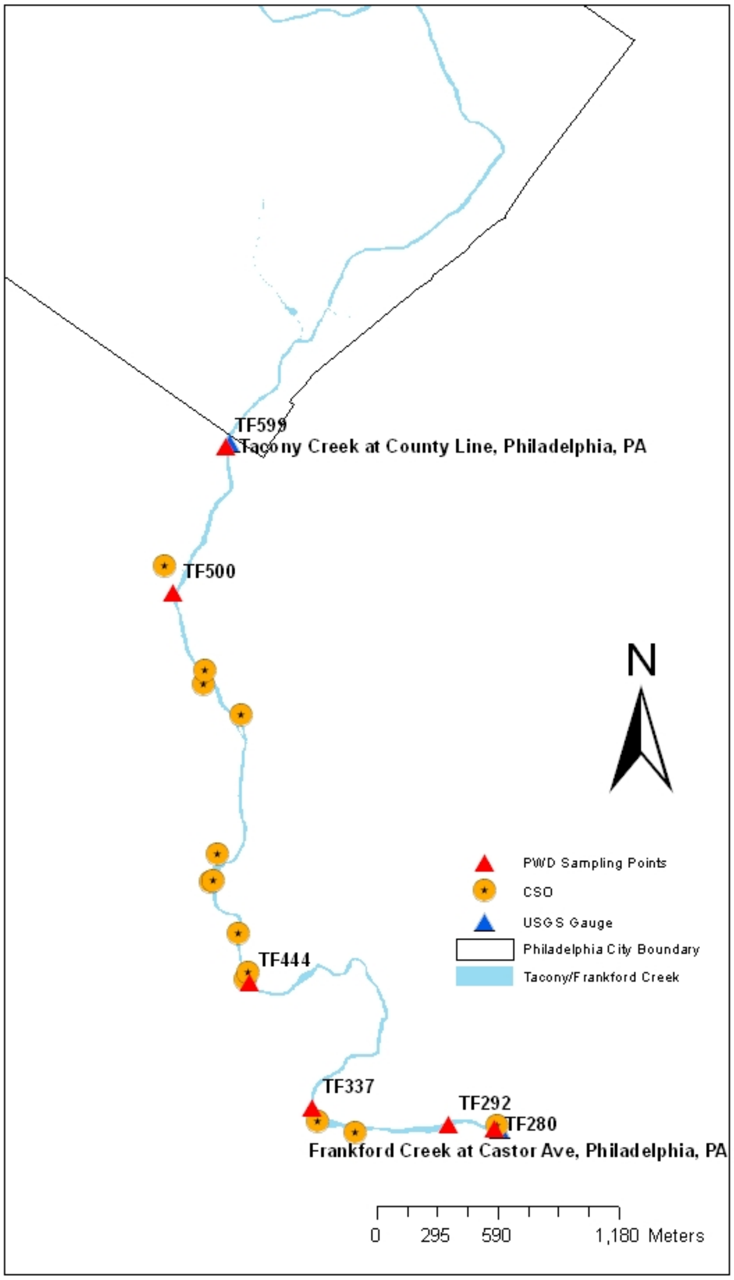

Figure 1a. Tacony Creek SOD monitoring site map

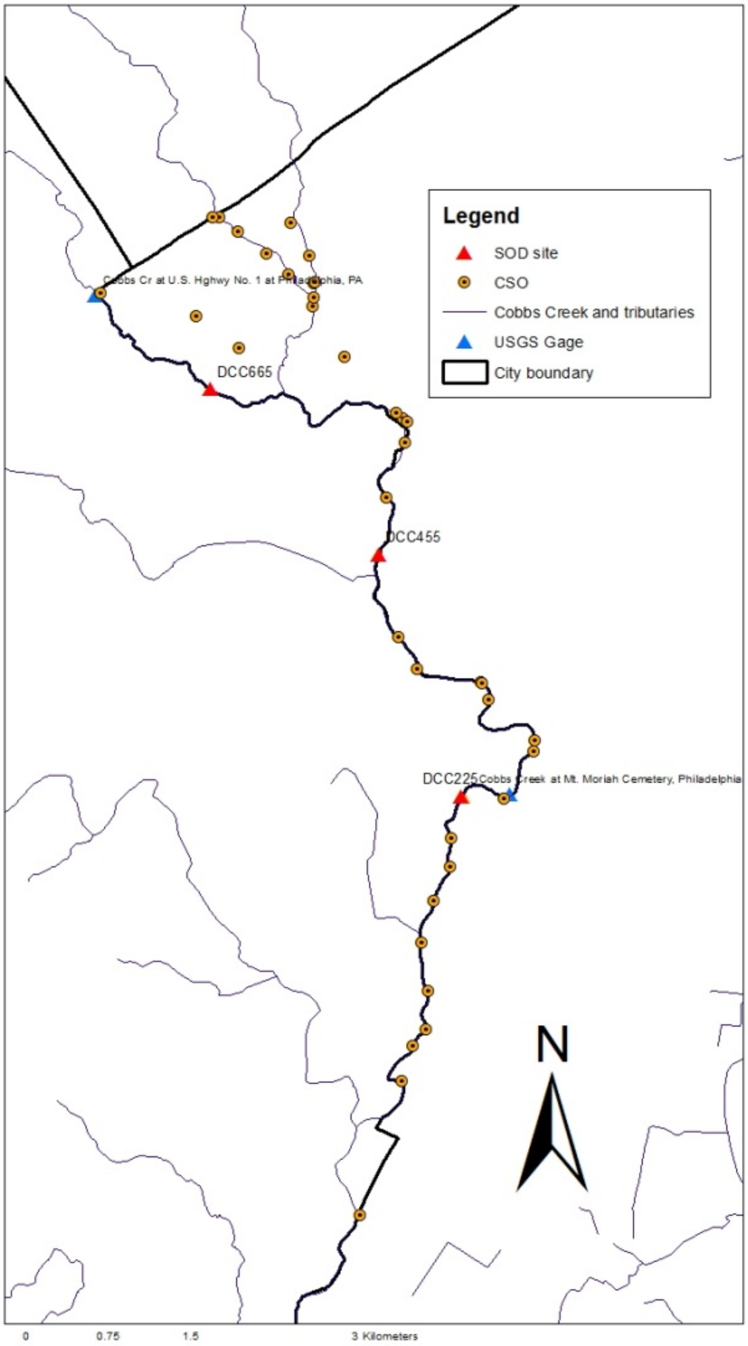

Figure 1b. Cobbs Creek SOD monitoring site map

Methodology: The gradient of dissolved oxygen concentrations was measured via three RDO Pro optical dissolved oxygen probes installed on a galvanized steel rack. The probes were typically at 11.4 cm, 21.6 cm and 31.8 cm above the sediment however these values varied with the stream bed contours. The vertical eddy diffusivity was calculated via the method presented by Elder (1959). This expression calculates the vertical eddy diffusivity as a function of the friction velocity, u*, elevation above the bed, z, and the depth, d, of the water.

$$\varepsilon_z = \kappa u^* z\left(1-\frac{z}{d}\right)$$

The value of κ is the von Karmen constant which has a value of 0.4, d is the water depth, z is the elevation above the stream bed, and u* is the friction velocity. The friction velocity is determined by taking the square root of the covariance of the turbulent fluctuations in the vertical and horizontal velocities, $u^* = \sqrt{\overline{u'w'}}$. These measurements were collected using a Sontek Acoustic Doppler Velicometer (ADV) which measured the velocity of the water at a point above the sediment surface located within dissolved oxygen profile measurements at a resolution 10 Hz. Using these measurements 1 minute average u* values were calculated. The u* values were then used to calculate the eddy viscosity. Since the dissolved oxygen gradient measurements were calculated using three probes 10.2 cm apart the average eddy viscosity was calculated by integrating the equation above between the probes and dividing by the interval. In this way the average flux was calculated between the probes.

$$q_{SOD} = \varepsilon_{\bar{z}} \frac{\Delta C}{\Delta z}$$

Three dissolved oxygen measurements were used in order to verify the dissolved oxygen profile. Although three dissolved oxygen measurements were collected, only the top to bottom SOD flux was calculated because the greater separation between these probes resulted in more significant gradients. During a single deployment, the two upper probes were used because (TF500 6/7/2012) the lower probe appeared to experience errors.

The system is built into a galvanized steel pipe rack structure that holds the three dissolved oxygen probes and the ADV in place for the length of the deployment. The structure was built to resemble a sawhorse. On either end of the structure are two legs connected by a 1.5 meter pipe. Mounted on the pipe are the ADV and the rack with the three dissolved oxygen probes. The probes are oriented perpendicular to the current and located 5 cm away from the sample volume of the ADV perpendicular to the direction of flow. The structure is placed on the river bed with the 1.5 meter pipe perpendicular to the direction of flow. The legs were located far enough from the sensors to avoid any disturbance to the sediment and the flow.

DO offset values: DO measurements were collected before and after each deployment to ensure consistent readings between sensors. In-Situ RDO probes were used for all measurements. Pre and post deployment tests consisted of placing all three DO probes in a vessel filled with stream water and allowing the readings to settle to constant values. Once the readings were constant, the mean and standard deviation of each offset was calculated for period of at least two minutes (Table 1). The offsets used for DO gradient measurements were calculated from the pre-test data except for those intervals when the temperature failed to stabilize in the pre-test.

The standard deviation of these readings represents the repeatability error of the DO differential between sensors (Table 1). This was used later to calculate the confidence interval for the DO gradient measurements. Offsets were calculated for all SDI-12 (digital) measurements. All data was checked for outliers via the Modified Z-score method (Iglewicz and Hoaglin 1993); this data was identified and removed.

Table 1. Measured Output Offset Summary Sheet

		Offset (Relative to Probe 1)			Standard Deviation		
		Probe 1	Probe 2	Probe 3	Probe 1	Probe 2	Probe 3
TF292*	4/24/2012	0.000	0.155	0.139	0.015	0.009	0.010
TF337*	4/24/2012	0.000	0.083	0.096	0.011	0.006	0.012
DCC225	5/8/2012	0.000	0.028	0.083	0.005	0.006	0.007
DC445	5/8/2012	0.000	0.039	0.096	0.007	0.006	0.006
TF500	5/11/2012	0.000	0.054	0.088	0.006	0.006	0.009
TF599	5/11/2012	0.000	-0.006	0.057	0.015	0.012	0.011
DC445*	5/17/2012	0.000	0.103	0.126	0.005	0.005	0.006
DC665*	5/17/2012	0.000	0.057	0.088	0.005	0.007	0.009
TF292	5/18/2012	0.000	0.079	0.085	0.021	0.024	0.014
TF337	5/18/2012	0.000	0.103	0.089	0.039	0.091	0.035
DCC225	5/24/2012	0.000	0.028	0.077	0.007	0.008	0.006
DCC445*	5/24/2012	0.000	-0.014	0.056	0.004	0.006	0.005
TF500	6/1/2012	0.000	0.115	0.124	0.008	0.005	0.006
TF599*	6/1/2012	0.000	-0.063	0.055	0.036	0.022	0.016
TF500	6/7/2012	0.000	0.043	0.096	0.007	0.007	0.009
TF599	6/7/2012	0.000	0.110	0.117	0.004	0.008	0.008
DCC225	6/19/2012	0.000	0.083	0.117	0.002	0.004	0.004
DCC665	6/19/2012	0.000	0.070	0.111	0.003	0.007	0.006
DCC225*	7/6/2012	0.000	0.645	0.382	0.006	0.006	0.004
DCC665	7/6/2012	0.000	0.196	0.206	0.007	0.012	0.009
TF292	7/12/2012	0.000	0.031	0.048	0.016	0.005	0.025
TF337*	7/12/2012	0.000	0.029	0.050	0.003	0.004	0.004
DCC225	7/13/2012	0.000	0.188	0.137	0.004	0.005	0.006
DCC665	7/13/2012	0.000	0.171	0.144	0.003	0.006	0.009
TF292	8/3/2012	0.000	0.115	0.124	0.009	0.009	0.006
TF500	8/3/2012	0.000	0.002	0.065	0.007	0.006	0.008
DCC225*	8/16/2012	0.000	-0.014	0.052	0.005	0.000	0.004
DCC665	8/16/2012	0.000	-0.087	0.032	0.009	0.010	0.007
TF337*	8/30/2012	0.000	0.016	0.046	0.002	0.002	0.004
TF500	8/30/2012	0.000	-0.05	-0.105	0.007	0.005	0.004

* Offset determined from post test.

DO gradient measurements*:* DO at three elevations above the stream bed was measured at 10 second intervals for the extent of the deployment at each location. Deployment durations were 30 minutes at TF292 and TF599, and 20 minutes at all other sites. The appropriate offset values were applied to each measurement to correct the value relative to DO probe 1, with probe 1 positioned closest to the surface, probe 3 closest to the sediment, and probe 2 in the center (Figure 2). The DO concentrations measured at probes 1 and 3 during the sampling events are presented in Appendix A.

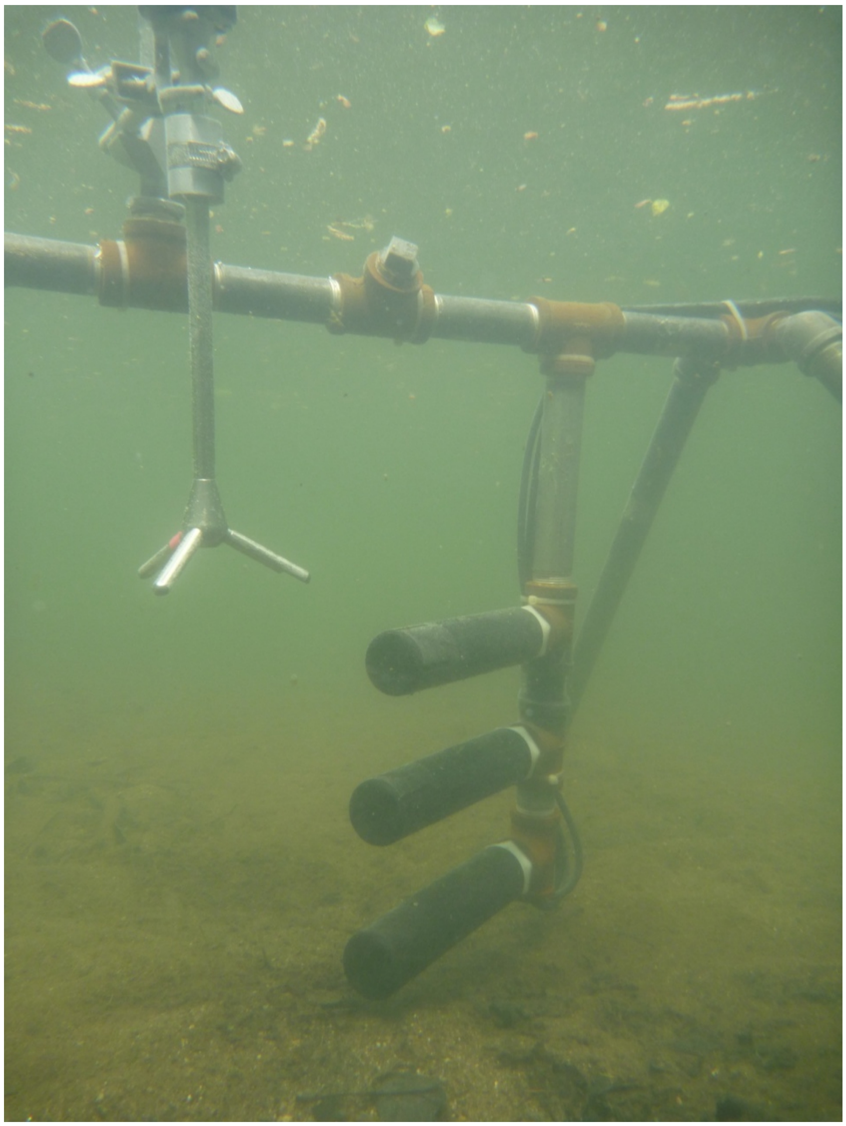

Figure 2. SOD sampling apparatus. DO probes 1, 2, and 3 are positioned at top, center and bottom, respectively. The ADV sensor is on the left.

It is important to note here that the absolute DO measurement is not used; rather the difference between probes is what is required for gradient calculation. The Modified Z-score method was employed to determine the presence of outliers in the measurement record. The only difference in the procedure was that the outlier test was completed for two minute intervals in order to account for fluctuations in the ambient DO concentration.

ADV Measurements: The ADV package measures velocity in 3 dimensions at a rate of 10 Hz. The output from the sensor includes a measure of signal quality. This measure was used to identify error in the velocity record. Errors typically arise from bubbles or elevated sediment concentrations that cause attenuation of the acoustic signal. All periods containing errors identified in this manner were simply excluded from the analysis. The remaining record was used to calculate the friction velocity. The manufacturer specified accuracy of the ADV is 1% of the measured velocity. Since the vertical and horizontal velocities are used to calculate the friction velocity, a sum of squares was calculated for both signals. The result is a combined uncertainty of 1.4% which was applied to the calculated value. This represents a fairly conservative approach however; the uncertainty from the velocity measurements are minor compared to the uncertainty associated with the DO gradient measurements.

Flux calculations: Fluxes were calculated for one minute intervals for each deployment. The uncertainty associated with the DO concentration gradient was calculated from the calculated standard deviations of the offset values. Using these values, a 95% confidence interval was calculated for the one minute mean gradient value. The product of the DO gradient uncertainty and the ADV uncertainty was then calculated and this value is presented in Appendix B alongside a summary of all data for each deployment. Table 2 is a summary of the SOD flux data for each of the deployments. The standard deviation presented in this table is a measure of the variation of the measured values and is not a measure of the combined uncertainty of each measurement. In addition to measured fluxes the flux corrected to 20˚ C is included in Table 2. These values were calculated using a form of the Ahrrenius Equation (Truax et al. 1995).

Table 2. Dissolved Oxygen Flux Summary Sheet

					Temperature corrected to 20˚C
Site	Date	SOD Flux		Temperature	SOD Flux
		Mean	Standard Deviation	Mean	Mean
		(g/m2/day)		˚C	(g/m2/day)
DCC225	5/8/2012	3.273*	3.948	15.49	4.35
DCC225	5/24/2012	7.133	5.174	20.24	7.03
DCC225	6/19/2012	3.214*	3.748	19.40	3.34
DCC225	7/6/2012	4.935	2.638	25.13	3.57

DCC225	7/13/2012	-4.316*	3.475	23.90	-3.38
DCC225	8/16/2012	4.378	3.947	23.38	3.54
DCC455	5/8/2012	9.631*	19.238	15.20	13.03
DCC455	5/17/2012	29.594	10.440	18.88	31.75
DCC455	5/24/2012	-1.191*	5.687	20.13	-1.18
DCC665	5/17/2012	7.079*	11.672	16.78	8.67
DCC665	6/19/2012	5.187*	10.289	18.25	5.79
DCC665	7/6/2012	25.106*	32.763	22.55	21.38
DCC665	7/13/2012	3.513*	12.546	22.00	3.10
DCC665	8/16/2012	-2.711*	6.540	22.00	-2.39
TF292	4/24/2012	7.395	2.693	10.66	13.32
TF292	5/18/2012	15.977	11.371	18.71	17.33
TF292	7/12/2012	1.365*	1.553	24.60	1.02
TF292	8/3/2012	13.177	8.033	24.67	9.82
TF337	4/24/2012	-0.688*	3.293	9.97	-1.29
TF337	5/18/2012	0.792*	2.028	18.27	0.88
TF337	7/12/2012	2.993*	3.006	24.30	2.28
TF337	8/30/2012	6.538	3.203	22.80	5.48
TF500	5/11/2012	4.959	4.140	14.06	7.21
TF500	6/1/2012	7.969	4.200	17.41	9.38
TF500	6/7/2012	1.85* (12.36)	4.09 (7.03)	20.05	1.84 (12.32)
TF500	8/3/2012	7.000	4.520	24.35	5.32
TF500	8/30/2012	10.356	9.236	21.03	9.71
TF599	5/11/2012	6.646	3.761	13.72	9.87
TF599	6/1/2012	19.013	11.311	17.22	22.65
TF599	6/7/2012	6.657	5.508	17.22	7.93

() Flux calculated between probes 1 and 2.
* No significant flux measured.

The measurements were analyzed to determine if a statistically significant flux (greater than zero) was present. This was completed by comparison of the SOD flux to the standard deviation of the measured flux. If the flux rate is greater than the standard deviation it is assumed that the measured flux is significant. Measurements that resulted in non-significant flux rates most often occurred at DCC445, DCC665, and TF337. In addition to the measured standard deviation, the instrument uncertainty was calculated for each sampling interval (columns I and J Appendix B). The instrument uncertainty was compared to the measured flux in the same manner as the standard deviation. The final quality control step involved a qualitative investigation of the data. Measurement intervals during which the pre- and post- offset test did not stabilize were identified as questionable (DCC255 7/13/2012, TF337 7/12/2012, TF599 6/1/2012). Measurement intervals during which the u* assumption of a steady state condition was violated were also identified (DCC665 7/6/2012, TF337 5/18/2012, TF500 8/30/2012). A violation of the u* assumption indicates a condition with unsteady flow in the channel.

References:

Boris Iglewicz and David Hoaglin (1993) "Volume 16: How to Detect and Handle Outliers", The ASQC Basic References in Quality Control: Statistical Techniques, Edward F. Mykytka, Ph.D., Editor.

Elder, J.,W. (1959) The dispersion of marked fluid in turbulent shear flow. *Journal of Fluid Mechanics*. *5* (4), 544-560.

Miskewitz, R., Francisco, K. and Uchrin, C. (2010) Comparison of a novel profile method to standard chamber methods for measurement of Sediment Oxygen Demand, *Journal of Environmental Science and Health,* Vol. 45 No. 7.

Truax, D., Shindala, A., and Sartain, H. (1995) Comparison of two sediment oxygen demand measurement techniques, Journal of Environmental Engineering Vol.121 No.9.

Appendix B

USGS Gage Data Processing & Analysis Procedures

USGS Gage Data Processing & Analysis Procedures

With 12 USGS gages collecting data for multiple water quality parameters at half-hour intervals, a large amount of data are produced. PWD Office of Watersheds (OOW) staff has developed procedures for the processing and analysis of these data using Microsoft Excel and Access software, as well as R, a free software environment for statistical computing and graphics. Most aspects of the data processing and analysis have been automated with custom Visual Basic and R code.

OOW independently maintains databases of water quality and streamflow via automated regular retrievals of these data from USGS NWIS. On a monthly basis, the databases are queried and results for each gage are imported into MS Excel workbooks. If available, any field data collected during that period (*e.g.*, hand meter readings from field maintenance checks, water quality grab samples, etc.) are also imported. Once all required data have been entered, separate plots are produced for each parameter (dissolved oxygen, turbidity, pH, specific conductance, and temperature) to enable a subjective review of data quality.

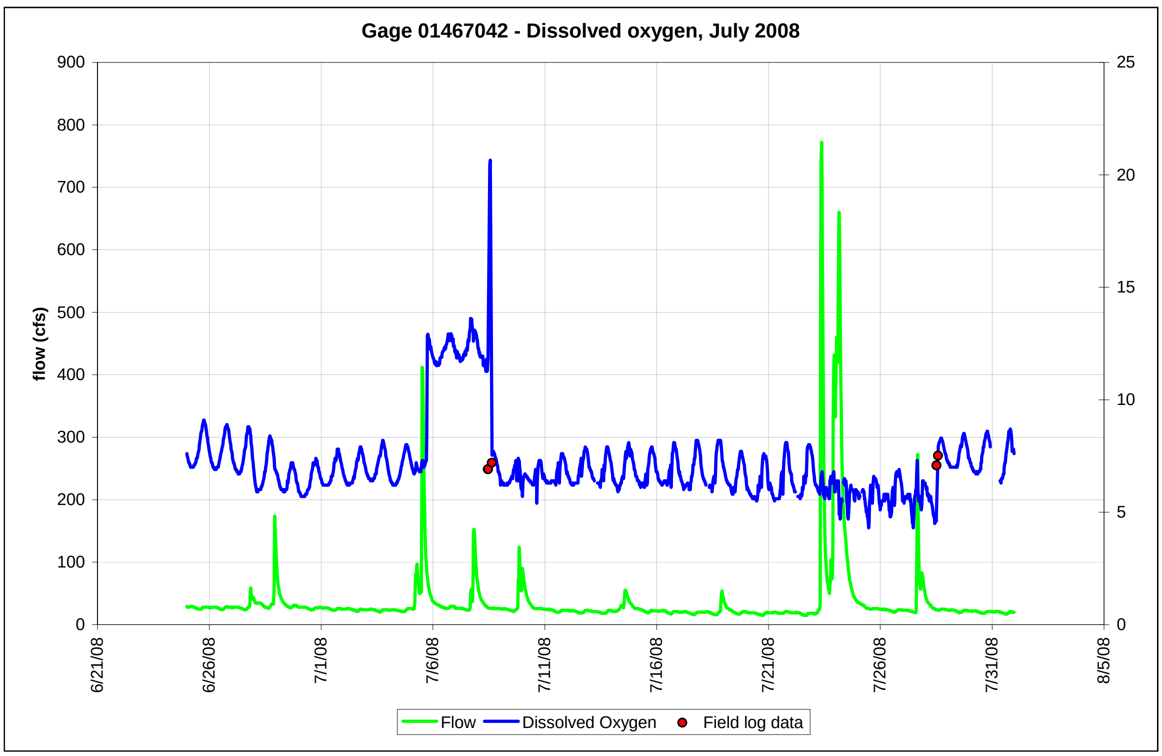

Figure B1: Example of an Excel-generated data processing/analysis plot; Gage 01467042, Dissolved Oxygen, July 2008.

These plots are examined and are the primary basis for the selection of good vs. questionable data for a given month. Intervals of questionable data are located and added to a table of "flagged" data for that particular parameter, which is then used to update the water quality database.

The final step of the procedure utilizes R, a statistical programming language and software environment. The R software code developed by OOW staff analyzes all of the water quality data in a database, as well as the good and questionable flags, and generates statistical and graphic results in a variety of forms. These include monthly plots for all data parameters for each site, showing accepted and questionable data, water quality criteria, grab sample data, and streamflow (Figure B2); assorted statistics including accepted and questionable data comparisons, monthly exceedance percentages, and comparisons of wet and dry weather periods; additional plots, including average dissolved oxygen (DO), percent DO saturation, and pH/percent DO saturation.

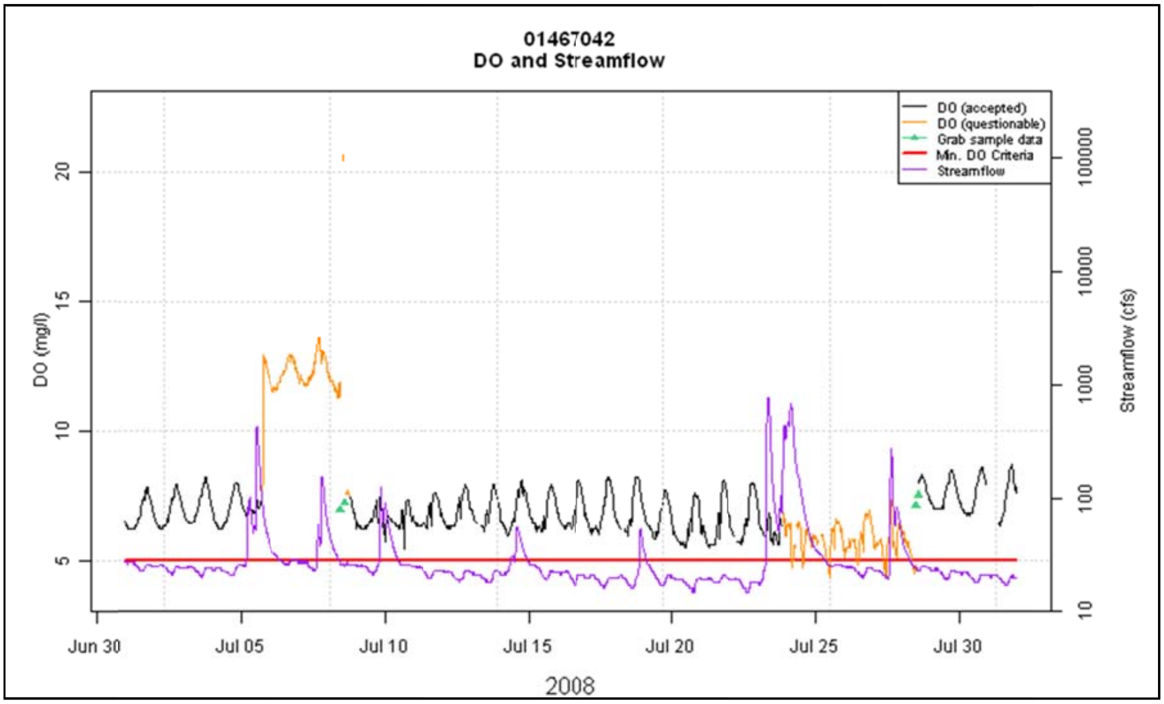

Figure B2: Example of an R-generated plot showing accepted and questionable data, and minimum water quality criteria; Gage 01467042, Dissolved Oxygen, July 2008.